Dynamique de l'infection grippale : modélisation et applications

Laetitia Canini

Thèse de doctorat de l'université Paris VI - Pierre et Marie Curie

Spécialité Biostatistiques et Biomathématiques

Ecole Doctorale Pierre Louis de santé publique

ED 393: épidémiologie et sciences de l'information biomédicale

Présentée par

Mademoiselle Laetitia CANINI

Pour obtenir le grade de

Docteur de l'université Paris VI - Pierre et Marie Curie

Dynamique de l'infection grippale
Modélisation et applications

Soutenue le 16 mai 2012 devant le jury composé de:

Mr le Pr Fabrice Carrat	Directeur de thèse
Mr le Dr Alan Perelson	Rapporteur
Mr le Pr Xavier de Lamballerie	Rapporteur
Mme le Dr Dominique Costagliola	Examinateur
Mme le Pr France Mentré	Examinateur
Mr le Dr Rodolphe Thiébaut	Examinateur

Laboratoire de rattachement

UMR-S 707, INSERM - Université Paris VI - Pierre et Marie Curie

"Epidémiologie, système d'information, modélisation"

Directeur: Guy THOMAS

Equipe "Epidémiologie des maladies infectieuses et modélisation"

Responsable: Guy THOMAS

Faculté de Médecine Pierre et Marie Curie, Site Saint-Antoine,

27 rue Chaligny,

75571 Paris Cedex 12,

France

Financement

Ce travail a été financé par le projet FLUMODCONT et par une allocation de recherche du Ministère de l'enseignement supérieur et de la recherche.

Remerciements

Je remercie très chaleureusement le Professeur Fabrice Carrat à l'initiative de ce travail. Merci de m'avoir si bien soutenue au cours de cette thèse et de m'avoir fait découvrir la Recherche. Merci pour ton encadrement scientifique, ta rigueur dans le travail et ta disponibilité.

I would like to thank Dr Alan Perelson for agreeing to participate on my thesis committee as an examiner-reviewer. I am particularly excited to work with you soon.

Je remercie le Professeur Xavier de Lamballerie d'avoir accepté de participer à mon jury de thèse en qualité de rapporteur.

Je remercie les Docteurs Dominique Costagliola et Rodolphe Thiébaut ainsi que le Professeur France Mentré d'avoir acepté de participer ŕ mon jury de thèse en qualité d'examinateur.

Je remercie MM. Paccioni, Courcier et Muller de GlaxoSmith Kline ainsi que MM. Morer et Maison Neuve de l'agence française de sécurité sanitaire des produits de santé (AFSSAPS) de nous avoir fourni les données individuelles d'excrétion virale.

Je remercie le Professeur Guy Thomas de m'avoir accueillie au sein de l'UMR S 707 ainsi que Liliane Narme et Isabelle Goderel pour leur aide dans les méandres administratifs et leur soutien.

Je remercie le Professeur Alain-Jacques Valleron et le Docteur Dominique Costagliola pour la qualité de l'école doctorale et des séminaires de doctorants à Saint Malo, agréables moments de partage entre doctorants, ainsi qu'Evelyne Guilloux pour son accueil, sa disponibilité et son aide au sein de l'école doctorale.

J'adresse un remerciement à toute l'équipe de Fabrice Carrat: Frédéric, Nasya, Erina, Khadija, Stéphanie, Grégory, Yoann, Anne-Sophie, Sylvain, Frédéric, Minh, Hubert, Henda, Cécilie, Nöelle et Céline.

Je remercie l'équipe de l'étude Gripmask, les médecins et les patients ayant participé à ce projet. Je remercie Pascal Ferrari et Romina D'Angelo pour leur travail et leur investissement dans ce projet.

Je remercie Rosemary pour les relectures et ses conseils précieux en anglais.

Je remercie très sincèrement mes amis thésards : Magali Lemaitre, Nathanël Lapidus, Yoann Mansiaux et Anne Cori pour leur amitié, leur soutien et leur aide très précieuse.

Enfin je remercie Maria et Marius pour leur aide sur des détails techniques et les relectures à distance ainsi que pour leur soutien.

A ma famille

A mes amis

Résumé de la thèse

La grippe est une maladie transmissible causant des épidémies saisonnières et occasionnellement des pandémies. Chaque année plus de 500000 morts sont dûes à la grippe. La transmission de la grippe a été largement étudiée afin de décrire et de prédire la propagation de la maladie au sein des populations. Ces modèles reposent sur de fortes hypothèses concernant les paramètres de l'histoire naturelle de la grippe tels que l'infectiosité, la période de latence, la période infectieuse ou le temps de génération.

Dans ce contexte, l'objectif principal de cette thèse était de définir un ensemble d'outil méthodologique pour décrire et étudier l'évolution au cours du temps de la grippe ainsi que les paramètres de son histoire naturelle. Le travail principal a été le dévelopement d'un modèle décrivant la chronologie de l'infection grippale et des symptômes associés. La cinétique virale (VK) de la grippe est utilisée pour représenter l'infectiosité alors que l'histoire naturelle de la grippe est décrite par la dynamique des symptômes (SD).

Dans un premier temps, nous décrivons l'évolution de l'infection grippale au cours du temps ou dynamique intra-hôte. Nous nous intéressons aux interactions existant entre le virus et son hôte et desquelles resulte le cycle de réplication virale. Puis, nous présentons les deux volets de la réponse immunitaire en cas d'infection grippale, avec leurs protagonistes, leurs rôles et leurs dynamiques. La réponse immunitaire innée intervient précocemment et confère une première défense non spécifique et la réponse immunitaire adaptative est mise en place après quelques jours et est spécifique. Enfin, nous décrivons l'expression clinique de la grippe et son évolution au cours du temps.

Il est généralement considéré que la grippe est une maladie aéroporté via des gouttelettes produites lors de la toux et/ou des éternuements et contenant du virus. La transmssion de la grippe d'un individu infecté à un individu susceptible dépend alors de la susceptibilité de l'individu contact, du taux de contact entre les deux individus et de la quantité de particules infectées produites par l'individu infecté. Or cette dernière hypothèse repose sur la caractérisation de la VK et de la SD des infividus infectés qui a été peu étudiée.

Nous définissons alors des paramètres de l'histoire naturelle de la grippe en nous basant sur l'hypothèse selon laquelle l'infectiosité est proportionnelle à la charge virale excrétée. Ces paramètres sont l'infectiosité, la période de latence, la durée d'infectiosité et le temps de génération.

L'infection grippale est variable d'un individu à l'autre aussi bien en ce qui concerne la VK, que la SD ou encore la réponse immunitaire. Nous nous intéressons alors aux différentes sources pouvant expliquer cette variabilité. Nous distinguons trois grandes sources de variabilité: variabilité environnementale, variabilité liée au virus et variabilité liée à l'hôte. Nous insistons en particulier sur l'évolution constante du virus et sa capacité à s'adapter rapidement en cas de pression de sélection et sur la variabilité de la réponse immunitaire de l'hôte qui peut être aussi bien qualitative que quantitative et toucher la réponse innée ou adaptative.

Pour modéliser la dynamique de l'infection grippale, il est donc important d'une part de représenter le phénomène infectieux et les relations entre le virus, les cellules cibles et l'immunité et d'autre part de prendre en compte les différents niveaux de variabilité. Nous présentons donc les modèles historiques de cinétiques virales initialement développés dans le cadre des infections par le VIH, puis les spécificités liées à la modélisation de la VK pour la grippe. Ces modèles, dits mécanistiques, se basent sur les connaissances concernant les interactions entre virus et son hôte et l'immunité. Ainsi, les paramètres utilisés ont une réelle signification biologique. Nous présentons ensuite l'approche de population qui est une mèthode de modèlisation statistiques permettant de prendre en compte plusieurs niveaux de variabilité et est donc adaptée au cas de la grippe.

C'est dans ce cadre que nous avons développé un modèle original de cinétique virale/dynamique des symptômes (VKSD) en utilisant une approche de population. Etant donné que les cytokines pro-inflammatoires produites lors de la réponse immunitaire innée sont responsable des symptômes systémiques, l'objectif de ce travail était de développer

un modèle qui lierait de manière causale la VK, la SD et la réponse immunitaire innée. De plus, précédemment, un seul modèle avait été ajusté sur des données humaines, avec un petit nombre de participant et la méthode utilisée ne prenait pas en compte la variabilité inter-individuelle. Le modèle que nous avons développé comporte sept compartiments: la charge virale, les cellules cibles, les cellules infectées en phase latente et productive, les cytokines pro-inflammatoire, les cellules NK et les symptômes systémiques. Nous avons utilisé l'approche de population pour modéliser la variabilité inter-individuelle. Ce modèle a été ajusté sur des données individuelles de charge virale et de score de symptômes systémiques, obtenu chez 56 volontaires expérimentalement infectés avec une souche de virus A/H1N1. Les données utilisées était particulièrement riches avec une mesure de la charge virale par jour et deux mesures de l'intensité des symptômes systémiques par jour. Bien que les participants aient été comparable en terme de données physiologiques et démographiques, les courbes de VK et SD étaient très variables. En effet, 12 volontaires n'ont pas excrété de virus et parmi les 44 restants, 19 n'ont pas développé de symptômes systémiques. L'approche de population était donc la mieux adaptée. Les paramètre du modèle ont été estimé en utilisant l'algorithme SAEM implémenté dans MONOLIX. A partir de ce modèle, nous décrivons la cinétique de la charge virale, des cytokines pro-inflammatoires, des cellules NK ainsi que la dynamique des symptômes systémiques. Nous mesurons également l'infectiosité comme étant l'aire sous la courbe VK. Nous trouvons que cette infectiosité est 15 fois supérieure chez les sujets avec de symptômes systémiques comparativement aux sujets qui en sont indemnes ($P<0.001$). La période de latence définie comme le temps nécessaire pour devenir infectieux variait de 0.7 à 1.9 jours et la période d'incubation qui est le temps nécessaire à l'apparition des premiers symptômes variait de 1.0 à 2.4 jours.

Notre modèle prolonge des travaux précédents en incluant la réponse immunitaire innée et en apportant des estimations réalistes des paramètres de l'infection et de la maladie, en prenant en compte la forte variabilité inter-individuelle.

Ce modèle pourrait être complété avec la description des symptômes respiratoires qui jouent un rôle central dans la propagation du virus dans l'environnment. De plus ce travail apporte des informations sur l'infectiosité qui est un paramètre clef pour la transmission de la grippe. Nous discutons plus particulièrement la proportion d'infectiosité ayant lieu avant l'apparition des symptômes et nous proposons une correction en prenant en compte la dynamique des symptômes respiratoires.
Enfin, concernant ce travail nous discutons l'applicabilité de ce modèle à des infections acquises naturellement et pour lesquelles la date d'infection est inconnue.

Etudier la VK de la grippe représent plusieurs défis. En effet, l'infection grippale est très rapide, le pic d'excrétion a lieu avant le début des symptômes et en cas d'infection acquise naturellement la date d'infection est inconnue. De plus, des problèmes d'identifiabilité des paramètres peuvent exister. Le choix du protocole est donc crucial afin d'obtenir des données suffisamment informatives et à un coût minimum. Nous nous sommes donc intéressé au développement de protocoles optimisés pour étudier la VK et la SD de la grippe. Déterminer un protocole consiste à identifier le nombre de prélèvements nécessaires ainsi que le temps de prélèvement pour chaque individu et à définir le structure du protocole: nombre de groupes, nombre de prélèvements par groupe et proportion d'individus dans chaque groupe. Nous présentons d'abord brièvement la méthode utilisée pour les analyses d'optimisation de protocoles. La matrice d'information de Fisher permet de quantifier l'information relative à un paramètre contenue dans une distribution. Le but qui est de minimiser les variances des paramètres, équivaut donc à maximiser la matrice d'information de Fisher par rapport au protocole de population.
Le choix des protocoles est crucial pour estimer précisemément les paramètres du modèle. À cet effet, nous avons réalisé une analyse d'optimisation de protocole afin de proposer des protocoles économiques et faciles à mettre en place. Un jeu de protocoles adaptés à l'étude de la VK, de la réponse immunitaire innée et/ou de la SD ont été élaborés. Nous

avons inclu des sites de prélèvement supplémentaires: les cytokines pro-inflammatoires et les cellules NK. En apportant de l'information dans ces compartiments, certains problèmes d'identifiabilité pourraient être résolus et la précision d'estimation des paramètres accrue. Ces protocoles pourraient aider à la mise en place de futures études de la VK de la grippe en diminuant l'inconfort des patients et le coût et permettraient d'affiner les résultats concernant la réponse immunitaire innée.

Enfin, nous avons réalisé une étude *in silico* de l'effet des inhibiteurs de neuraminidase sur la VK et la SD grippales et sur l'émergence de résistance. En utilisant le modèle VKSD, nous avons exploré l'efficacité virologique et clinique de l'oseltamivir en modélisant la pharmacocinétique du produit pour différentes posologies. Nous avons simulé pour chaque cas une population de sujets immunocompétents et une population de sujets immunodéficients. Une administration précoce assure une efficacité élevée. L'immunodéficience était associée à une nette augmentation de la proportion de sujets excrétant du virus résistant et un effet dose a été clairement identifié.

Cette thèse illustre l'importance de la prise en compte des connaissances sur la biologie de la grippe dans les modèles à l'échelle de la population afin de faire face à l'infection grippale et d'atténuer son impact.

***

Mots clefs: Grippe, Virus grippal, Cinétique virale, Symptômes systémiques, Immunité, Traitement antiviral, Inhibiteur de neuraminidase, Résistance aux antiviraux, Modèles Non linéaires à effets mixtes, Optimisation de protocole.

Thesis summary

The main objective of this PhD was to define a set of methodological tools to describe and study the time course of influenza and to measure its natural history parameters. The principal work was the development of a model to describe influenza infection and illness timeline. Influenza virus kinetics (VK) is used as a surrogate of infectiousness, while the natural history of influenza is described by symptom dynamics (SD). We developped an original virus kinetics/symptom dynamics (VKSD) model based on a population approach. Our approach extends previous works by including the innate response and providing realistic estimates of infection and illness parameters, taking into account the strong interindividual variability.

We were then interested in defining optimized designs to study influenza VK and SD. The choice of the study design, *i.e.* when and how many times samples are to be collected in individuals depending on the sample size, is crucial to accurately estimate the model parameters. For this purpose we performed an optimal design analysis to propose cost-effective and practical designs. A set of designs adapted to study influenza VK, innate immune response and/or SD was elaborated and could help design further studies on influenza viral kinetics with decreased discomfort and cost.

Finally, we realised an *in silico* analysis studying the effect of neuraminidase inhibitors on influenza infection and illness and on resistance emergence. Using the VKSD model, we explored the virological and clinical efficacy of oseltamivir through simulated pharmacokinetics for differents regimens. We simulated each time a population of immunocompetent subjects and one of immunodeficient subjects. An early administration provided a high efficacy, but led to resistant virus emergence. Immunodeficiency was associated with a substantially increased proportion of subjects shedding resistant virus and a clear dose effect was found on resistance emergence.

This thesis illustrates the need of incorporating biological knowledge in models at population scale to improve the accuracy of the predictions.

***

Key-words: Influenza, Influenza virus, Viral kinetics, Systemic symptoms, Immunity, Antiviral, Neuraminidase inhibitor, Antiviral resistance, Nonlinear mixed effect modeling, Optimal design.

Production scientifique

Publications

Canini L., and F. Carrat. Impact of different oseltamivir treatment regimens in the otherwise healthy or immunocompromised influenza infected patients: insights from a modelling study. *In preparation*

Canini L., and F. Carrat. (2012) Ready-to-use optimized designs to study influenza infection dynamics. *In review in PLoS ONE*

*__Canini L.__, and F. Carrat. (2011) Viral kinetics on influenza: When and how many times are nasal samples to be collected? *Influenza and other Respiratory Viruses* 5(suppl 1):144-47

Canini L., and F. Carrat. (2011) Population modeling of influenza A/H1N1 viral kinetics and symptom dynamics. *Journal of Virology* 85(6):2764-70

*__Canini L.__, L. Andréoletti, P. Ferrari, R. D'Angelo, T. Blanchon, et al. (2010) Surgical Mask to Prevent Influenza Transmission in Households: A Cluster Randomized Trial. *PLoS ONE* 5(11): e13998

** Prepared during the PhD period but not included in the manuscript*

Communications orales et posters

Canini L., and F. Carrat. "Viral kinetics studies on influenza: when and how many times are nasal samples and symptoms scores to be collected?", Poster presented at the international conference 51st ICAAC, in Chicago IL, USA, in September 2011

Canini L., and F. Carrat. "Impact of different oseltamivir treatment regimens in the otherwise healthy or immunocompromised influenza infected patients: insights from a modelling study", Poster presented at the international conference 4th ESWI conference, in Malta, in September 2011

Canini L., and F. Carrat. "Optimal designs to study influenza viral kinetics", Talk at the 5ème conférence d'épidémiologie clinique in Marseille, France, in May 2011

Canini L., and F. Carrat. "Viral kinetics studies on influenza: when and how many times are nasal samples to be collected?" Poster presented at the international conference Option for the control of influenza VII, in Hong Kong SAR, China, in September 2010

Canini L., and F. Carrat. "Population modeling of influenza A/H1N1 viral kinetics and symptom dynamics", Talk at the international conference Epidemics^2 in Athens, Greece, in December 2009

Contents

1 Introduction

Influenza is a transmissible disease. Influenza virus' structure, its genome, the immune response elicited against it, vaccines to protect against it and its epidemiology have been the subjects of overwhelming attention. The pathogens responsible for the disease are RNA viruses from the *Orthomyxoviridae* family, namely the *Orthomyxoviruses* A, B and C. This classification is based on the type-specific nucleoprotein and matrix protein antigens.

The type A virus which was first isolated in 1933, is associated to the most serious clinical manifestations. It can be found in human beings as well as in different animal species such as birds, horses, pigs, seals, whales, dogs... [1–3]. The type B virus was first isolated in 1940 and was only described in human beings [4]. The type C virus rarely circulates in human populations at present [5].

Influenza virus is continuously evolving and is highly contagious which is why the disease is considered a major problem in Public Health. It induces a cost in terms of human lives during pandemics and can generate economical losses (absenteeism, medical cares, hospitalizations...) which are generaly mild but can be sometimes severe.

Influenza viruses are also classified in subtypes depending on their genetic structure and on the antigenic properties of their surface glycoproteins: the haemagglutinine (HA) and the neuraminidase (NA). Sixteen different HA were identified: H1 to H16 and nine NA: N1 to N9 [6–8]. Most of the circulating subtypes are responsible for animal infections and only the subtypes A/H1N1, A/H2N2 and A/H3N2 were formally identified in human epidemics. Subtypes were not identified for type B virus [5].

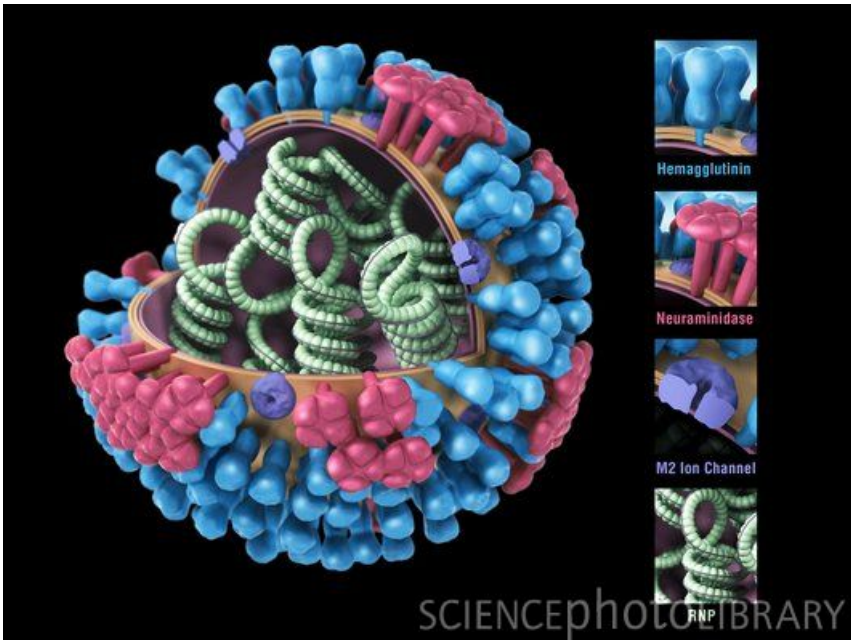

Figure 1.1: Influenza virus structure. (Credit: CDC/SCIENCE PHOTO LIBRARY)

Viruses of type A and B are responsible for annual epidemics in humans. The seasonal characteristic of influenza is marked in the temperate regions where the disease appears in winter months whereas in tropical regions cases may occur all year long [9].

Each year 5 to 20% of the population is infected with 3 to 5 million severe infectious cases and results in more than 500,000 deaths worldwide [10, 11]. Besides these yearly epidemics, influenza can lead to pandemics during which millions of persons might die.

Outbreaks of human influenza virus infection is believed to have happened since as far back as 430 BC [12]. During the XXth century, three pandemics were identified. In 1918, a A/H1N1 virus emerged and replaced the A/H3N8 virus previously circulating and caused the "Spanish flu" which was responsible for the death of more than 40 millions persons [13–15]. Then in 1957–1958, a A/H2N2 virus appeared causing the "Asian flu" and circulated until 1968–1969 when a A/H3N2 virus emerged and led to the "Hong Kong" flu [16]. More recently, the emergence of the A/H1N1pdm virus in April 2009, which spread rapidly around the world, caused the first pandemic of the XXIst century [17].

Several works have focused on modeling the spread of the disease in the populations and the effect of public health measures [18–25]. These models are based on strong hypotheses concerning influenza natural history parameters, its transmission and the efficacy of the measures to control its spread. One hypothesis is that infectiousness (cf. definition in part 2.2.2) which is a key-parameter is proportional to the viral shedding [18, 26, 27]. Mechanistic models were developed to represent the evolution of viral shedding in time (also called viral kinetics) [28–32], however all of these models used only viral kinetics data. Moreover, influenza shows great variability in terms of virus shedding as well as in clinical expression. The between subject variability of influenza remains poorly explored but could provide meaningful insights to the study of influenza disease and epidemiology. By using other sources of information, the evolution of the symptoms or a more accurate description of the immune response could be provided.

This work began in this context and was aimed at providing an accurate description of influenza infection and illness dynamics. In the first part, we expose briefly the dynamics of influenza infection and illness as well as the underlying biological mechanisms. We then explain how the within-host dynamics of influenza virus plays a role in the disease transmission and how it is linked to its epidemiology (or between-host dynamics). We also study the origin and consequences of influenza infection variability. We then present the different models used to study infectious diseases and the "population approach" aimed at describing and analyzing different levels of variability. The core work of this project is then presented. It consist of a within host model describing the viral kinetics as well as the dynamics of systemic symptoms. We used the "population approach" to study the between subject variability. We also deduced several epidemiological parameters from the viral kinetics and symptoms dynamics curves.

We then present the designs used to study influenza dynamics and an approach used

to optimize them. We present the second article in which we propose a series of designs to study influenza dynamics in several situations. Indeed, due to the quick evolution of the infection, appropriately choosing the sampling times is crucial to obtain informative data. We used a model-based approach to derive well-balanced designs for studying viral kinetics, innate immune response dynamic and/or systemic symptoms dynamics.

We continue by describing the different possible measures to mitigate influenza infection and how their efficacy relies on the disease dynamics. We present a simulation study comparing the effect of different oseltamivir regimen in immunocompromised and otherwise healthy subjects. For this purpose, we simulated the pharmacokinetics of oseltamivir and the viral kinetics and symptoms dynamics in 1000 subjects. We used a stochastic process to take into account the emergence of resistant virus. We assessed the virological and clinical efficacy as well as the proportion of subjects shedding resistant virus.

This work stresses that influenza infection is a complex process which needs appropriate statistical and methodological tools for its study. We also show that the great variability observed must be taken into consideration when planning the strategies for influenza mitigation as the success of disease control depends on the timing of the onset of infectiousness relative to the onset of detectable clinical signs.

2 Timeline of influenza infection and epidemiologic considerations

2.1 Dynamics of influenza infection

The dynamics of influenza infection reflects the effects of the virus on the host and conversely the effects of the host's reaction on the virus population. The replication cycle describes the interaction between influenza virus and the host at the molecular and cellular level and can be depicted by viral kinetics data. The short-term as well as the long-term immune response will be associated with the host's susceptibility. The dynamics of influenza infection can be modified by the use of antivirals or vaccine. Here we present the dynamics of influenza in the case of an otherwise healthy subject who would neither be immune nor have received treatment.

2.1.1 Host – virus interactions

The influenza virus replication cycle is a complex phenomenon resulting from the interactions between the virus and the host cells (cf. Figure 2.1). First, the virus binds to receptors on the surface of the host cell with the HA and is internalized into endosomes. M2 ion channel proteins allow for the acidification of the endosome which triggers the fusion and the uncoating. The viral genome is released in the form of viral ribonucleoproteins (vRNPs) into the cytoplasm. The vRNPs are then imported into the nucleus

for replication. The positive-sense viral messenger RNAs (mRNAs) are exported out of the nucleus into the cytoplasm for protein synthesis. Some of the proteins are imported into the nucleus to assist in viral RNA replication and are assembled with the negative-sense RNA to form new vRNPs, which also occur in the nucleus. Later in the infection, vRNPs form and leave the nucleus, and progeny viruses assemble and bud from the plasma membrane [33].

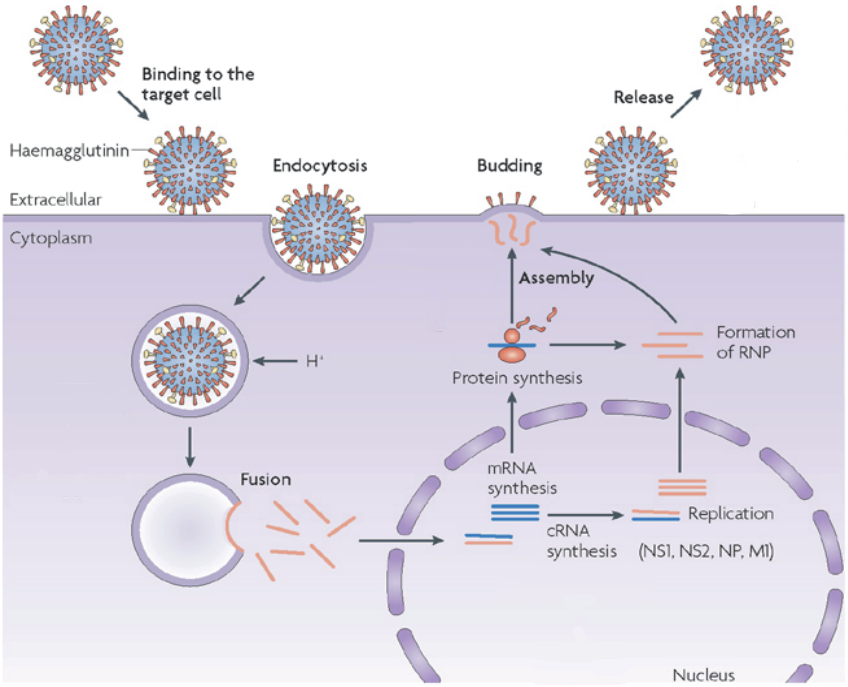

Figure 2.1: Influenza virus replication cycle (from [34])

Previous works depicted influenza viral kinetics as follows: The standard influenza virus kinetic pattern includes rapid exponential growth, peak viral load occurring 2 to 3 days after infection, and a decline toward virus undetectability over the following 3 days [28, 35, 36] (cf. Figure 2.2).

2.1.2 Immune response to influenza infection

Immunity finds its etymology in the latin word *immunis* meaning "to make safe". The medical meaning is related to the ability of an organism to defend itself against a disease [37]. The immune response follows a timeline during which the innate immune response which is unspecific is first activated before the adaptive immune response which is antigen-specific.

2.1.2.1 Innate immune response

During the first days of infection, the innate immune response, mediated by pro-inflammatory cytokines, chemokines, sentinelle cells and natural killer (NK) cells, provides nonspecific defenses pending activation of adaptive responses [38]. It does not require a preliminary immunization. A recent study showed that after influenza infection the host antiviral program is activated 36 hours before symptoms onset [39]. Its different actors have several effects such as a strictly speaking antiviral action, a mutual potentialization and the induction of the adaptive immunity (cf. Figure 2.2).

Among the principal cytokines, interferons (IFN) α and β are produced by the infected cells and the dendritic cells. They induce the production of antiviral proteins which block the transcription of the viral mRNA in viral proteins. They also stimulate the NK cells. IFN γ activates the macrophages and also acts as an antiviral. The tumor necrosis factor α (TNF-α) activates the neutrophile cells. Interleukine-2 (IL-2) induces the proliferation of the T lymphocytes and stimulates the NK cells. Interleukine-6 (IL-6) stimulates the B and T cells. Interleukine-12 stimulates the NK cells. The chemokines recruit monocytes and B and T lymphocytes. The sentinelle cells, namely dendritic cells and macrophages, produce several cytokines, induce the internalization and the processing of viral antigens, and migrate to the lymph nodes to inform the T and B lymphocytes. Finally, NK cells recognize the infected cells and cause their lysis and shed several cytokines.

2.1.2.2 Adaptive immune response

The adaptive immune system comes into play a few days later and eventually clears the virus [31, 40]. It also confers a long-time protection to the host.

The effector cells are mainly the B and T CD8+ and T CD4+ lymphocytes. The main role of the B lymphocyte is to produce antibodies whereas the T CD8+ lymphocytes, also called cytotoxic T lymphocyte (CTL) induce the lysis of the infected cells. Each lymphocyte targets a specific antigen thanks to specific receptor. The T CD4+ lymphocytes, once informed by the dendritic cells, promote the evolution of B lymphocytes in circulating plasmocytes producing antibodies and activate the CTLs.

It takes several days for the adaptive immunity to take place. However, in case of reinfection by a similar virus, the adaptive immune response can be rapidly deployed thanks to the memory B or T lymphocytes which have a long life span and are specific to the immuno-inducing antigen [41].

2.1.3 Clinical expression of influenza infection

Influenza-like illness is an association of systemic and respiratory symptoms. In several trials the case-definition used was a temperature over 37.8°C with cough or sore throat [42–44]. Cytokines have a protective role, but their levels also correlate with systemic symptom dynamics. In particular, IL-6 and IFN-α levels in nasal washing fluid are causally linked to viral titers, body temperature, mucus production, and symptom scores [45].

Influenza virus replication takes place in the epithelial cells of the upper respiratory tract and major central airways. The infection leads to the desquamation of the epithelium of the nasal mucosa, the larynx and the tracheobronchial tree. The resulting loss of respiratory epithelial cells is one major reason for several of the symptoms that accompany infection such as cough, depressed tracheobronchial clearance, and altered pulmonary function [46, 47].

A review from experimentally challenged volunteers showed that the average total symptoms score increased one day after the inoculation and that the total symptom score peaked by day 2 or 3 after inoculation to return to baseline at day 8 after inoculation. Systemic symptoms (fever, muscle aches, fatigue, headache) peaked earlier, by day 2 after inoculation, and resolved faster than respiratory or nasal symptoms [35] (cf. Figure 2.2).

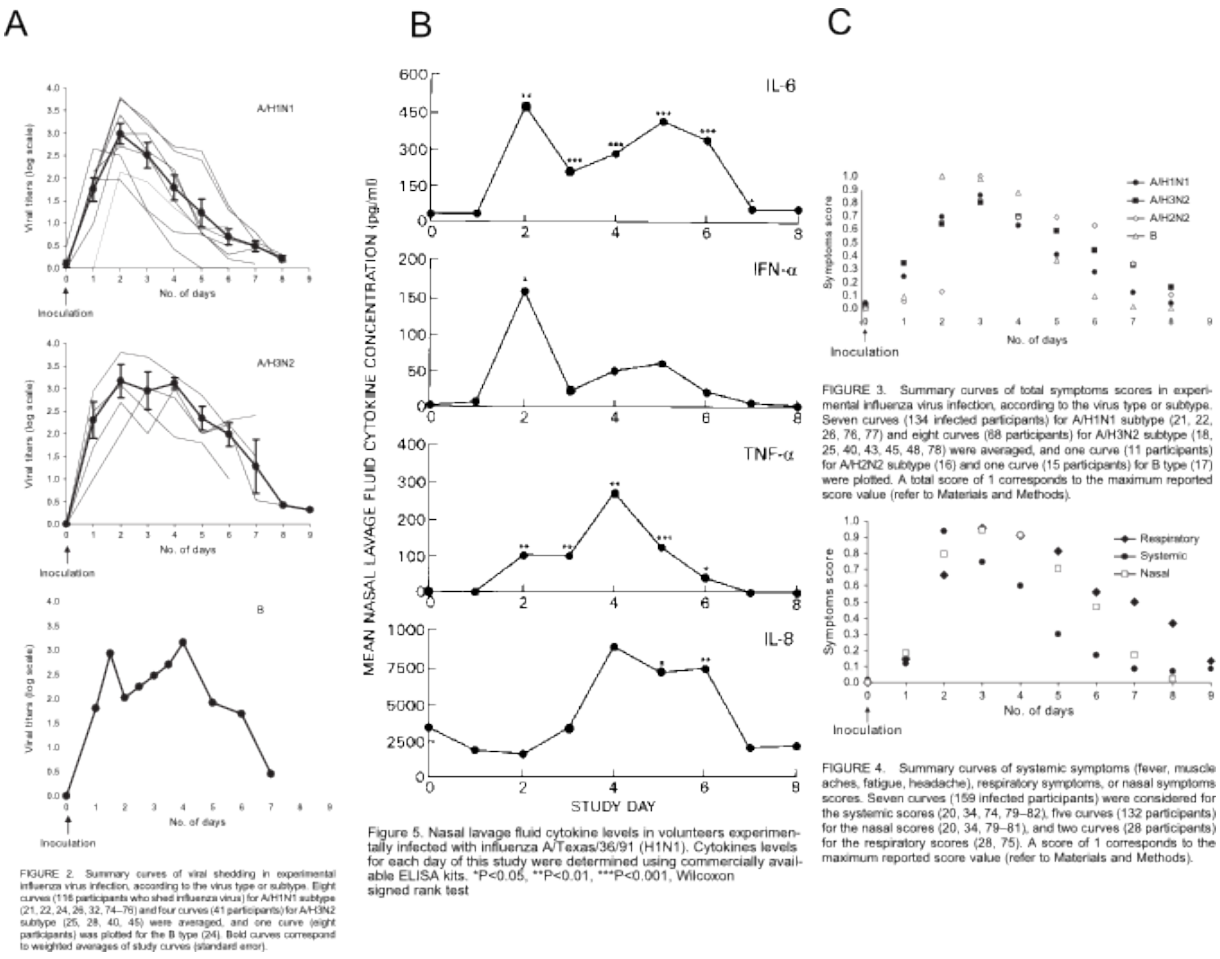

FIGURE 2. Summary curves of viral shedding in experimental influenza virus infection, according to the virus type or subtype. Eight curves (116 participants who shed influenza virus) for A/H1N1 subtype (21, 22, 24, 26, 32, 74–76) and four curves (41 participants) for A/H3N2 subtype (25, 28, 40, 45) were averaged, and one curve (eight participants) was plotted for the B type (24). Bold curves correspond to weighted averages of study curves (standard error).

Figure 5. Nasal lavage fluid cytokine levels in volunteers experimentally infected with influenza A/Texas/36/91 (H1N1). Cytokines levels for each day of this study were determined using commercially available ELISA kits. *P<0.05, **P<0.01, ***P<0.001, Wilcoxon signed rank test

FIGURE 3. Summary curves of total symptoms scores in experimental influenza virus infection, according to the virus type or subtype. Seven curves (134 infected participants) for A/H1N1 subtype (21, 22, 26, 76, 77) and eight curves (68 participants) for A/H3N2 subtype (18, 25, 40, 43, 45, 48, 78) were averaged, and one curve (11 participants) for A/H2N2 subtype (16) and one curve (15 participants) for B type (17) were plotted. A total score of 1 corresponds to the maximum reported score value (refer to Materials and Methods).

FIGURE 4. Summary curves of systemic symptoms (fever, muscle aches, fatigue, headache), respiratory symptoms, or nasal symptoms scores. Seven curves (159 infected participants) were considered for the systemic scores (20, 34, 74, 79–82), five curves (132 participants) for the nasal scores (20, 34, 79–81), and two curves (28 participants) for the respiratory scores (28, 75). A score of 1 corresponds to the maximum reported score value (refer to Materials and Methods).

Figure 2.2: Dynamics of influenza infection: A) Viral kinetics of influenza A/H1N1 virus in the upper panel, A/H3N2 virus in the middle panel and B virus in the lower panel, B) Cytokines dynamics with the IL-6 in the upper panel, $IFN-\alpha$ in the second panel, $TNF-\alpha$ in the third panel and IL-8 in the lower panel, C) Symptoms dynamics: total symptoms score for A/H1N1, A/H3N2, A/H2N2 and B virus in the upper panel and systemic symptoms, respiratory symptoms and nasal symptoms score in the lower panel (from [35, 45])

2.2 From within host dynamics to between host dynamics

2.2.1 Influenza transmission

Influenza is considered an airborne disease, though its transmission remains not fully understood. Droplets are produced during sneezing, coughing and exhalation and may contain different amounts of virus [48, 49]. Droplets small enough evaporate, leaving microscopic particles or aerosols that can remain suspended in the air [50]. Bigger particles will tend to sedimentate and cover the surrounding surfaces. They can then be transferred by hand contact which would represent another transmission route [51–53]. The role played by each of these routes remains under discussion [54].

Therefore the transmission of influenza from an infected subject i to a susceptible subject j at time t will depend on [55]:

- **The quantity of infected particles produced by the subject** i. This quantity will vary in time according to the quantity of virus shed in the upper respiratory tract and to the frequency and intensity of cough and sneeze. The characteristics of the environment (humidity, ventilation, ...) can impact the dynamics of the infected particles.
- **The susceptibility of the subject** j which can be modified by vaccination, previous exposition to influenza virus or by the use of antivirals as prophylaxis.
- **The contact rate between the subjects** i **and** j.

Whereas the second and third aspects have been widely studied, the studies on the effect of viral kinetics / symptoms dynamics on influenza transmission remain scarce. The parameters of interest quantifying the duration and intensity of exposition (for instance the viral particles concentration, the distance between subjects, the exposition duration) were not described in human beings and remain scarce in animals [56, 57].

2.2.2 Definition of epidemiological parameters

The **infectivity** refers to the efficiency of infection for a particular viral strain. It is an intrinsic characteristic of the virus. The **infectiousness** of a subject i at the time t and at the place P is the probability for the virus that he shed to reach a susceptible subject who would be in contact with him at this place and at this time [55].
Consequently, under the hypothesis of homogeneous mixing, the **duration of infectiousness** is defined as the average period during which a subject is capable of transmitting the virus and the **latent period** as the period during which a subject is infected but not yet infectious. The **incubation period** is defined as the average time from infection to apparition of disease symptoms [58].

Under the hypothesis that viral titer is a surrogate of infectiousness [18, 26, 27] and for a given infectiousness threshold, latent period, infectiousness and its duration can be easily derived from the viral kinetics (VK), as shown in Figure 2.3. The incubation period can be derived from the symptom dynamics (SD) curve. Infectiousness is then computed as the area under the VK curve. However, this definition remains theoretical as a subject shedding virus but without contact would not infect anybody. The efficient infectiousness depends on the theoretical infectiousness and the contact rate. For the latent period and the duration of infectiousness, it is necessary to choose a threshold above which subjects will be considered as infectious. The latent period would hence be the time from inoculation to VK curve exceeding this threshold whereas the duration of infectiousness would be the period during which the VK curve is above this threshold. These two parameters have to be considered with caution as they depend on an arbitrarely chosen threshold to represent the transition to infectiousness which is in fact a continuous process as shown in the Figure 2.3.

The **generation time,** T_g**,** is an epidemiological parameter representing the mean interval between infection of a primary case and his/her secondary cases and indicating the speed at which an epidemic spreads [59]. The shorter the generation time is, the faster

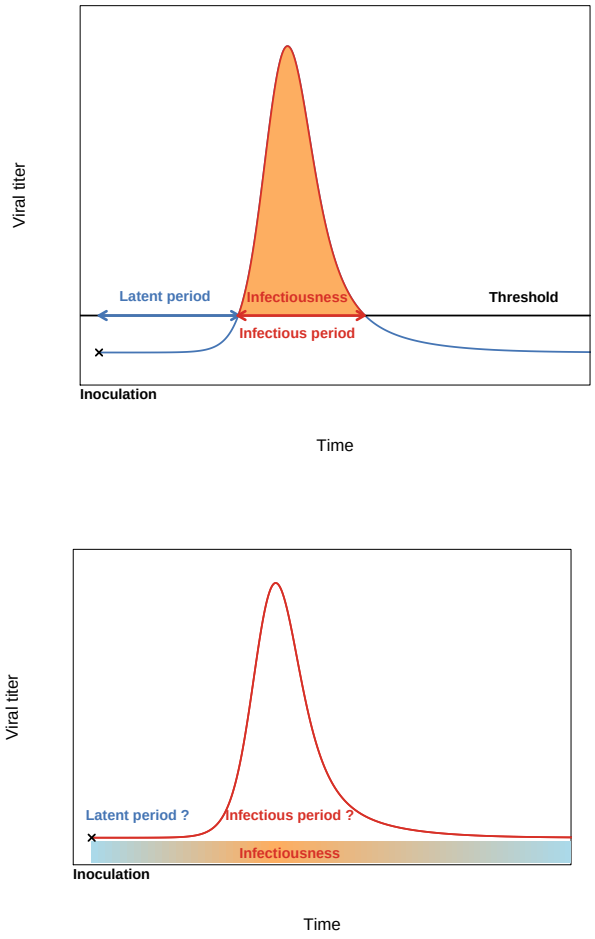

Figure 2.3: Definition of the epidemiological parameters from the VK curve: The upper panel shows how the parameters are computed from the VK curve. The lower panel shows a more realistic representation of influenza infection timeline with a continuous transition from non-infectious (blue) to infectious (orange) states.

the epidemic spreads. Generation time distribution was shown to be quantitatively similar to viral shedding curves from experimental infection studies in human volunteers [18].

Assume that contacts between individuals occur according to a homogeneous Poisson process, and that the probability of infection when a contact occurs is proportional to the current viral excretion level. In this description, secondary infections caused by a case occur according to a time in homogeneous Poisson process with intensity $\omega V(t)$, where ω is a positive random number and $V(t)$ is the viral load at time t after infection. We assume that V and ω are independent. The density function of the generation time is

obtained as the normalized average viral excretion profile:

$$f(t) = \frac{V(t)}{\int_0^{+\infty} V(x).dx} \tag{2.1}$$

And the average generation time T_g is $T_g = \int_0^{+\infty} t \times f(t).dt$ [35].

Of course, if the process of contacts is not homogeneous or depends on viral load, this formula does not hold and it is necessary to differentiate a theoric generation time from an efficient generation time. The first one depends only on the infectiousness whereas the second one takes into account the contact rate. If the contact rate decreases in time (due to mitigating measures for instance), then the efficient generation time will be shorter than the theoretical generation time.

3 Variability of influenza infection and illness

3.1 Sources of variability

Exposure to an infectious agent does not always result in infection. Whether or not an infection develops depends on innate immunity, alone or together with adaptive immunity. Biological and/or clinical expression might be detectable after infection is established and immunity is involved. The process that goes from exposure to an infectious agent to the development of a clinical disease is subject to host and environmental variability. Host factors might be genetic or not, and might act at the level of exposure to or infection with the pathogen. Environmental factors might be microbial or related to the mode of exposure, and might have an impact at each stage of the interaction (cf. Figure 3.1).

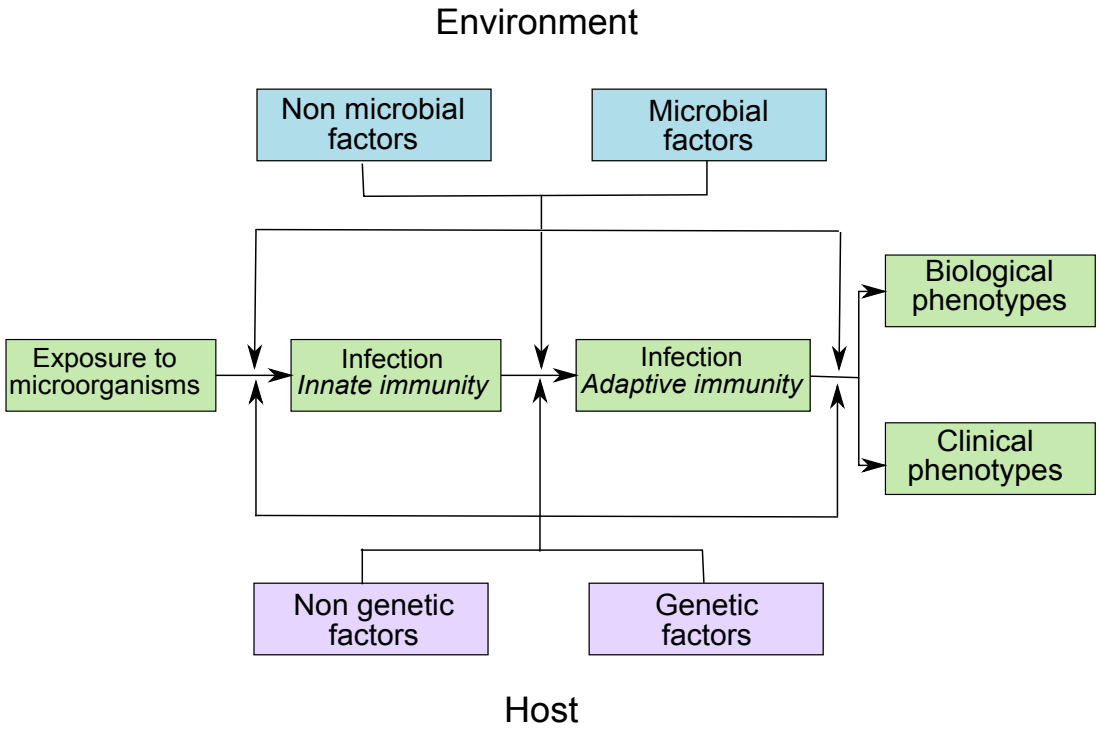

Figure 3.1: A schematic showing the stages of the host–environment interaction in the course of infection [60].

3.1.1 Environmental variability

Several factors from the environement could explain a part of the observed variability. The virus infectivity may be modified by the changes in the environment characteristics. For instance, the stability of the virus in the aerosol is associated with the level of humidity [61]. Cold temperatures are also associated with influenza virus increased infectivity as breathing cold air would slow mucociliary clearance and thereby encourage viral spread within the respiratory tract [62].

Also vitamin D, which is activated by the UVB rays from the sun [63] triggers the innate immune response [64,65]. It has been hypothesized that its variations due to the duration of daylight could be one of the factors explaining influenza seasonality in temperate regions [66–68], though it remains controversial [69].

3.1.2 Virus variability

Influenza virus is continuously evolving. The mechanisms of influenza virus evolution include mutation and genome reassortment. Mutations are random events that generate genetic variations. By changing the properties of the virus it allows it to persist in the host population despite selective pressures such as the immunity to strains from previous years or antiviral use [70, 71].

It is important to note that influenza virus as other RNA viruses has a high mutation rate and rapid replication cycles which lead to its rapid evolution. For the purpose of comparison, RNA virus mutation rate varies between 10^{-3} and 10^{-5} per base per generation [72] whereas human genomic mutation rate was estimated to $\approx 2.5 \times 10^{-8}$ per base per generation [73]. Influenza viruses are hence "moving targets" as they can quickly develop resistance to antiviral drugs and escape the immune response.

One of the consequences of this dynamic evolution is the existence of quasispecies which are collections of similar variants generated by mutations and with related sequences. The cloud of variants can hence quickly react to selective pressure by selecting the best adapted candidate genome [74]. The mutations conferring beneficial functional alteration are more likely to be preserved.

However, even though mutations often directly cause a beneficial functional alteration (such as antigenic shift or drug resistance), they can be deleterious to protein-level properties such as folding, stability or expression. Secondary mutation can reinforce the protein-level properties damaged by the functional mutation, but by itself may confer no major adaptive benefit.

For instance, the $His^{274} \rightarrow Tyr^{274}$ (H274Y) mutation confers influenza virus oseltamivir resistance [75, 76] but also compromises viral fitness [77]. H274Y also induces a protein-level defect that decreases the amount of neuraminidase expressed on the cell surface and hence reduces the infectivity of the virus [78]. Secondary "permissive" mutations can occur that restores the virus fitness [79]. Both mutations are needed to yield a protein

that possesses the beneficial functional alteration and the requisite protein-level properties [80].

Another consequence of the virus evolution is that the antibodies produced during a previous infection or after vaccination are not always efficient against the new variant in which case the subject will be susceptible to infection [5].

3.1.3 Host biology variability

The host susceptibility and clinical expression is highly variable between subjects. Both the innate and adaptive immune response can be variable and can explain partly the observed variability. The variability of the immune response could result from a polymorphism of the genes which might be regulated in an age-dependant manner and from the history of previous infections which might enhance the adaptive response to influenza.

3.1.3.1 Host genetic effect on susceptibility

Host genetic effect on susceptibility to influenza was increasingly studied in recent years [81,82]. Hints came from a review of epidemiological patterns of A/H5N1 cases in humans which noted apparent familial clustering of cases, a relative lack of nonfamilial clusters, cases separated by time and place among related individuals, and relatively few cases in some highly exposed groups [83] and from an investigation of the influenza death records over the past 100 years in the population of Utah which provided evidence for an increased risk in close and distant related relatives [84]. However the analysis of influenza related deaths in the population of Iceland during the Spanish flu pandemic did not find any conclusive evidence for a genetic contribution [85].

In a recent study, the transcriptional responses of human hosts towards influenza viral pathogens was studied. It revealed an over-stimulation of multiple viral sensing pathways in symptomatic hosts and that their temporal trajectory was associated with development

of diverse clinical signs and symptoms [39] suggesting that:

- viral sensing and inflammation correlate to clinical symptoms dynamic in symptomatic subjects
- asymptomatic subjects have a rapid innate immune response quickly clearing the virus from the organism
- anti-oxydant response may be an antiviral mechanism by which aberrant immune response are avoided in asymptomatic subjects

3.1.3.2 Antibodies with cross reactivity

Antibodies with cross reactivity allow a subject to be protected against a subtype strain when he/she was previously exposed to another strain of this subtype. Hence older subjects, as they have a longer infectious history, tend to have a lower risk for influenza infection [86]. This is particularly obvious for the A/H1N1 and B viruses for which the genetic evolution is slower than for the A/H3N2 viruses [87].

3.1.3.3 Immunosenescence

Immunosenescence is the decline of the immune function due to aging. While the ability to recall antigens might be conserved, the ability to initiate a primary immune response against novel antigens decreases. Both the innate and adaptive immunity are modified [88]:

- the production of pro-inflammatory cytokines increases,
- the NK cells number increases while their function decreases,
- the number of CD4, CD8, B lymphocytes, macrophages and the antibody decrease.

3.2 Consequences

Influenza infection can present variability both within subjects and between subjects. The within subject variability results from the evolution of immune response during the lifetime and from the evolution of the virus. One of the consequences is that children are more susceptible and more infectious than adults [23, 36, 89]. Hence they play a specific role in the transmission of the disease in the population and can be the target for mitigating interventions. Another consequence is the increased risk of death for the elderly due to immunosenescence.

Second, the between host variability due to genetic background of the subjects as shown previously is associated with the speed and "quality" of the innate immune response [39]. Therefore asymptomatic subjects resolve rapidly the infection and are less infectious. Finally, the between host variability of the clinical expression leads to the undetection of infected subjects as they do not match the case-definition.

4 How to model infectious diseases dynamics

We will limit the presentation here to the mechanistic models which are based on the knowledge about the interaction between the virus and its host as presented in 2.1.1. It is noteworthy that the parameters of these models have a biological meaning.

4.1 The first models

The first models describing viral kinetics were developed for HIV infection. If the virus is produced by infected cells at the rate P and the virus is cleared at the rate c, then the equation corresponding to the evolution of the viral titer V in time t is:

$$dV/dt = P - cV \tag{4.1}$$

If the virus production is blocked then $P = 0$ and $V(t) = V_0 e^{-ct}$, where $t = 0$ is the treatment initiation time and $V(0) = V_0$. The minimal viral clearance, c, can hence be estimated. If we assume that at the treatment initiation the viral kinetics is at a steady state, then $P = cV_0$ and the virus production rate P can be determined. The virus half-life, $T_{1/2}$, is the time necessary for the viral titer to be divide by 2. It can be deduced as $T_{1/2} = ln(2)/c$ [90].

The model was then refined by taking into account the dynamical interaction between the virus and the target cells T. A set of ordinary differential equations was used. In the absence of infection, the target cells are produced at the rate λ and die at the rate d. The infection was modeled as follows: the target cells are infected by the virus. Infected cells I produce virus at the rate p and die at the rate δ. The measured response is the viral titer, V. We will call it the "classic model" thereafter.

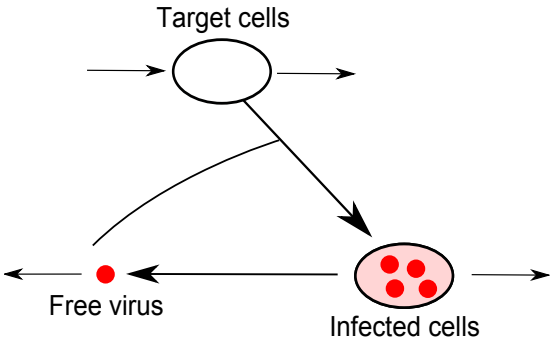

$$\begin{cases} dT/dt &= \lambda - kVT - dT \\ dI/dt &= kVT - \delta I \\ dV/dt &= pI - cV \end{cases} \tag{4.2}$$

Several biological entities can be deduced such as the average life-times of uninfected cells and infected cells which are given by $1/d$ and $1/\delta$ respectively. The average number of virus particles produced over the lifetime of a single infected cells is p/δ [91].
Similar models were also used to study HBV, HCV and cytomegalovirus infection dynamics [92, 93]. This model can then be adapted to various situations. Here we present the models developed for treatment effect and for drug resistance.

Drug resistance raises several issues. Were resistant viruses present in the drug-naive quasispecy or did they emerge during the treatment [94]? If so, what is the probability of obtaining a mutant during the treatment? What role does treatment selective pressure play? How should decreased viral fitness be taken into account?

If resistant virus is present before the treatment begins, the following model can depict the dynamic of both sensitive and resistant virus in the absence of treatment [95]:

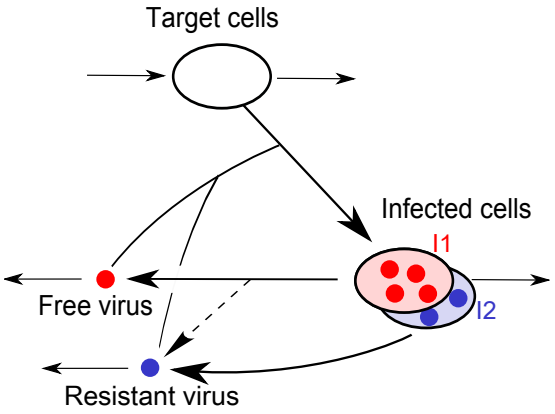

$$\begin{cases} dT/dt &= \lambda - k_1 V_1 T - k_2 V_2 T - dT \\ dI_1/dt &= (1-\mu) k_1 V_1 T + \mu k_2 V_2 T - \delta I_1 \\ dI_2/dt &= \mu k_1 V_1 T + (1-\mu) k_2 V_2 T - \delta I_2 \\ dV_1/dt &= p_1 I_1 - c V_1 \\ dV_2/dt &= p_2 I_2 - c V_2 \end{cases} \tag{4.3}$$

where I_1, I_2, V_1, and V_2,are respectively cells infected by sensitive virus, cells infected by mutant virus, free sensitive virus, and free mutant virus. μ represents the mutation rate.

In case of rare events the deterministic approach used so far might not be realistic. A strain created by mutation can be lost due to stochastic effect as its frequency is very small. In this case, each event (production of uninfected cells, infection of target cells, death of target cells, death of infected cell...) is assigned a probability which is related to the deterministic rates. Hence the stochastic expression of the equation of the classic model 4.2 is represented in table 4.1 [96].

Table 4.1: Structure of the stochastic process

Event	Population at t	$\rightarrow$	Population at $t + \Delta t$	Probability
Production of uninfected cell	T	$\rightarrow$	T+1	$\lambda \Delta t$
Death of uninfected cell	T	$\rightarrow$	T-1	$dT\Delta t$
Production of infected cell	$\left\{ \begin{array}{c} \text{I} \\ \text{T} \end{array} \right\}$	$\rightarrow$	$\left\{ \begin{array}{c} \text{I+1} \\ \text{T-1} \end{array} \right\}$	$kTV\Delta t$
Death of infected cell	I	$\rightarrow$	I-1	$\delta I \Delta t$
Production of free virus	V	$\rightarrow$	V+1	$pI\Delta t$
Clearance of free virus	V	$\rightarrow$	V-1	$cV\Delta t$

4.2 Models for influenza dynamics

More recently, models have been developed for *in vivo* influenza infection [28–32, 97, 98].

Target cell-limited model

The classic model was modified to accurately represent the dynamics of influenza infection. First, considering the short duration of influenza, target cells' production and death were ignored. Second, a latent phase in the infected cells dynamic was included assuming that infected cells do not die before they begin to produce viruses [99]. The model in which influenza virus infection is limited by the availability of susceptible target cells is hence written [28]:

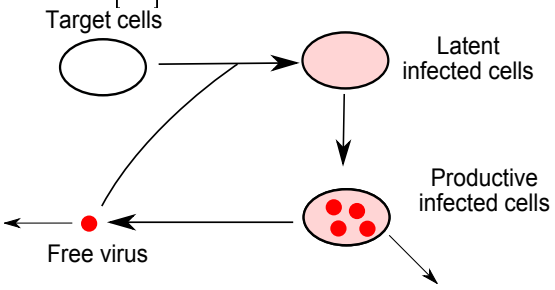

$$\begin{cases} dT/dt &= -\beta TV \\ dI_1/dt &= \beta TV - kI_1 \\ dI_2/dt &= kI_2 - \delta I_2 \\ dV/dt &= pI_2 - cV \end{cases} \tag{4.4}$$

where T is the target cells, I_1 the latent infected cells, I_2 the virus-producing cells and V the free virus, β is the rate at which target cells are infected by free virus, k the rate at which latent cells move into the virus-producing state, δ the mortality rate of virus-producing cells, p the virus production rate and c the virus clearance. However, it is more realistic to consider that the innate immune response controls the viral growth and that the adaptive immune response helps to eliminate the virus.

Innate immune control

Only the dynamics of pro-inflammatory cytokines such as IFN have been modeled for influenza. The first model proposed for the innate immune response was an extension of the previous one describing the IFN kinetics as

$$dF/dt = sI_2(t-\tau) - \alpha F \tag{4.5}$$

where F is the IFN level, s is the rate at which IFN is secreted by virus-producing cells, τ is the lag-time necessary for the virus-producing cells to secrete IFN and α is the

IFN clearance rate [28]. The effect of interferon was modeled as a decrease of the virus production rate, p, and/or as a decrease of the rate at which latent cells move into the virus-producing state, k.

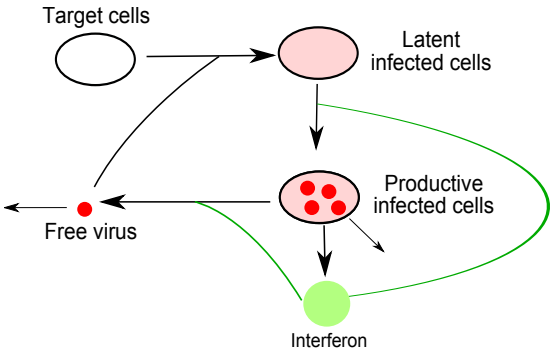

$$\begin{cases} p = \dfrac{\hat{p}}{1+\varepsilon_1 F} \\ k = \dfrac{\hat{k}}{1+\varepsilon_2 F} \end{cases} \tag{4.6}$$

where $\hat{p}$ and $\hat{k}$ are the value of these parameters in the absence of IFN and ε_1 and ε_2 represent the IFN efficiencies [28]. Another way to describe IFN effect is to model the production of cells that are refractory to infection [32, 97].

Adaptive immune control

The acquisition of both CTLs and specific antibodies and their role in virus clearing were modeled [29, 100, 101].

However, in all the experiments, subjects were primo-infected. Thus the effect of pre-existing immunity on the infection settlement remains unstudied.

Antiviral treatment

A model similar to the one used for protease inhibitors in HIV infection was used for the neuraminidase inhibitors in the case of influenza [30].

4.3 Conclusion on modeling viral kinetics

The modeling of viral kinetics has increased over the past fifteen years and has provided a better understanding of the mechanisms underlying infection dynamics. It allows to simulate various *scenarii* and to debate the biological relevance of several hypotheses.

The parameters estimates quantify the interactions between the virus, its host and the immune response and allow to measure the effect of interventions such as antiviral treatment. Finally, it can be used to make predictions.

However, there are several limitations. First, identifiability is a problem often raised in viral kinetics modelling [28, 30, 32]. Indeed the models used to describe viral kinetics are complex, nonlinear and depends on unknown parameters [102]. Three possible solutions in case of non-identifiability are 1) simplifying the model, 2) fixing parameters with biologically plausible value and 3) enriching the data with additional sampling sites or measurements [99, 102]. The two first are often used and simplified models were proposed to help identify the parameters [103]. However, as these models focus on viral kinetics, information about the dynamics of the infected cells or about the immune response is lost. Concerning the third option, beside the numerous different responses that could be collected (different types of cytokines levels [45], symptoms score [35], NK cells activity), only viral titer was used in most of the studies fitting models to dynamics data. These observations would bring additional information which would allow more complex models [104].

4.4 How to model the variability

4.4.1 Between-subjects variability

Nonlinear mixed effect models, or "population approach" were first developed to study the pharmacokinetics of drugs [105]. They allow to describe the population characteristics (mean parameters) as well as different levels of variability such as the interindividual variability or the variability observed at different stages of the treatment, namely the interoccasion variability [106].

Let y_i be the vector of the n_i observations of subject i, with i varying from 1 to N. Let f be a function describing the phenomenon to model, depending nonlinearly from θ_i, the

vector of the p parameters of the subject i. Suppose that ξ_i represents the vector of times at which samples are collected from subject i, $\xi_i = (t_{i1}, t_{i2}, ..., t_{in})$. The statistical model for the subject i is then:

$$y_i = f(\theta_i, \xi_i) + \varepsilon_i(\sigma_{inter} + \sigma_{slope} f(\theta_i, \xi_i))$$

where ε_i is the vector of the residual errors which is the part of the observations unexplained by the model f. We will suppose that these errors are independant from one observation to another and that their distribution is gaussian $\varepsilon_i \sim \mathcal{N}(0, I_{n_i})$, where I_{n_i} is an identity matrix of dimensions (n_i, n_i). σ_{inter} and σ_{slope} are two parameters characterizing the error model variance.

In nonlinear mixed effect models, the model f is common to all the subjects, but the vector of parameters θ_i for the subject i may vary from one subject to another. The interindividual variability is modeled with the vector of random effect parameters b_i. The vector of parameter θ_i for the subject i can then be expressed as a "second level" model which links with the function g the vector of fixed effect parameters β common for all subject and the vector of random effects b_i specific for the subject i: $\theta_i = g(\beta, b_i)$. The vector of random effect is supposed to follow a gaussian distribution $b_i \sim \mathcal{N}(0, \Omega)$, b_i and ε_i are supposed to be independant for the subject i and $b_i|\varepsilon_i$ is supposed independant from one subject to another. Ω is the matrix of random effect variance. Most of the time, the function g is an additive or exponential model. The vector of parameters is hence written $\theta_i = \beta + b_i$ or $\theta_i = \beta^{b_i}$ respectively.

4.4.2 Covariate modeling

The inter-individual variability can either be related to natural variations, or caused by differences in covariate values between and/or within subjects [107]. As the number of extra parameters to be estimated tends to grow considerably with the inclusion of covariates and their associated random effects in the model, the decision on whether or not to include a covariate has to be carefully considered.

4.4.3 Estimation approaches

The estimation approach the most frequently used for influenza viral kinetics was a "two-stage approach". In the first step, each individual's data were separately fitted using nonlinear least squares. In the second step, the geometric mean of the individual parameters is computed and represents the average population parameter. However, this approach leads to an overestimation of the variability as the parameter uncertainty is ignored in the second step [108], thus an appropriate method is required to model the different levels of variability.

For nonlinear mixed effect models, several methods are available. The objective is to maximize the likelihood. However, with such models the integral of likelihood function cannot be explicitly solved.

- **Estimation method based on model approximation**

  A first-order linearization of the regression function with respect to the random effects, as the first-order method and first-order conditional estimation methods implemented in NONMEM and in the nlme function in Splus and R, allows to obtain an analytical expression of the likelihood [109,110]. Laplace or Gaussian quadrature approximation can also be used [111]. These two algorithms are implemented in SAS procedure NLMIXED.

  However, several limitations are noteworthy: 1) these methods needs very long computation times, 2) convergence problems occur frequently and 3) the number of parameters that can be estimated is limited [112].

- **Bayesian inference**

  Here, a prior distribution of the parameters is included in the mixed model and the objective is to assess the posterior distribution which is proportional to the likelihood. Markov Chain Monte Carlo (MCMC) methods is a class of algorithms for generating samples that mimic a target distribution. In bayesian statistics, the

Gibbs sampling and the Metropolis-Hastings algorithm are the most frequently used. It was developped to approximate the posterior distribution and is implemented in the BUGS softwares [113].

- **Expectation-Maximization (EM) based methods**

  This iterative method allows an exact maximization of the model likelihood. Each iteration is performed in two steps: expectation (E) step, which computes the expectation of the log-likelihood evaluated using the current estimate for the parameters, and a maximization (M) step, which computes parameters maximizing the expected log-likelihood found on the E step [114]. A variant algorithm called Stochastic Approximation EM was developped [115,116] and implemented in MONOLIX software.

4.5 Population modeling of influenza A/H1N1 viral kinetics and symptom dynamics

As shown in the part 2.1, the dynamics of influenza infection is a complex phenomenon during which the virus interact with the host. The innate immune response leading to the clearance of the virus is also responsible for the systemic symptoms. The objective of this first work was to provide a model which would causally link the viral kinetics to the systemic symptoms dynamic through the dynamic of the innate immune response.

Only one influenza viral kinetics model was previously fitted to human data, with a relatively small number of subjects [28] and a two-stage approach was used. The parameters were estimated with a two-stage approach which as we showed in part 4.3.2 leads to an underestimation of the between subject variability.

We used data from fives studies in which 56 healthy volunteers under placebo were experimentally challenged with a A/H1N1 virus. The participants were carefully monitored with one viral sample and two symptoms measures each day collected. It was the first time that such a rich dataset was analyzed. Even though the volunteers were comparable on a

physiological and demographical point of view, the viral kinetics and systemic symptoms dynamics patterns showed a high variability. Indeed, 12 participants did not shed virus and from the 44 remaining 19 did not exhibit any systemic symptom.

Considering the number of subjects from the dataset and the observed variability, we used the population approach which allowed us to give a first description of the between subject variability. Moreover this rich dataset allowed us to refine the innate immune response model in which we included the dynamics of the NK cells.

The parameters estimates were coherent with previous findings [28–32, 97, 98]. Moreover, the predicted cytokines response with a sharp increase and a peak occuring a few hours after the viral titer's was in agreement with what was previously found [45]. Information concerning the NK dynamics remains scarce for influenza infection, however our findings showing a later peak and a slow decrease seems in line with the result from the study of another acute disease, the Epstein-Barr virus infection [117].

We also derived several epidemiological parameters and their between subject variability: the latent period, infectiousness, duration of infectiousness, generation time and incubation. We computed them based on the assumption than infectiousness is proportional to the viral titer. Once again, the results obtained were consistent with previous findings from challenge and epidemiological studies [18, 20, 22, 35].

4.5.1 Article *Published in Journal of Virology*

JOURNAL OF VIROLOGY, Mar. 2011, p. 2764–2770 Vol. 85, No. 6
0022-538X/11/$12.00 doi:10.1128/JVI.01318-10

Population Modeling of Influenza A/H1N1 Virus Kinetics and Symptom Dynamics[▽]

Laetitia Canini[1,2] and Fabrice Carrat[1,2,3]*

UPMC Université Paris 06, UMR-S 707, Paris F-75012, France[1]; Inserm, UMR-S 707, Paris F-75012, France[2]; and Assistance Publique Hôpitaux de Paris, Hôpital Saint Antoine, Paris F-75012, France[3]

Received 21 June 2010/Accepted 21 December 2010

Influenza virus kinetics (VK) is used as a surrogate of infectiousness, while the natural history of influenza is described by symptom dynamics (SD). We used an original virus kinetics/symptom dynamics (VKSD) model to characterize human influenza virus infection and illness, based on a population approach. We combined structural equations and a statistical model to describe intra- and interindividual variability. The structural equations described influenza based on the target epithelial cells, the virus, the innate host response, and systemic symptoms. The model was fitted to individual VK and SD data obtained from 44 volunteers experimentally challenged with influenza A/H1N1 virus. Infection and illness parameters were calculated from best-fitted model estimates. We predicted that the cytokine level and NK cell activity would peak at days 2.2 and 4.2 after inoculation, respectively. Infectiousness, measured as the area under the VK curve above a viral titer threshold, lasted between 7.0 and 1.3 days and was 15 times lower in participants without systemic symptoms than in those with systemic symptoms ($P < 0.001$). The latent period, defined as the time between inoculation and infectiousness, varied from 0.7 to 1.9 days. The incubation period, defined as the time from inoculation to first symptoms, varied from 1.0 to 2.4 days. Our approach extends previous work by including the innate response and providing realistic estimates of infection and illness parameters, taking into account the strong interindividual variability. This approach could help to optimize studies of influenza VK and SD and to predict the effect of antivirals on infectiousness and symptoms.

Viral shedding kinetics and symptom dynamics (SD) are often used to describe the natural course of infections. In influenza virus infection, virus kinetics (VK) is used as a surrogate for infectiousness, and parameters such as the latent period, the duration of infectiousness, and the generation time can be deduced directly from viral shedding data (13). The standard influenza virus kinetic pattern includes rapid exponential growth, peak viral load occurring 2 to 3 days after infection, and a decline toward virus undetectability over the following 3 days (5, 8, 10).

This kinetic pattern results from interactions between the virus, host target cells, and the immune system. During the first days of infection, the innate immune response, mediated by cytokines and natural killer (NK) cells, provides nonspecific defenses pending activation of adaptive responses (16). Cytokines have a protective role, but their levels also correlate with systemic symptom dynamics. In particular, interleukin 6 (IL-6) and alpha interferon (IFN-α) levels in nasal washing fluid are causally linked to viral titers, body temperature, mucus production, and symptom scores (20).

Nonlinear models have previously been used to characterize the kinetics of agents causing chronic infections, such as HIV (29), hepatitis B virus (28), and hepatitis C virus (27), and have proved useful both for explaining sustained replication and for studying the effect of antiviral drugs. Few nonlinear models of influenza have been published (4, 6, 17–19, 21, 24, 26, 31), and only one used actual human data (3). The latter model was fitted to viral shedding data from six experimentally challenged subjects and was based on compartments describing target epithelial cells (infected or uninfected), the virus titer, and the interferon response.

We extended this model and used an original virus kinetics/symptom dynamics (VKSD) "population" approach to estimate infection parameters and to characterize the overall pattern and variability of influenza virus infection and illness. Our approach fits VK and SD simultaneously, using predicted (unobserved) cytokine and NK cell effects.

Data came from the experimental influenza virus infection of healthy volunteers who showed substantial variability in viral shedding and symptoms, with some individuals remaining asymptomatic (32). In the "population" approach, widely employed in pharmacokinetic/pharmacodynamic studies, the data are modeled with structural equations and a statistical model to capture the full intra- and interindividual variability of virus kinetics and symptoms.

MATERIALS AND METHODS

Design. We used data from five randomized, double-blind, placebo-controlled registration studies of zanamivir treatment of H1N1 influenza virus (NAIA1001, NAIA1002, NAIA1003, NAIA1004, and NAIA1010). The studies were conducted between 1993 and 1997 and involved experimentally challenged volunteers. All were approved by ethics committees, and the volunteers gave their written informed consent.

Volunteers were eligible for these studies if they were Caucasian men or women aged from 18 to 40 years, with serum hemagglutinin antibody titers of ≤1:8 to the relevant virus strains. They were nonsmokers or smoked an average of less than 10 cigarettes per day and agreed not to smoke for the duration of the isolation period. They had normal pulmonary function, were within ±30% of their ideal weight for height, were using effective contraception (women), and were judged to be healthy based on medical history taking, physical examination,

* Corresponding author. Mailing address: Epidémiologie, Systèmes d'Information, Modélisation, UMR-S 707, Faculté de Médecine Saint Antoine, 27 Rue Chaligny, 75571 Paris, Cedex 12, France. Phone: 33 1 44 73 84 51. Fax: 33 1 44 73 84 53. E-mail: carrat@u707.jussieu.fr.

▽ Published ahead of print on 29 December 2010.

routine laboratory investigations, screening electrocardiograms (ECGs), and the absence of lymphadenopathy.

The volunteers were challenged with 10^5 median (50%) tissue culture infective doses ($TCID_{50}$) of influenza A/Texas/91 (H1N1) virus intranasally and were monitored daily for the following 7 or 8 days. A sample for viral shedding kinetics analysis was taken from each volunteer 8 or 9 times. In four studies (48 subjects), sample collection took place on day 0 (D0) before the challenge, and then on D1, D2, D3, D4, D5, D6, D7, and D8; no D8 sample was collected in the fifth study (8 subjects). The following symptoms were noted: earache, runny nose, sore throat, coughing, sneezing, breathing difficulties, muscle ache, fatigue, headache, a feverish feeling, hoarseness, and chest discomfort. The intensity of each symptom was scored by the patient from 0 (none) to 3 (severe). The symptom data were collected twice a day, at 0800 and 2000 on the same days as the viral titer samples.

A systemic symptom score (range, 0 to 12) was constructed by summing the scores for muscle ache, fatigue, headache, and a feverish feeling. We focused on these systemic symptoms as they occurred first (8) and adequately delineated the incubation period. In addition, these symptoms are causally related to the cytokine level (20).

We also summed all the systemic symptom scores over the entire study period. Volunteers with total systemic symptom scores below 2 over the 7 or 8 days of follow-up were considered free of systemic symptoms.

On the whole, 56 volunteers were included in the placebo arms of these trials. For this study, we selected subjects who had virus-positive samples on at least one occasion after the challenge, leading us to exclude 12 volunteers who were considered to not have been infected as they did not shed virus.

Forty-four volunteers with a mean age of 22.7 ± 4.2 years (range, 18 to 35 years) were selected, of whom 35 (80%) were male. The mean body mass index (BMI) was 24.3 ± 3.5 kg/m^2 (range, 18.8 to 33.6 kg/m^2).

The subjects were influenza virus positive for 1 to 8 days (at least), and the observed viral titer peak ranged from 0.75 to 9.5 $\log_{10}$ ($TCID_{50}$/ml).

The observed systemic symptom scores ranged from 0 to 10 points, and systemic symptoms lasted between 0 and 8 days (or more). Six volunteers had no respiratory symptoms and no systemic symptoms and were thus considered totally asymptomatic. Maximal viral shedding did not correlate with the maximal systemic symptom score (Spearman's rho, −0.28; $P = 0.18$).

Viral shedding. Daily nasal washing fluid samples, first taken on the day before virus inoculation, were collected by introducing 5 ml of phosphate-buffered saline per nostril and allowing it to dwell for 10 to 15 s before the volunteer gently blew into a sterile container that was then transported to the laboratory for processing. Two milliliters of each sample was combined with 0.5 ml of concentrated virus transport medium. The residual sample was stored at −70°C until titration. Aliquots of 0.2 ml were inoculated on quadruplicate monolayers. Samples were incubated at 33 to 35°C for 14 days and examined for cytopathic effects every day. Negative controls were conducted each day. Titers were calculated from 10-fold dilutions of positive samples by the Karber method and expressed as $TCID_{50}$ per ml (14).

Modeling. (i) Population VKSD model. Population VKSD models were constructed with MONOLIX software version 3.1, and population parameters were estimated with the maximum likelihood method and the stochastic approximation expectation maximization algorithm (23). The two responses (viral shedding titer and systemic symptom score) were fitted simultaneously.

(ii) Structural VK model. This model extended the IFN compartmental model proposed by Baccam et al. (3) and used a set of ordinary differential equations. The compartments were uninfected target cells (T), infected but not yet virus-producing cells (I_1), productively infected cells (I_2), cytokines (F), natural killer (NK) cells, and infectious viral titers expressed in $TCID_{50}$/ml (V) (Fig. 1). Note that the cytokine compartment is taken "as a whole" and is not restricted to IFN as in the Baccam et al. model. Cytokine production was assumed to be directly proportionally to the number of infected cells and was attributed either to infected cells themselves (30) or to activated macrophages and dendritic cells (2). The cytokine compartment included all cytokines, such as IFN-α and IL-6, that are causally linked to systemic symptoms, NK cell activation, and virus production (34).

The equations describing the VK model are as follows: $dT/dt = -\beta TV$; $dI_1/dt = \beta TV - kI_1$; $dI_2/dt = kI_1 - \delta I_2 - \tau I_2 NK$; $dF/dt = I_2 - \alpha F$; $dNK/dt = F - \xi NK$; and $dV/dt = pI_2/(1 + \psi F) - cV$; where β is the target cell infection rate, k is the transition rate from I_1 to I_2, δ is the mortality rate of infected cells, τ is the effect of NK cells on infected cells, α is the cytokine clearance, ξ is the mortality rate of NK cells, p is the rate of virus production by I_2, ψ is the effect of cytokines on p, and c is the virus clearance. T_0, the initial number of target cells in the upper respiratory tract, was set at 4×10^8 (3). We set the cytokine and NK cell production rates to 1, as this changes only the units in which the early immune response is measured and does not lead to a loss of generality.

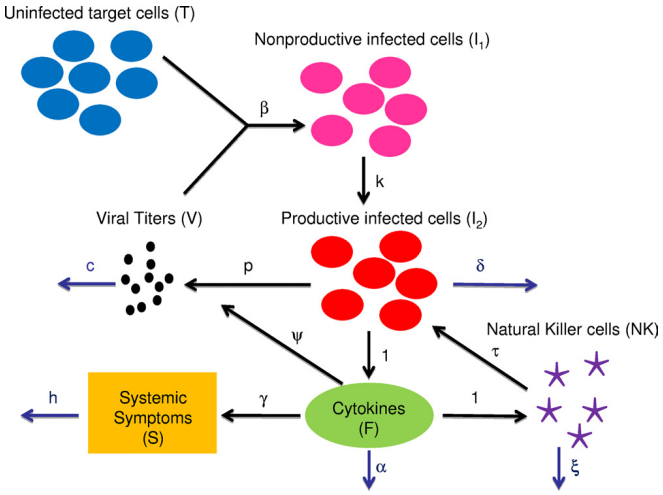

FIG. 1. Graphical presentation of the VKSD model. The free virus (V) infects target epithelial cells (T), which become infected cells not yet producing virus (I_1), before becoming productively infected cells (I_2). These latter cells produce free virus and lead to the production of cytokines (F), either directly or via activation of macrophages or dendritic cells. Cytokines reduce the virus production rate, activate natural killer (NK) cells and induce systemic symptoms (S). NK cells kill infected cells. The symbols above each arrow represent model parameters. Parameters between I_2 and F, or F and NK, were fixed at 1.

The average life span of infected cells is about 1 day (35), and δ was thus set at $k/(k - 1)$.

We defined the half-life of free virus (i.e., the time required for a 50% decline in the quantity of shed virus) as $\ln(2)/c$, the half-life of cytokines as $\ln(2)/\alpha$, and the half-life of NK cells as $\ln(2)/\xi$ (3, 36).

(iii) Structural SD model. Systemic symptoms were modeled as being dependent on the level of cytokines (20), as follows: $dS/dt = \gamma F - hS$, where γ is the rate at which systemic symptoms (S) appear and h is the rate of symptom resolution.

(iv) Modeling the different degrees of variability. In the population approach, each model parameter can be decomposed into a "population" parameter (a fixed effect) and an interindividual variability (IIV) parameter (a random effect). We illustrate this approach in a simple modeling example (Fig. 2). In our VKSD model, the IIV parameters were tested one by one to determine if they significantly improved the model. The three different error models (additive, multiplicative, and mixed) (12) were tested to model residual variability. The model was fitted for two responses: the viral titer and the systemic symptom score. The minimum value of the objective function (−2 log likelihood) was the main criterion used for model selection. Nested models were compared by using the likelihood ratio test (11). Model selection was also based on goodness-of-fit plots, and the precision of the parameter estimates, in terms of the relative standard error (RSE), was calculated as the standard deviation (STD) estimate divided by the parameter estimate.

Influenza infection and illness parameters. We estimated the latent period, infectiousness and its duration, the incubation period, and the generation time. The latent period is defined as the time during which a subject is infected but not yet infectious, while the duration of infectiousness is the average period for which an individual is capable of transmitting the infection; the incubation period is defined as the average time from infection to the appearance of symptoms of disease (1).

As the viral shedding titer above which a subject will enter the infectious period is unknown, we calculated the latent period, infectiousness, and the duration of infectiousness for various thresholds of viral shedding titers. The latent period was calculated as the time from inoculation to viral shedding exceeding a given threshold for the first time. Infectiousness was calculated as the area under the predicted VK curve (AUC) above the threshold (maximal infectiousness corresponding to the AUC calculated with no threshold), and the

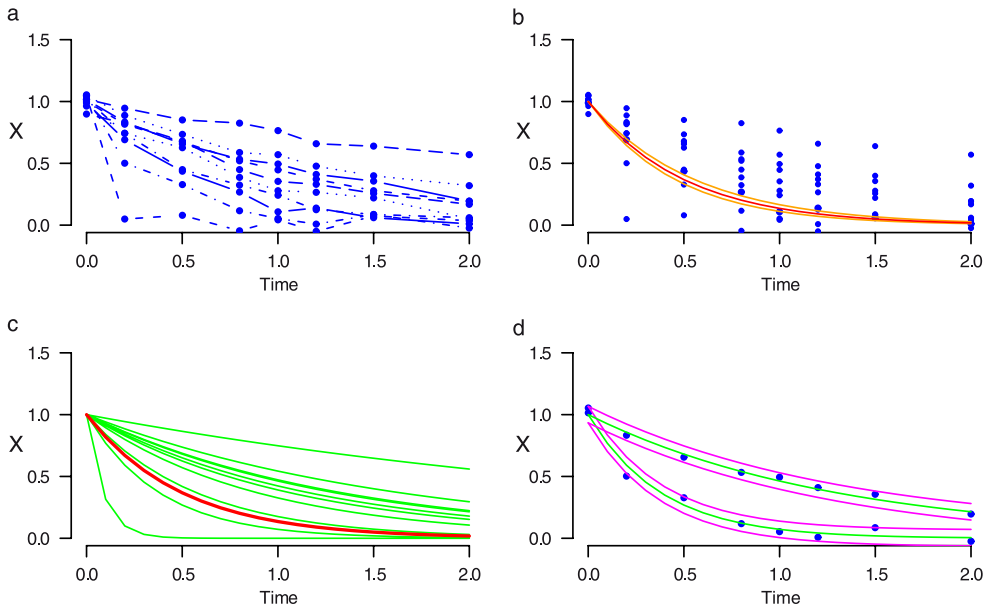

FIG. 2. Illustrative explanation of the population approach. We illustrate the statistical population approach with a simple monocompartmental model simulated on individuals ($i = 10$) and described by the equation $dX/dt = -kX$ [i.e., $X(t) = X(0) \times e^{-kt}$], with a single parameter, the elimination rate k. Parameter k was the population estimate but was assumed to vary across individuals such that k_i equals $k \exp(\eta_i)$, with η_i being normally distributed $(0,\omega^2)$. In the example, k equals 2 and ω equals 1, leading to an interindividual variability of 100%. To model residual variability, i.e., the difference between predicted and observed values, the following three different error models can be tested: additive $[X_i(t) = \hat{X}_i(t) + \varepsilon_1]$, multiplicative $[X_i(t) = \hat{X}_i(t)(1 + \varepsilon_2)]$, or mixed $[X_i(t) = \hat{X}_i(t)(1 + \varepsilon_2) + \varepsilon_1]$, where ε_1 and ε_2 follow $N(0,\sigma_1^2)$ and $N(0,\sigma_2^2)$, respectively, and $\hat{X}_i(t)$ is the individual predicted value. (a) Simulated data for 10 subjects. (b) Population predictions (red line), the population confidence interval (orange lines), and the simulated data (blue dots) are shown. (c) Predicted individual curves (green). The population curve (red) is shown for information. (d) For two subjects, we present the individual prediction (green) and the prediction interval (magenta) obtained with the additive error model.

duration of infectiousness was defined as the period during which viral shedding exceeded the threshold.

The incubation period was calculated as the time from inoculation to the onset of a systemic symptom score of ≥1 in volunteers with systemic symptoms.

Finally, for the different thresholds, we calculated the generation time (T_g), an epidemiological parameter representing the mean interval between infection of a primary case and his/her secondary cases (33) and indicating the speed at which an epidemic spreads.

Assuming infectiousness to be proportional to the viral shedding titer, random contacts between infectious and susceptible individuals (i.e., homogeneous mixing) which do not depend on the viral shedding titer, T_g can be calculated (8, 15) as follows:

$$T_g = \frac{\int_{-\infty}^{+\infty} t \times V(t)\,dt}{\int_{0}^{+\infty} V(x)dx}$$

We used the trapezoidal rule as a numerical integration method to compute the generation time from individually predicted VK curves.

RESULTS

Population VKSD model. The population VK and SD parameter estimates are shown in Table 1. The best results were obtained with an additive error model for both the VK and SD components. Interindividual variability on all parameters significantly improved the model.

The estimated average viral shedding titer increased sharply from day 1 and peaked 2.0 days after inoculation (Fig. 3), then fell rapidly to 1 $\log_{10}$ ($TCID_{50}$/ml) between days 6 and 7. The cytokine level and systemic symptom score showed roughly the same dynamic pattern, and their peaks lagged behind the viral titer peak by 0.2 and 0.4 days, respectively. The NK cell number peaked at 4.2 days but decayed slowly, remaining at 82% of the peak on day 8.

The half-life of free virus was 2.3 h (STD, 0.4 h). The average cytokine half-life was 9.1 h (STD, 1.8 h), and the average half-life of NK cells was 11.4 days (STD, 4.7 days).

Virus kinetics and symptom dynamics were highly variable across the volunteers, as shown in Fig. 4. Volunteers with the highest viral titers usually had the strongest predicted innate responses but not necessarily the highest symptom scores. Nineteen volunteers had no systemic symptoms, and these subjects had significantly lower peaks of viral shedding than volunteers with systemic symptoms ($P < 0.001$). The effect of cytokines on virus production and the virus clearance were significantly higher in volunteers without systemic symptoms than in volunteers with systemic symptoms (Table 2).

Influenza infection and illness parameters. The average latent period ranged from 0.4 days (STD, 0.3 days) to 1.5 days (STD, 0.6 days), depending on the chosen viral titer threshold (Fig. 5). In the same way, infectiousness lasted 1.3 days (STD, 0.8 days) at a threshold of 4 $\log_{10}$ ($TCID_{50}$/ml) and 7.0 days (STD, 2.1 days) when no threshold was applied. In the latter case, 95% of the total amount of infectiousness was concentrated between day 1.2 and day 3.9 after inoculation. The incubation period was 1.9 days on average (STD, 0.7 days) and ranged from 0.9 to 4.5 days.

The average generation time was 2.1 days (STD, 1.0 day),

TABLE 1. Population VKSD parameter estimates and their precision[a]

Parameter	Parameter description	Unit	Estimates (% RSE)	% IIV (% RSE)
β	Infection rate	$(TCID_{50}/ml)^{-1} \cdot day^{-1}$	3.0×10^{-5} (18)	74 (19)
k	Transition rate from non productive to productive infected cells	Day^{-1}	2.8 (7)	28 (23)
τ	Effect of NK cells on infected cells		3.8×10^{-6} (49)	126 (36)
α	IFN clearance rate	[F]/day	1.82 (20)	111 (14)
ξ	Mortality rate of NK cells		0.061 (41)	114 (33)
p	Virus production rate	$TCID_{50}/ml \cdot day^{-1}$	0.043 (16)	60 (22)
c	Virus clearance rate	Day^{-1}	7.1 (17)	91 (15)
ψ	Effect of cytokines on virus production rate (p)	$[F]^{-1}$	2.4×10^{-7} (145)	778 (14)
V_0	Initial no. of viruses	$TCID_{50}/ml$	0.50 (13)	67 (15)
γ	Rate characterizing systemic symptoms	Symptom score point $\cdot$ day^{-1}	2.2×10^{-6} (34)	78 (37)
h	Systemic symptom resolution rate	Day^{-1}	6.1 (26)	64 (40)
ε_V	Additive part of the model error for the viral titer	$TCID_{50}/ml$	1.2 (5)	
ε_S	Additive part of the model error for systemic symptoms	Symptom score point	0.59 (3)	

[a] The estimates column provides the population fixed effect parameters or "average value of the parameter in the population" with their precision of estimation (relative standard error [RSE] as a percentage), while the IIV column represents the predicted interindividual variability for each parameter in the population and is shown along with its own precision of estimation.

while the times computed from individual predictions ranged from 1.2 to 6.2 days (Fig. 5).

Infectiousness was on average 14 to 16 times lower in volunteers without systemic symptoms than in volunteers with systemic symptoms (Fig. 5). The latent period was 0.2 days longer with the 0.5 $\log_{10}$ ($TCID_{50}$/ml) threshold (Mann-Whitney test; $P = 0.045$), and the generation time was 1 day longer (Mann-Whitney test; $P = 0.002$) in subjects without systemic symptoms than in volunteers with systemic symptoms. However, regardless of the threshold, no significant difference in the duration of infectiousness was found between subjects with and without systemic symptoms.

DISCUSSION

We used an original model to characterize influenza virus shedding kinetics and symptom dynamics. This model offers a mechanistic approach to influenza infection and illness and an overall view of the disease time course. Relative to previous work, our approach comprises three novelties: influenza infection and illness were fitted simultaneously, the innate immune response was modeled and predicted, and we used a statistical population approach which contributes to the description and explanation of different levels of variability, including interindividual variability. We also characterized major influenza infection and illness parameters. Our model parameter estimates for virus kinetics were of the same order as those found in other studies. The infection rate, β, was 2.7×10^{-5} to 3.2×10^{-5} $(TCID_{50}/ml)^{-1} \cdot days^{-1}$ (3); the virus clearance, c, was 3.0 to 5.2 $days^{-1}$ (3, 26); and we found 3.0×10^{-5} $(TCID_{50}/ml)^{-1} \cdot days^{-1}$ (95% confidence interval [CI], 1.4×10^{-5} to 4.6×10^{-5}) and 7.1 $days^{-1}$ (95% CI, 3.6 to 11), respectively. The average lifetime of infected cells was fixed at 1 day, as overfitting occurred when this parameter was estimated. The use of other lifetimes (12 h to 4 days) did not modify the main findings. The VK and SD curves were also consistent with those obtained in a previous study (8) in which the viral titer and systemic symptoms peaked on day 2. However, ours is the first study to quantify the interindividual variability of parameters describing viral shedding and symptoms. We showed that some of these parameters were highly variable across individuals, such as parameter ψ (the effect of cytokines on the virus production rate), while others were relatively constant across individuals, such as parameter k (the transition rate from I_1 to I_2).

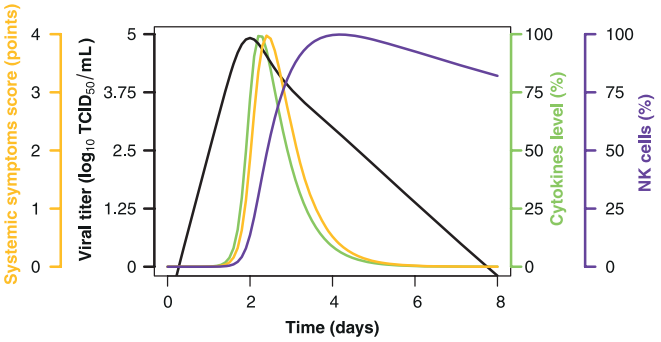

FIG. 3. Population predictions of viral titer (black), cytokines (green), and NK cell (purple) kinetics and systemic symptom intensity (orange) dynamics. The cytokine and NK cell kinetics were scaled in proportion to their maximum values.

As we had no data on cytokine or cellular responses, we designed the innate response compartments as a "black box," representing the pooled cytokine response, and an NK cell compartment. We predicted that the cytokine level peaked at 2.2 days and had a half-life of 9.1 h. This pattern was similar to the IL-6 and IFN-α kinetics observed in a volunteer challenge study of influenza virus (20). The NK cell kinetics was in line with that found in a study of young subjects with Epstein-Barr virus infection (36). Our model does not take into account the adaptive immune response, as the early adaptive immune response, and particularly cytotoxic T lymphocyte destruction of virus-infected cells, would tend to appear a certain time after infection (nearly 5 days) and would peak later (between 9.5 to 11 days) (7). The adaptive response is unlikely to have a marked effect on the observed kinetics during the first days of infection.

The model predictions were then used to calculate several influenza virus infection and illness parameters. We arbitrarily

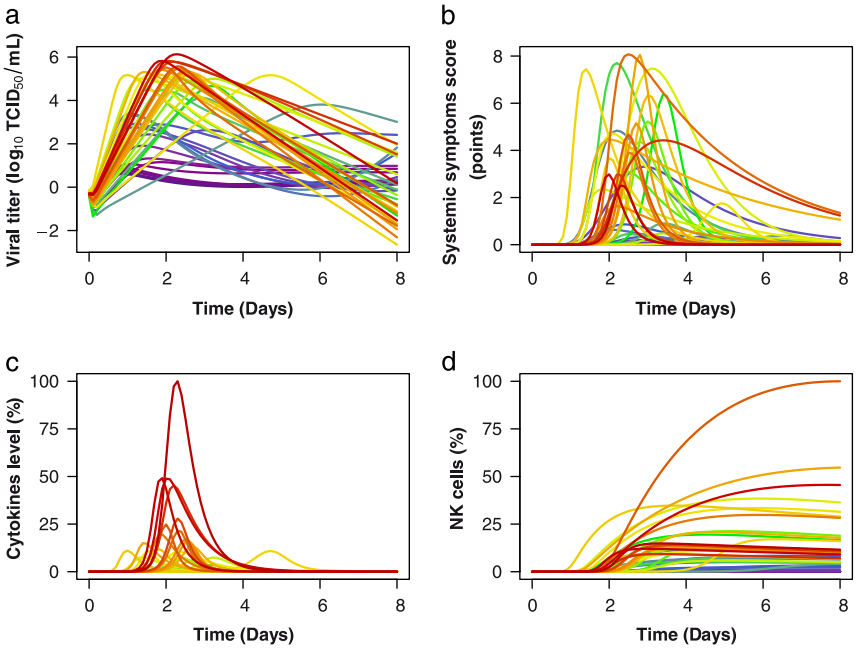

FIG. 4. Individual predictions of the viral titer (a), cytokines (c), and NK cell (d) kinetics and systemic symptom dynamics (b). The curves are ordered from the lowest peak viral titer (dark blue) to the highest (red). The order of the cytokines and NK cells peaks roughly follows that of the viral titers, contrary to the order of the peak systemic symptom scores.

chose viral titer thresholds to distinguish between infectious and noninfectious individuals, as there is no clear boundary. We deduced from these thresholds a series of values for infectiousness, its duration, and the latent period. These parameter values were consistent with the results of previous studies (8, 9, 13, 25). The generation time was calculated assuming (i) infectiousness proportional to the viral titer, thus ignoring other key factors contributing to virus transmissibility, such as respiratory symptoms; and (ii) homogeneous random contacts independent of viral shedding. Our estimated generation time (2.1 days) was consistent with the values obtained in a meta-analysis of volunteer challenge studies (8) and with epidemiological data (13) but showed increased variability (range, 1.2 to 6.2 days), which may be important from an epidemiological standpoint. We found that participants without systemic symptoms were on average 15 times less infectious than participants with systemic symptoms, confirming and extending the results of a study of naturally acquired infection in which asymptomatic subjects had lower viral titer peaks than symptomatic subjects (22). We believe that this result is particularly important, as poorly symptomatic individuals who go undiagnosed are poorly infectious and would not markedly influence the effectiveness of interventions (antivirals, isolation, etc.) aimed at controlling epidemics.

Our study has two main limitations. First, the analysis was based on a relatively homogeneous population, and second, the data came from experimental rather than naturally acquired infection. The applicability of our model to the natural infection depends on the pathogenicity of the virus used to challenge the volunteers, as well as preexisting immunity and the relevance of the challenge method to natural influenza virus acquisition (8). We believe that these issues are unlikely to affect the validity of our modeling approach: the viral shedding data and the rate of symptomatic infection, as well as the estimated infection and illness parameters, are consistent with the results of studies based on epidemiological data (13, 25).

Our findings have several important implications. First, similar models could be used to predict the time course of respiratory symptoms in influenza, thereby providing more realistic estimates of infectiousness by taking into account the high interindividual variability. Second, our approach could be used to predict the effect of antiviral treatment on infectiousness and symptoms. Finally, this approach might

TABLE 2. Differences in mean individual VKSD parameters between volunteers with and without systemic symptoms

Parameter	Parameter description	Unit	Systemic symptoms	No systemic symptoms	*P*
p	Virus production rate	$TCID_{50}/ml \cdot day^{-1}$	0.047	0.038	0.009
ψ	Effect of cytokines on virus production rate (p)	$[F]^{-1}$	7.1×10^{-6}	1.7×10^{-3}	0.0001
c	Virus clearance rate	Day^{-1}	7.6	10.3	0.03
γ	Rate characterizing systemic symptoms	Symptom score point $\cdot$ day^{-1}	2.6×10^{-6}	2.0×10^{-6}	0.012

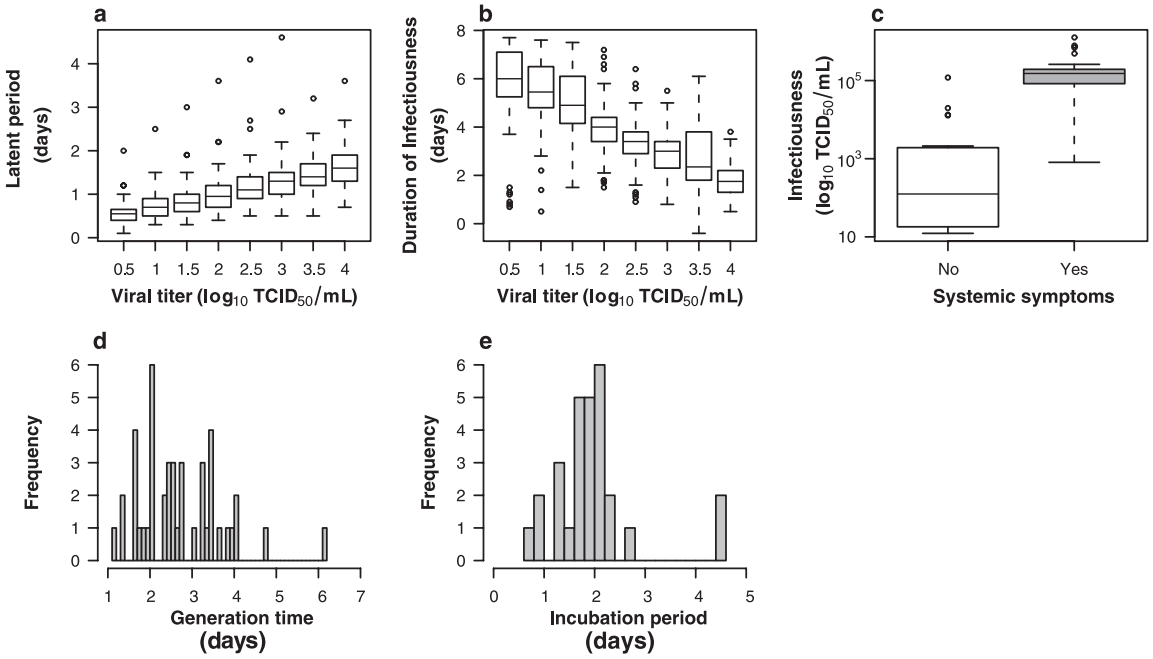

FIG. 5. Distribution of individual infection and illness parameters for the latent period (a) and infectiousness duration (b) computed for eight viral titer thresholds (0.5, 1, 1.5, 2, 2.5, 3, 3.5, and 4 $\log_{10}$ [$TCID_{50}$/ml]), infectiousness (white, absence of systemic symptoms; gray, presence of systemic symptoms) (c), generation time (d), and incubation period (e).

help to optimize the design of future influenza VK and VKSD studies with respect to the necessary number of participants and samples.

ACKNOWLEDGMENTS

We thank J. P. Paccioni, S. Courcier, and S. Muller from GlaxoSmithKline and I. Morer and P. Maison Neuve from the French Medicines Agency (AFSSAPS) for kindly providing the data used in this paper. We thank David Young, Marie-Lise Gougeon (Institut Pasteur, Paris, France), Béhazine Combadière (INSERM, Paris, France), and Brigitte Autran (Université Paris 06 and INSERM, Paris, France) for their advice on the manuscript.

This work was supported by a grant from the European Union FP7 project FLUMODCONT (no. 20160) and by a grant from the French Ministère de l'Enseignement Supérieur et de la Recherche.

REFERENCES

1. **Anderson, R. M., and R. M. May.** 1982. Directly transmitted infections diseases: control by vaccination. Science **215:**1053.
2. **Asselin-Paturel, C., and G. Trinchieri.** 2005. Production of type I interferons: plasmacytoid dendritic cells and beyond. J. Exp. Med. **202:**461–465.
3. **Baccam, P., C. Beauchemin, C. A. Macken, F. G. Hayden, and A. S. Perelson.** 2006. Kinetics of influenza A virus infection in humans. J. Virol. **80:**7590–7599.
4. **Beauchemin, C., J. Samuel, and J. Tuszynski.** 2005. A simple cellular automaton model for influenza A viral infections. J. Theor. Biol. **232:**223–234.
5. **Bell, D. M.** 2006. Non-pharmaceutical interventions for pandemic influenza, international measures. Emerg. Infect. Dis. **12:**81–87.
6. **Bocharov, G. A., and A. A. Romanyukha.** 1994. Mathematical model of antiviral immune response. III. Influenza A virus infection. J. Theor. Biol. **167:**323–360.
7. **Brown, D. M., E. Roman, and S. L. Swain.** 2004. CD4 T cell responses to influenza infection. Semin. Immunol. **16:**171–177.
8. **Carrat, F., et al.** 2008. Time lines of infection and disease in human influenza: a review of volunteer challenge studies. Am. J. Epidemiol. **167:**775–785.
9. **Cauchemez, S., F. Carrat, C. Viboud, A. J. Valleron, and P. Y. Boelle.** 2004. A Bayesian MCMC approach to study transmission of influenza: application to household longitudinal data. Stat. Med. **23:**3469–3487.
10. **Cowling, B. J., et al.** 2010. Comparative epidemiology of pandemic and seasonal influenza A in households. N. Engl. J. Med. **362:**2175–2184.
11. **Cox, D. R., and D. V. Hinkley.** 1997. Theoretical statistics. Chapman & Hall, London, United Kingdom.
12. **Davidian, M., and D. M. Giltinan.** 1995. Nonlinear models for repeated measurement data. Chapman & Hall/CRC Press, London, United Kingdom.
13. **Ferguson, N. M., et al.** 2005. Strategies for containing an emerging influenza pandemic in Southeast Asia. Nature **437:**209–214.
14. **Finney, D. J.** 1964. The Spearman-Kärber method, p. 524–530. *In* Statistical methods in biological assay. Charles Griffin and Co., London, United Kingdom.
15. **Fraser, C., S. Riley, R. M. Anderson, and N. M. Ferguson.** 2004. Factors that make an infectious disease outbreak controllable. Proc. Natl. Acad. Sci. U. S. A. **101:**6146.
16. **French, A. R., and W. M. Yokoyama.** 2003. Natural killer cells and viral infections. Curr. Opin. Immunol. **15:**45–51.
17. **Hancioglu, B., D. Swigon, and G. Clermont.** 2007. A dynamical model of human immune response to influenza A virus infection. J. Theor. Biol. **246:**70–86.
18. **Handel, A., I. M. Longini, Jr., and R. Antia.** 2007. Neuraminidase inhibitor resistance in influenza: assessing the danger of its generation and spread. PLoS Comput. Biol. **3:**e240.
19. **Handel, A., I. M. Longini, Jr., and R. Antia.** 2010. Towards a quantitative understanding of the within-host dynamics of influenza A infections. J. R. Soc. Interface **7:**35–47.
20. **Hayden, F. G., et al.** 1998. Local and systemic cytokine responses during experimental human influenza A virus infection. Relation to symptom formation and host defense. J. Clin. Invest. **101:**643–649.
21. **Larson, E. W., J. W. Dominik, A. H. Rowberg, and G. A. Higbee.** 1976. Influenza virus population dynamics in the respiratory tract of experimentally infected mice. Infect. Immun. **13:**438–447.
22. **Lau, L. L., et al.** 2010. Viral shedding and clinical illness in naturally acquired influenza virus infections. J. Infect. Dis. **201:**1509–1516.
23. **Lavielle, M.** 2005. MONOLIX (MOdèles NOn LInéaires à effets miXtes). The MONOLIX Group, Orsay, France.
24. **Lee, H. Y., et al.** 2009. Simulation and prediction of the adaptive immune response to influenza A virus infection. J. Virol. **83:**7151–7165.
25. **Longini, I. M., Jr., et al.** 2005. Containing pandemic influenza at the source. Science **309:**1083–1087.
26. **Miao, H., et al.** 2010. Quantifying the early immune response and adaptive immune response kinetics in mice infected with influenza A virus. J. Virol. **84:**6687–6698.
27. **Neumann, A. U., et al.** 1998. Hepatitis C viral dynamics in vivo and the antiviral efficacy of interferon-alpha therapy. Science **282:**103–107.
28. **Nowak, M. A., et al.** 1996. Viral dynamics in hepatitis B virus infection. Proc. Natl. Acad. Sci. U. S. A. **93:**4398–4402.

29. **Perelson, A. S., A. U. Neumann, M. Markowitz, J. M. Leonard, and D. D. Ho.** 1996. HIV-1 dynamics in vivo: virion clearance rate, infected cell life-span, and viral generation time. Science **271:**1582–1586.
30. **Pichlmair, A., and C. Reis e Sousa.** 2007. Innate recognition of viruses. Immunity **27:**370–383.
31. **Saenz, R. A., et al.** 2010. Dynamics of influenza virus infection and pathology. J. Virol. **84:**3974–3983.
32. **Samson, A., M. Lavielle, and F. Mentré.** 2006. Extension of the SAEM algorithm to left-censored data in nonlinear mixed-effects model: application to HIV dynamics model. Comput. Stat. Data Analysis **51:**1562–1574.
33. **Svensson, A.** 2007. A note on generation times in epidemic models. Math Biosci. **208:**300–311.
34. **White, M. R., M. Doss, P. Boland, T. Tecle, and K. L. Hartshorn.** 2008. Innate immunity to influenza virus: implications for future therapy. Expert Rev. Clin. Immunol. **4:**497–514.
35. **Zdanov, V. M., and A. G. Bukrinskaja.** 1969. Myxoviruses reproduction. Medicina, Moscow, Russia.
36. **Zhang, Y., et al.** 2007. In vivo kinetics of human natural killer cells: the effects of ageing and acute and chronic viral infection. Immunology **121:**258–265.

4.5.2 Comments and perspectives

4.5.2.1 About the VKSD model

This model is in line with the previous models used to describe influenza viral kinetics [28, 29, 31]. These complex models raise the problem of identifiability. However, it takes into account two responses for the first time which allow the model to be more complex.

Modeling the respiratory symptoms dynamics would be of great interest. Indeed, influenza virus is mainly spread in the environment by sneezing and coughing. The infectiousness should also be associated with respiratory symptoms intensity then. However, the underlying physiological mechanisms for respiratory symptoms such as sneezing and coughing are complex. They are related to local inflammation at different sites such as nasopharynx, larynx or below. The virus spreads from one site to another and causes local inflammation responsible for these symptoms [118]. Therefore spatially-structured model to represent influenza virus tropism could be developped supposing that the intensity of respiratory symptoms depends on the quantity of infected cells.

We also found that 19 of the 44 subjects did not exhibit systemic symptoms, suggesting that the proportion of asymptomatic infections is coherent with a study finding that 59% of the infection of the Royal Air Force personnel in 1918 were asymptomatic [119].

4.5.2.2 About the natural history parameters

The evolution of infectiousness in time is one central question for those who want to control influenza pandemic, and assuming that infectiousness is proportional to viral shedding, our study brings with relevant and original information regarding infectiousness in these subjects. However, as we mentioned in section 2.1.2, the infectiousness that we computed is theoretical.

The proportion of infectiousness prior to symptom onset and prior to physician consultation may play a major role in the disease transmission. Also infectiousness of poorly

symptomatic individuals is of major interest as these spreaders are undetectable and might not be subjects to the measures aiming to decrease the contacts. The Figure 4.1 shows that in average 29% of the infectiousness occurs prior to symptom onset, 94% until 1 day after symptom onset and that 2% remains after the systemic symptoms alleviation (Figure 4.1 - upper left panel).

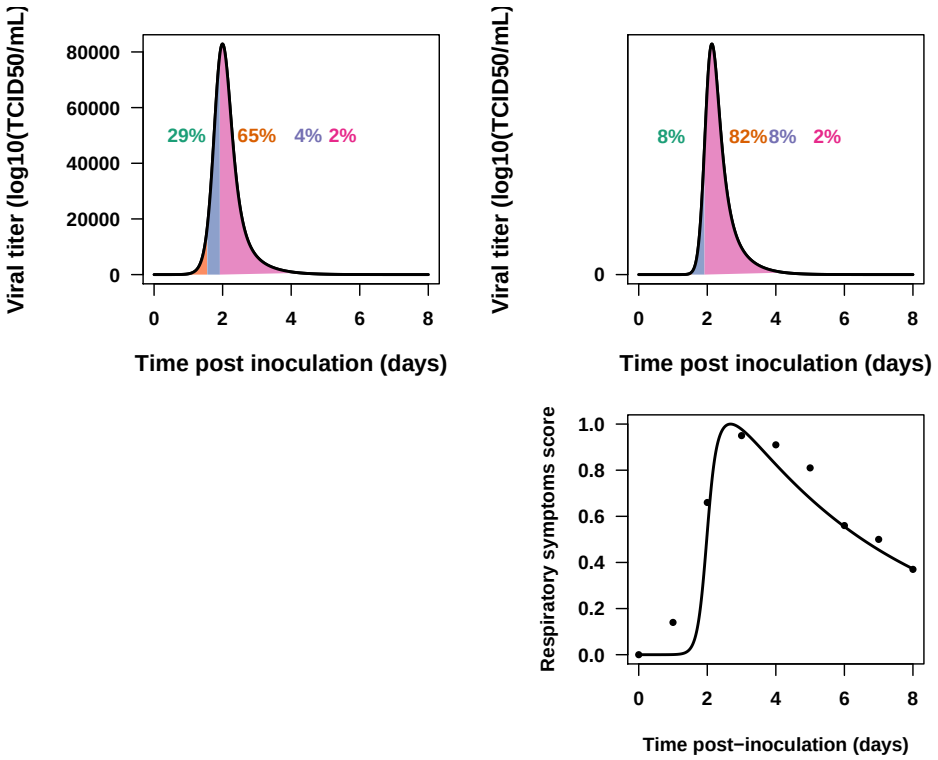

Figure 4.1: Proportion of infectiousness. Upper left panel: Infectiousness is proportional to the VK only as in [120]. Upper left pannel: Infectiousness is proportional to VK and respiratory symptoms. Lower panel: respiratory symptoms intensity depending on time. The dots represents the average respiratory symptoms observed as presented in [35]. The line is the fit used to compute infectiousness

Respiratoy symptoms have a different dynamics from systemic symptoms (cf. Figure 4.1 - lower panel). They peak 1 to 2 days later and then decrease slowly until the eighth or nineth day post inoculation [35]. If we use the average observed respiratory symptoms [35] and consider infectiousness proportional to both viral titer and respiratory symptoms intensity, we find that in average 8% of the infectiousness occurs prior

to symptom onset, 90% during the first day of symptoms and that 2% remains after the systemic symptoms alleviation (cf. Figure 4.1 - upper right panel). Using the respiratory symptoms dynamics provides a generation time lasting in average 2.3 days vs. 2.1 days with the previous method. In both cases, we find that more than 65% of the total infectiousness occurs during the first day of symptoms and that at the end of this first day of symptoms less than 15% of the total infectiousness remains, suggesting that interventions are probably inefficient or poorly efficient if began after.

Modeling accurately respiratory symptoms dynamics and its variation would hence have a great importance and could provide estimates of the effective natural history parameters. It would be however more realistic to consider 1) a constant baseline virus spread due to exhalation and 2) an increase of the spread linked to the intensity of respiratory symptoms.

4.5.2.3 Modeling naturally acquired infections

For naturally acquired infections, studying influenza dynamics remains challenge. In an epidemiological study where the viral titer was measured, three samples were collected each three days after symptom onset of households index case [36]. The data are presented in the Figure 4.2. 61% of the samples were below the limit of detection ($0.3log_{10}(TCID_{50}/mL)$ [36]). The incubation period was previously shown to be variable and to range from 0.9 to 4.5 days [120] and in the case of naturally acquired infections, the time of infection is unknown. If we represent viral load data depending on the time from symptoms onset, the ditsribution is stretched as shown in Figure 4.5.2.3

The variability observed for incubation period, responsible for the "'data stretch"' could lead to misinterpretations in transmission studies. Let us consider a household where two subjects 1 and 2 are co-infected in the same time. Subject 1 has a shorter incubation period than subject 2, then subject 1 will be considered as an index case whereas subject 2 will be considered as a transmission case. Similarly, it can lead to a

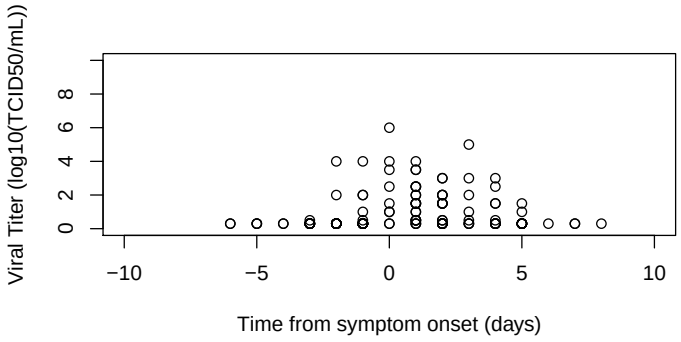

Figure 4.2: Viral load data in naturally infected subjects. Data available from [36] at `http://web.hku.hk/~bcowling/influenza/HK_NPI_study.htm`

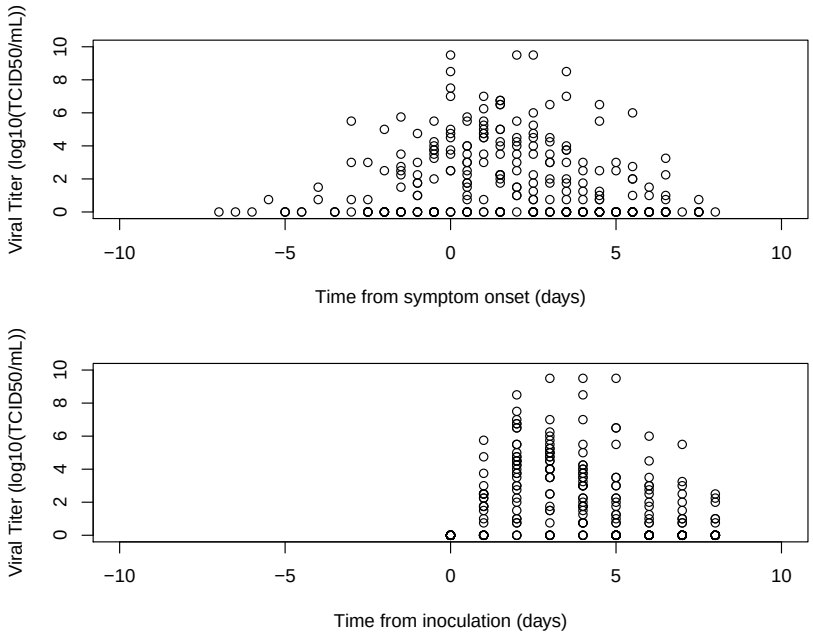

Figure 4.3: Viral load depending on the time scale used. Upper panel: viral load depending on time from inoculation. 0 stands for symptom onset. Lower pannel: viral load depending on time from inoculation. 0 stands for inoculation time

confusion of secondary and tertiary cases [121]. Determining the timeline of influenza infection within host would therefore help to understand transmission timeline.

5 Optimizing designs to study influenza dynamics

Influenza as an acute infection represents several challenges. Indeed the infection and illness are very brief and the peak of viral shedding occurs before the peak of systemic symptoms, or around the first day of symptoms. Thus, finding an appropriate design is crucial to study influenza dynamics.

5.1 Sampling design for population model

Let N be the number of subjects from the population to study. An elementary design ξ_i with i varying from 1 to N is defined by the number of samples to collect n_i and by the sample time allocation: $\xi_i = (t_{i1}, t_{i2}, ..., t_{in})$. The population design is the set of elementary designs: $\Xi = (\xi_1, ..., \xi_N)$. It is described by the N elementary designs for a total number of observation n such as $n = \sum_{i=0}^{N} n_i$. When there are Q groups of subjects having the same elementary designs ξ_q with q varying from 1 to Q, the population protocol is written $\Xi = \{[\xi_1, N_1]\,; [\xi_2, N_2]\,; ...; [\xi_Q, N_Q]\}$, where each N_q is the number of subject with the same design ξ_q, with $\sum_{q=1}^{Q} N_q = N$ and $n = \sum_{q=1}^{Q} n_q \times N_q$ [122].

Determining a design implies the identification of the sample times allocation for each subject and to define the structure of the design: the number of groups, the number of samples per group and the proportion of subjects in each group for a total number of

samples n.

5.2 Design optimization

Simulation studies showed that the balance between the number of groups, the number of subjects per group and the sample times allocation in each group has an effect on parameters estimates accuracy and that unbalanced designs can lead to uninterpretable studies [123, 124]. Therefore it is important to carefully choose the design, and even more so in populations such as paediatrics, elderly or patients with chronic diseases for which the number of samples is often limited [125–127]. Hence a well-balanced design can increase the efficiency of the study while being ethical and less expensive as the number of samples per subject is minimized and that all samples are informative.

The simulation approach to optimize designs, while being reliable, is expensive in term of computation time. Another approach using the non-linear regression consist in minimizing the variance-covariance matrix of parameter estimates [128, 129]. Now, according to the Rao-Cramer inequality, the Fisher information matrix inverse is the lower bound of variance-covariance matrix of any unbiased estimator.

There is no exact analytical expression for the Fisher information matrix when used for nonlinear mixed effect models. However several approximations have been proposed and validated by simulation. By linearizing the model $f(g(\beta, b, Z), \xi)$ with a first-order Taylor approximation around the expectation of random effects [130–132], analytical values for the elements of the Fisher information matrix can be obtain.

For the covariate vector Z and for the elementary design ξ, the matrix can be written as follow: $E_{y|Z}\left(-\frac{\partial^2 L(\Psi; y)}{\partial \Psi \partial \Psi'}\right)$, where $L(\Psi; y)$ is the log-likelihood of observations vector y for the population parameters vector Ψ.

The expression of the Fisher information matrix in the nonlinear mixed effect models depends on the sampling design and on the population parameters vector. Minimizing

the variances is equivalent to maximizing the Fisher information matrix regarding the population design. The most classical criterion used is D-optimality for which the determinant of the Fisher information matrix is maximized. However other criteria are available such as A-optimality (minimization of the sum of the asymptotic variances), C-optimality (minimization of the sum of the estimates squared variation coefficient) and E-optimality (maximization of the smallest peculiar value of the Fisher information matrix) [128, 133].

5.3 Ready-to-use optimized designs to study influenza infection dynamics

5.3.1 Article *In review in PLoS One*

Ready-to-use optimized designs to study influenza infection dynamics

Laetitia Canini[1,2] and Fabrice Carrat[*,1,2,3].

Affiliations:

[1] UPMC – Paris 6, UMR-S 707, Paris, F-75012, France

[2] Inserm, UMR-S 707, Paris, F-75012, France

[3] Assistance Publique Hôpitaux de Paris, Hôpital Saint Antoine, Paris, F-75012, France

Address for correspondence:

F Carrat,

Epidémiologie, systèmes d'information, modélisation,

UMR-S 707,

Faculté de médecine Saint Antoine,

27, rue Chaligny,

75571 PARIS CEDEX 12,

phone: +33 1 44 73 84 51

fax: +33 1 44 73 84 53

e-mail: carrat@u707.jussieu.fr

Abstract

Background: Viral kinetics is increasingly used to study influenza infectiousness. The choice of the study design, *i.e.* when and how many times samples are to be collected in subjects is crucial to efficiently estimate the viral kinetics parameters.

Material and methods: We performed a model based analysis to derive the optimal design for studying influenza viral kinetics, innate immune response dynamic and/or systemic symptoms dynamics. In a first step, we defined a set of possible sample times as well as the number of possible subgroups of subjects with different sampling protocols. In a second step, we computed the requested number of subjects to accurately estimate the model parameters.

Results: We provided a set of optimized designs with up to 6 sample times per subject. In a parsimonious design, viral titre and pro-inflammatory cytokines or NK cells would be measured in 8 subjects at 6 different sampling times over 9 days.

Conclusions: These findings should help designing further studies on influenza viral kinetics. It also provides an original set of protocols for the study of pro-inflammatory cytokines and NK cells dynamics in influenza.

Word count: 182

Key words: optimal design, influenza, viral kinetics, innate immunity

Introduction

Volunteer challenge studies have been widely used to describe viral shedding kinetics during influenza infection [1]. Recently, viral kinetics (VK) was also studied in naturally acquired influenza infection [2,3]. These studies are helpful to provide information on the influenza infection timelines and to estimate natural history parameters such as the latent period or the duration of infectiousness [1,2,3,4].

In the 56 studies describing VK which were reported in a meta-analysis [1], the number of subjects varied from 6 to 76, the follow-up from 6 to 17 days and the number of samples collected from 1 over the entire follow-up to 3 per day. These differences led to a highly variable amount of information across the studies to accurately estimate the parameters describing VK. When the number of sample collections and the number of subjects are too limited, uncertainties on parameter estimates are huge and no relevant conclusions can be drawn from the study findings. In contrast, a large number of repeated collections in a large number of subjects will provide accurate estimates of VK parameters, but with a dramatic increase of general discomfort for enrolled subjects and elevated cost of experiments.

In order to correctly estimate the parameters it is crucial to determine a design to collect sufficiently informative data. This is the objective of optimal design approach, which determines from previous experiments, the number and allocation of sample times per subject as well as the number of subjects to include in another experiment [5]. Over the last ten years, optimal design analysis has been used increasingly in the general field of pharmacokinetic/pharmacodynamic studies to provide cost-efficient designs [6]. Few optimized designs have already been used and proved to be useful in pharmacokinetic studies [7,8]. Recently, the optimal design approach has been

used to describe VK in Hepatitis C Virus infection [9]. In influenza, this approach has never been used. Moreover, the dynamics of pro-inflammatory cytokines [10], or NK cells, or systemic symptoms [4], have received little attention in influenza but would be interesting to describe in addition to VK.

Our objective was to apply the optimal design approach for studies describing the VK, the pro-inflammatory cytokines, NK cells and/or systemic symptoms dynamics in influenza infection. We estimated the number of participants, the number of samples to collect and their time allocations.

Methods

We used a previously published viral kinetics – symptoms dynamic model of influenza infection [4]. This model used a set of ordinary differential equations (Figure 1). The compartments were uninfected target cells (T), unproductive infected cells (I1), productive infected cells (I2), infectious viral titers expressed in TCID50/mL (V), natural killer cells (Nk) and cytokines (F). Note that here the cytokines compartment is taken “as a whole" and not restricted to the IFN only as in the Baccam model. It involves a large number of cytokines as immunomodulators [11].

$$\frac{dT}{dt} = -\beta TV$$

$$\frac{d\,I_1}{dt} = \beta TV - k\,I_1$$

$$\frac{d\,I_2}{dt} = k\,I_1 - \delta\,I_2 - \tau\,I_2 NK$$

$$\frac{dF}{dt} = I_2 - \alpha F$$

$$\frac{d\,NK}{dt} = F - \xi\,NK$$

$$\frac{dV}{dt} = \frac{p}{1+\psi F}\,I_2 - cV$$

The compartmental model was parameterized in terms of the infection rate (β), cytokines clearance (α), the transition rate from unproductive to productive infected cells (k), the mortality rate of infected cells (δ), the rate of virus production by infected productive cells (p), the effect of cytokines on p (ψ), the effect of NK cells on infected cells (τ), the NK cells clearance (ξ) and the virus clearance (c). T0, the initial number of target cells in the upper respiratory tract, was set to $4x10^8$ cells [12]. We set the cytokines and NK cells production rates to 1, as this changes only the units in which the early immune response is measured and does not lead to a loss of generality.

It was shown that infected cells lifespan lasts in average 1 day. We set $\frac{1}{k} + \frac{1}{\delta} = 1$ and estimated only k [12].

Systemic symptoms were modeled as being dependent on the level of cytokines [10].

$$\frac{dS}{dt} = \gamma F - hS$$

where γ is the rate at which systemic symptoms appear and h is the rate of symptom resolution.

We used a population approach in which each coefficient of the structural model is composed of a fix and a random parameter. The fix parameter represents the average value observed in the population whereas the random parameter models the inter-individual variability. We will call the random parameter η variable thereafter. Each η variable was assumed to have a mean of zero and a variance of ω^2. Assuming that the distribution of the individual parameters around the population value was lognormal, each ω^2 was estimated with an exponential error model.

For example, the IIV on virus clearance was modeled as follows:

$$c_i = c \times \exp\left(\eta_i^c\right) \qquad \eta_i^c \sim N\left(0, \omega_c^2\right)$$

where c_i is the predicted viral clearance in the i^{th} subject, c is the population viral clearance value, and η_i^c are random variables that are independent and identically and normally distributed.

The magnitude of the IIV in viral kinetic parameters was equal to ω.

The differences between the observed and predicted values were regarded as random quantities and were modeled with ε variables. Each ε variable was assumed to have a mean value of zero and a variance of σ^2.

The additive error was modeled as follows

$$V(t) = \overline{V}(t) + \varepsilon \qquad \varepsilon \sim N\left(0, \sigma^2\right)$$

where V(t) is the observed viral titer at time t, $\overline{V}(t)$ is the predicted viral titer at time t, ε is the error, σ^2 is the variances of the error.

The parameters were estimated from a follow-up over 9 days of 56 experimentally challenged volunteers with daily viral titre and twice daily systemic symptoms

measurements. Estimated fixed effect parameters were used as reference values and our goal was to derive optimized sampling protocols, involving a limited number of sample collections and a limited number of subjects while leading to accurate estimation of the model parameters. Therefore the optimal design analysis is a model-based approach [4]. The optimal design analysis was conducted in two steps: first, optimization of the sample times was performed using the maximization of the Fisher information matrix determinant (criterion of "D-optimization)"[13]. We used the Fedorov-Wynn algorithm implemented in PFIM 3.2 [14]. Second, we calculated the requested number of subjects as the number providing a sufficient accuracy on fixed effect estimates. We defined the accuracy as the ratio of the fixed effect parameter to its standard error. An accuracy above 2 would correspond to a relative standard error below 50% and hence we used this value as a threshold to select the optimized designs.

The random effect parameters' accuracies were examined to reinforce the selection process of the optimized designs.

The requested number of subjects was finally inflated by 25% to take into account that 25% of volunteers experimentally inoculated with influenza virus did not shed virus [4]. For the purpose of comparison, we also computed the accuracy for designs with the total number of subjects set to 20 and 5.

Four coefficients were fixed (i.e. not to be estimated) to avoid numerical problems, namely: the virus production rate, the effect of pro-inflammatory cytokines on virus production rate, the rate characterizing the systemic symptoms and the systemic symptoms resolution rate [4]. We also fixed the inoculation time to 8:00 and we limited the choice of sampling times to 8:00 and 20:00 for each day.

Three sets of designs were optimized, each including measurements of viral titre obtained from isolation from nasal washing according to described methods [4,10]. In set 1 (S1), pro-inflammatory cytokines is measured from the nasal wash fluid and can be determined using commercially kits [10]. In set 2 (S2) NK cells response is measured from simultaneous peripheral blood collection as the proportion of NK cells expressing the CD69 receptor [15]. In set 3 (S3) systemic symptoms are assessed as the sum of muscle ache, fatigue, headache, and feverish feeling rated on a four-point scale: 0–3 corresponding to absent to severe [4]. We considered designs with at least 3 sample times. For each set, we selected the most parsimonious design, i.e. the design with the lowest total number of sample collections.

Results

The number of sampling times per subject would vary between 5 and 6 in all optimized parsimonious designs.

In designs involving less than 5 time-dependent measurements per individual, individual predictions would not be accurate as the parameter distribution would shrink towards the mean population value.

More specifically, for S1 six samples should be collected in 8 subjects as follow: on day 1 at 20:00, on day 2 at 8:00 and 20:00, on day 3 and on day 4 at 8:00 and on day 5 at 20:00 in 12% of the subjects, at inoculation time, on day 1 at 20:00 and on day 2, 3, 7 and 8 at 8:00 in 38% of the subjects and on days 1 and 2 at 8:00, on day 6 at 20:00, on day 7 at 8:00 and 20:00 and on day 8 at 8:00 in 50% of the subjects.

For S2 six samples should be collected in all subjects at inoculation time and on days 2, 3, 4, 6 and 8 at 8:00 (cf. Figure 1).

For S3 five samples should be collected in all subjects on day 2 at 8:00 and 20:00, on days 3 and 4 at 20:00 and on day 8 at 8:00.

The figure presents the accuracy for each fixed effect parameter with the different designs and the different population sizes.

Overall, the parameters were more precisely estimated with S2 and the accuracy was lower with S3. With 20 subjects included, the number of sample times would be decreased by 76% for S1 and S2 and by 80% for S3, compared to the design used in the original study where 56 subjects were sampled 9 times. For S1 and S2, the accuracy of all the parameters would exceed 2 and for S3 one parameter, the mortality rate of the NK cells, would not be accurately estimated (cf. figure 2).

In optimized designs, the number of subjects would vary from 8 for S1 and S2 to 850 for S3 and the total number of sample collections from 48 for S1 to S2 and 4250 S3. The total number of viral titre samples collected would be decreased by 91% with the optimized designs for S1 and S2.

The model performing the best in term of random effects accuracy is the parsimonious S2 design (not shown).

Discussion

We used the optimal design approach to derive optimised protocols combining simultaneous collections of VK with pro-inflammatory cytokines, NK cells or systemic symptoms, in order to estimate the viral kinetics-symptom dynamics model parameters with sufficient accuracy. These designs are well balanced between the amount of necessary information and the expected accuracy of estimation, leading to a number of collected samples decreased by up to 91% compared with the original data set. It is important to note that the optimal design approach is developed for a

particular model. Therefore our findings cannot be transposed to other models describing influenza infection or illness with different parameterizations. The choice of this particular model was motivated because it provided the most complete picture of acute influenza infection, by describing the viral shedding, the pro-inflammatory cytokines and NK cell responses as well as the course of illness [4].

We retrieved one study with pro-inflammatory cytokines measurements during experimental human influenza A virus infection [10]. In this study 19 volunteers were sampled 9 times leading to a total of 171 paired collections of viral titre and cytokines to analyse. Our optimized design with pro-inflammatory cytokines involves 8 volunteers and 6 samples per subjects, thus would decrease the total number of collected samples by 72% and would provide accurate estimates for both fixed and random parameters.

NK cells dynamics has been to our knowledge the subject to only one human influenza infection study [15]. The optimized design with 6 samples per subject would provide precise estimates for both fixed and random parameters.

The design combining viral titre and systemic symptoms measurements was potentially the easiest to implement with limited volume of blood collection per subject. The implementation of this design with only 5 point measurements per subject and 20 subjects would not achieve our accuracy objective for the mortality rate of the NK cells. Similarly in the original study [4], one parameter implied in the innate immune response modelling, the effect of the pro-inflammatory cytokines on virus production rate, was roughly estimated. The parameters accuracy is similar for the S3 design with 20 subjects. To obtain precise estimates of all fixed effect parameters, 850 volunteers would have to be recruited - this design is meaningless from a practical standpoint.

It is worth noting that the original model was fitted on viral titre and symptoms data obtained from healthy volunteers with low serum haemagglutinin antibody titre and intranasally inoculated with influenza A/Texas/91 (H1N1) virus [4]. Consequently, the optimized designs could be unsuited for studying naturally acquired influenza infections or experimental infections with other influenza viruses or for studies intended in other populations.

Our approach has several limitations. First, four coefficients of the model were fixed to avoid numerical problems. These parameters exhibited wide inter-individual variability when they were initially estimated [4] - and the selected optimized designs are therefore not adapted for measuring these parameters.

Second, we did not optimize designs with viral titre measurement only for which simpler models involving only VK should be used [12].

Finally, we forced sample collection during daytime and simultaneous measurements of different outcomes in order to ensure practicability of the design. It is however possible that optimized designs with a lower number of total measurements could be obtained if these constraints were removed.

Our findings should help in designing further studies on influenza viral kinetics. It also provides an original set of protocols for the study of pro-inflammatory cytokines and NK cells dynamics in influenza. The approach could also be extended to estimate treatment-related parameters in population pharmacokinetic / pharmacodynamic studies of influenza antivirals.

Financial support

This work was supported by a grant from the European Union FP7 project FLUMODCONT [grant number 201601] and by a grant from the French Ministère de l'Enseignement Supérieur et de la Recherche. The funders had no role in study design, data collection and analysis, decision to publish, or preparation of the manuscript

Aknowledgement

We thank Caroline Bazzoli (Université Pierre Mendès-France, Grenoble, France) for her advice on PFIM use.

Potential conflict of interest

None to declare

Authors' contribution

LC performed the analyses and LC and FC have been involved in drafting the manuscript. All authors read and approved the final manuscript.

Author's information

LC received her Master in Clinical epidemiology from Toulouse III University in June 2008 and her diploma of Doctor of Veterinary Medicine from the Ecole Nationale Vétérinaire de Toulouse in October 2010. Since October 2008, she has been a PhD student in Biostatistics at UMR-S 707 ("Epidemiology, Information Systems and Modelling"). Her research focuses on influenza infection dynamics modelling: viral

kinetics, symptoms and innate immune response dynamics and effects of antivirals on influenza infection dynamics.

FC is a Senior Lecturer in Epidemiology at Institut National de la Santé et de la Recherche Médicale (INSERM), Paris; Professor at the Department of Public Health, Université Pierre et Marie Curie, Paris; and Public Health practitioner at Saint-Antoine Hospital, Paris. He has been involved in influenza epidemiological research since 1992. His research interests include influenza epidemiology and modelling, surveillance, burden-of-illness, and evaluation of preventive interventions. He is also a member of a number of public health expert panels on influenza pandemic planning.

References

1. Carrat F, Vergu E, Ferguson NM, Lemaitre M, Cauchemez S, et al. (2008) Time lines of infection and disease in human influenza: a review of volunteer challenge studies. Am J Epidemiol 167: 775-785.
2. Cowling BJ, Chan KH, Fang VJ, Lau LL, So HC, et al. (2010) Comparative epidemiology of pandemic and seasonal influenza A in households. N Engl J Med 362: 2175-2184.
3. Lau LL, Cowling BJ, Fang VJ, Chan KH, Lau EH, et al. (2010) Viral shedding and clinical illness in naturally acquired influenza virus infections. J Infect Dis 201: 1509-1516.
4. Canini L, Carrat F (2011) Population Modeling of Influenza A/H1N1 Virus Kinetics and Symptom Dynamics. J Virol 85: 2764-2770.
5. Federov VV (1972) Theory of optimal experiments: Academic Press, New York.
6. Mentre F, Mallet A, Baccar D (1997) Optimal design in random-effects regression models. Biometrika 84: 429.
7. Hennig S, Waterhouse TH, Bell SC, France M, Wainwright CE, et al. (2007) A d-optimal designed population pharmacokinetic study of oral itraconazole in adult cystic fibrosis patients. Br J Clin Pharmacol 63: 438-450.
8. Mentre F, Dubruc C, Thenot JP (2001) Population pharmacokinetic analysis and optimization of the experimental design for mizolastine solution in children. J Pharmacokinet Pharmacodyn 28: 299-319.
9. Guedj J, Bazzoli C, Neumann AU, Mentre F (2011) Design evaluation and optimization for models of hepatitis C viral dynamics. Stat Med 30: 1045-1056.
10. Hayden FG, Fritz R, Lobo MC, Alvord W, Strober W, et al. (1998) Local and systemic cytokine responses during experimental human influenza A virus infection. Relation to symptom formation and host defense. J Clin Invest 101: 643-649.
11. White MR, Doss M, Boland P, Tecle T, Hartshorn KL (2008) Innate immunity to influenza virus: implications for future therapy. Expert Rev Clin Immunol 4: 497-514.
12. Baccam P, Beauchemin C, Macken CA, Hayden FG, Perelson AS (2006) Kinetics of influenza A virus infection in humans. J Virol 80: 7590-7599.
13. Atkinson AC, Donev AN (1992) Optimum Experimental Designs: Clarendon Press, Oxford.
14. Retout S, Comets E, Samson A, Mentré F (2007) Design in nonlinear mixed effects models: Optimization using the Fedorov-Wynn algorithm and power of the Wald test for binary covariates. Statistics in medicine 26: 5162-5179.
15. Jost S, Quillay H, Reardon J, Peterson E, Simmons RP, et al. (2011) Changes in cytokine levels and NK cell activation associated with influenza. PLoS One 6: e25060.

Figure legends

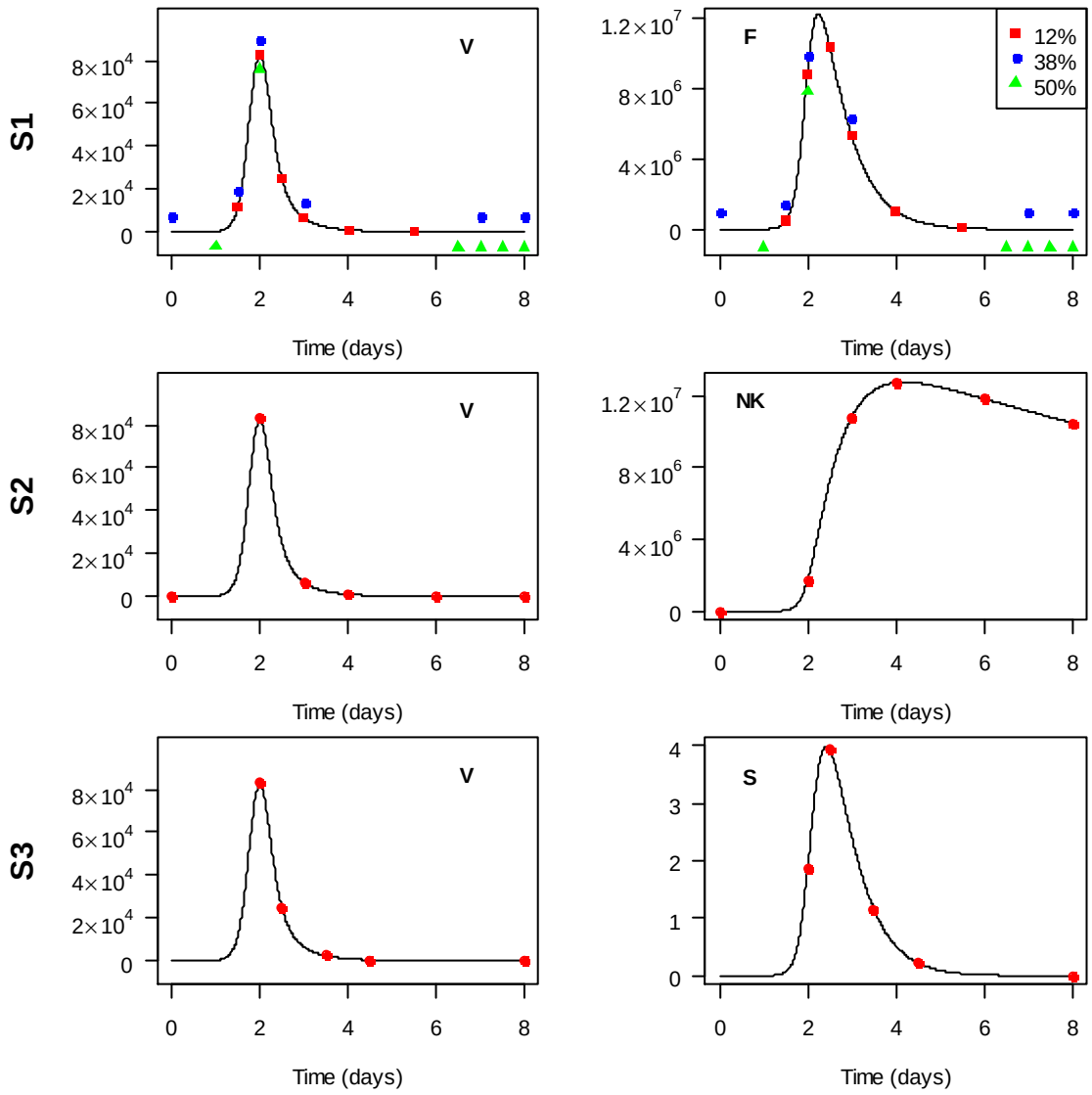

Figure 1: Optimized designs. For each case, we indicate the data points where the viral load (left panels) and the second response (right panels) is sampled. The upper panels represent the dynamics for the S1 design where viral kinetics and pro-inflammatory cytokines are sampled. The percentages presented in the corner correspond to the proportion of subject in each group. The middle panels represent the dynamics for the S2 design where viral kinetics and NK cells are sampled. The lower panels represent the dynamics for the S3 design where viral kinetics and systemic symptoms are sampled.

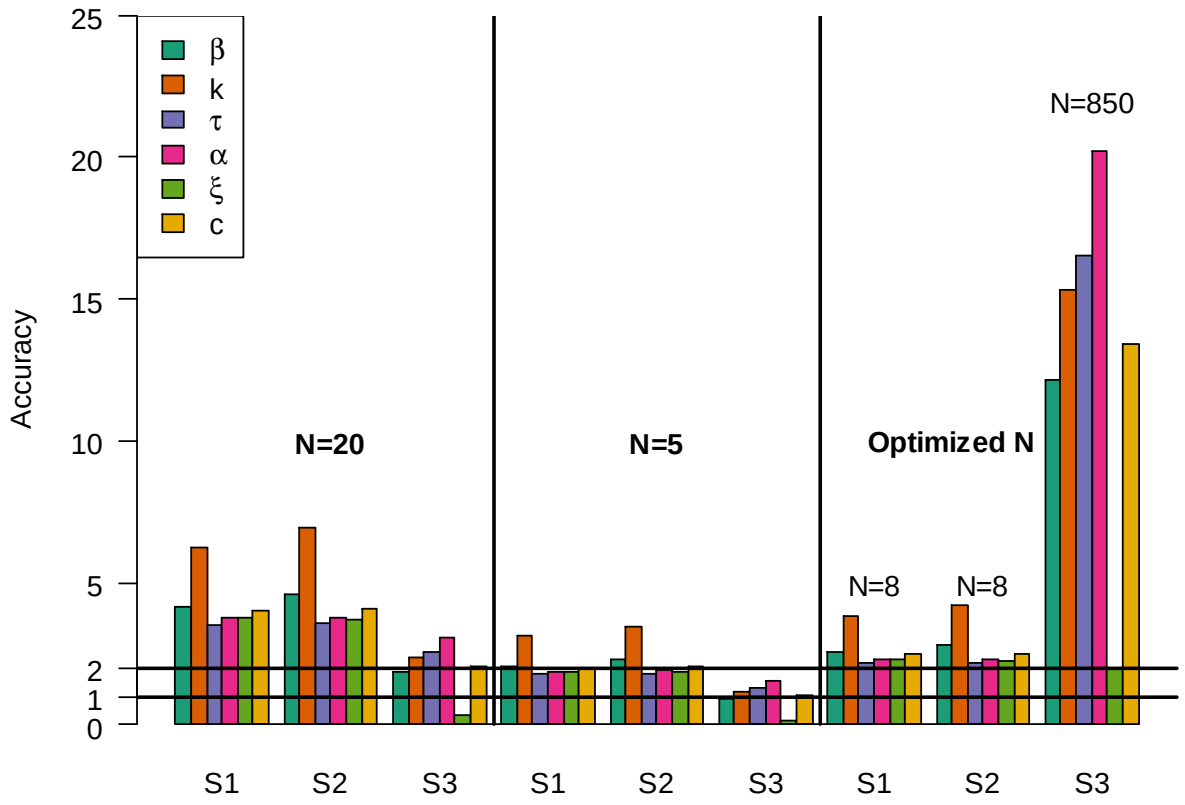

Figure 2: Predicted accuracy for each fixed effect parameter for the three sets of designs with different population size: the accuracy was defined as the ratio of the parameter prediction to the predicted standard error and was set to a minimum of 2 in optimized designs. β stands for the viral infection rate, k for the transition rate from non productive to productive infected cells, τ for the effect of NK cells on infected cells, α for the pro-inflammatory cytokines clearance rate, ξ for the mortality rate of the NK cells and c for the virus clearance rate.

5.3.2 Comments

The designs proposed here were developed to both be practical and provide precise estimates of the model parameters. They are adapted for experimental infections as the time is scaled on the inoculation time and as we supposed that inoculation time is known. The designs proposed here enhance the identifiability of the model. As expected, enriching the data with additional sampling sites or measurements such as cytokines level or NK cells activity greatly improved the estimates precision (cf. part 4.3.1).
The effect of pro-inflammatory cytokines on virus production rate, ψ, was less precisely estimated than other parameters. Indeed, ψ links the innate immune response to the viral kinetics and is associated with a high degree of nonlinearity [134, 135], indicating that linear approximation does not perform as well as with the other parameters [136, 137]. This problem could be resolved by fixing this parameter with biologically plausible value.

***

Even though optimal designs has been subject to numerous study [128, 130–133, 138, 139], few optimized designs were actually used for trials [125, 126, 138, 140, 141]. It is possible that investigators have little confidence in this type of analyses, eventhough the results were promising.

6 Interventions to mitigate influenza

Three possible ways of mitigating influenza can be envisaged: 1) increasing the immunity with vaccines, 2) limiting the contamination of the environment with non-pharmaceutical interventions and 3) decreasing the subjects' infectiousness with antiviral treatment and decreasing the transmission between subjects with non pharmaceutical interventions.

6.1 Vaccines

Vaccination is aimed at enhancing the immunity to a particular disease and thus to decrease the susceptibility of the subjects.

Most countries use split virion (virus particles have been partially or completely disrupted by physicochemical means) or subunit (the preparation consists predominantly of haemagglutinin and neuraminidase antigens) non-adjuvanted inactivated vaccines [142]. The vaccines used are trivalent: they contain since 1977 a A/H1N1, a A/H3N2 and B strain. Its fabrication depends on the strains that circulated the previous year and in the Northern hemisphere on the strains that ciruculated in the Southern hemisphere [5]. Live attenuated seasonal influenza vaccines have been shown to be more effective in immunologically naive individuals than un-adjuvanted and inactivated seasonal influenza vaccines [143]. Figure 6.1 shows that while being in general less reactogenic, purified influenza virus surface antigens are less immunogenic than purified whole virion vaccines in immunologically naive individuals such as small children and subjects with no contact to circulating influenza viruses [144].

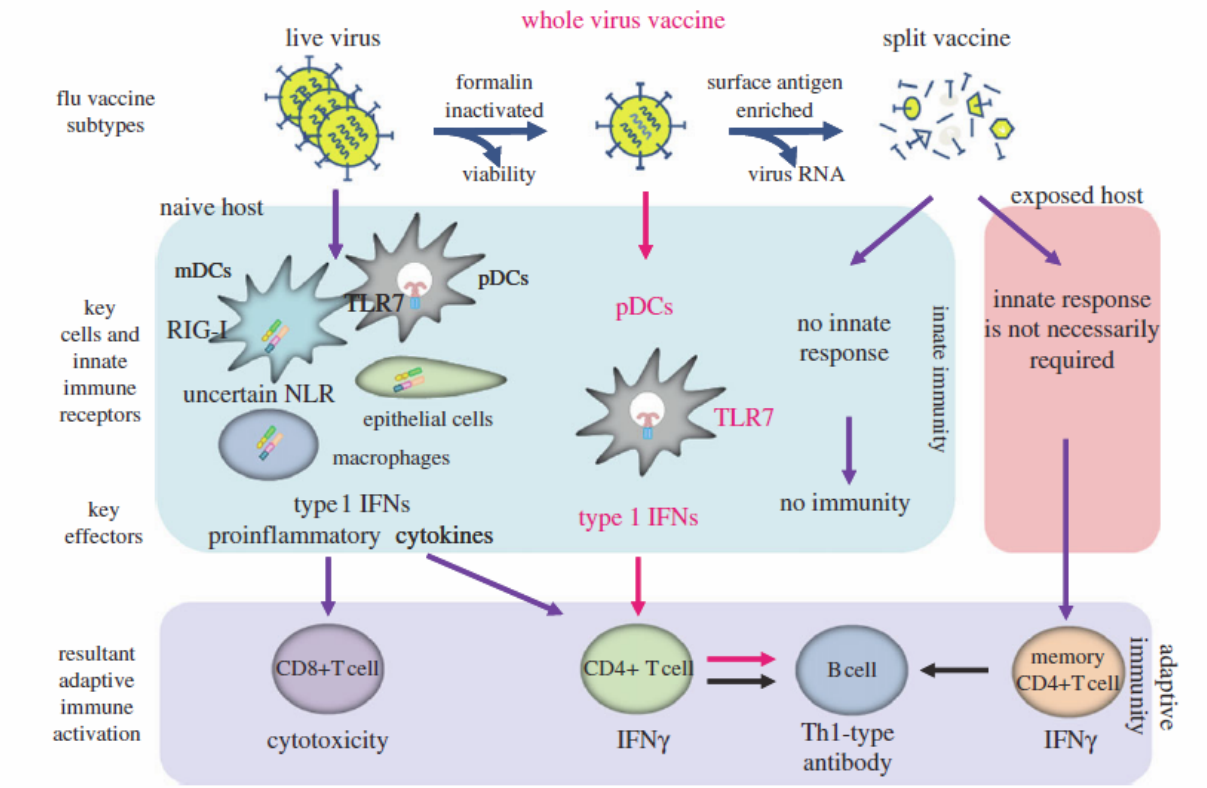

Figure 6.1: Activation of the adaptive immunity by vaccination (from [144]): In the case of live influenza viruses, the viruses infect a variety of cells except for plasmacytoid dendritic cells (pDC) and produce RNAs resulting in type 1 interferon production. pDCs are resistant to infection and phagocytose the viral particle, and RNA is liberated in the phagolysome, which result in activation of Toll-like receptors (TLR)-dependent pathway and type 1 interferon production. In the case of inactivated whole virus vaccine, this cannot infect but pDCs engulf the inactivated virus, and subsequent activation of TLR-dependent pathway leads to production of type 1 interferon. This pathway is also essential to induction of adaptive immunity against influenza virus. Split vaccine lacking RNA is not effective in naive persons but can play a role in protection by activating memory B cells in people who have already experienced influenza viral infection

Vaccination against influenza is recommended for subjects over 65 years in France and in the United States. Specific recommandations include subjects susceptible to develop severe infections such as immunocompromised patients or patients suffering from respiratory pathologies.

6.2 Non-pharmaceutical interventions

Several non-pharmaceutical interventions are available for influenza such as using facemasks [43,44,145–148] and respirators [147], hand hygiene [149], social distancing measures and isolation of patients or quarantine of contacts [150].
These measures are aimed at limiting the contamination of the environment and thus influenza transmissio. However none of these measures appeared to be effective to limit influenza transmission.

6.3 Antiviral treatments

Among the pharmaceutical ways of counteracting influenza virus, antivirals can be used as well for prophylaxis as for treatment to reduce the symptoms intensity and infectiousness [151–153]. Figure 6.2 shows the different anti-influenza-virus compounds and their target [34]:

1. M2 ion channel inhibitors
2. Neuraminidase inhibitors
3. RNA polymerase inhibitors

Two classes of antivirals are currently available: M2 ion chanel inhibitors and neuraminidase inhibitors [154]. **The M2 ion chanel** is a membrane protein which is highly expressed at the surface of infected cells and plays a major role during the internalization

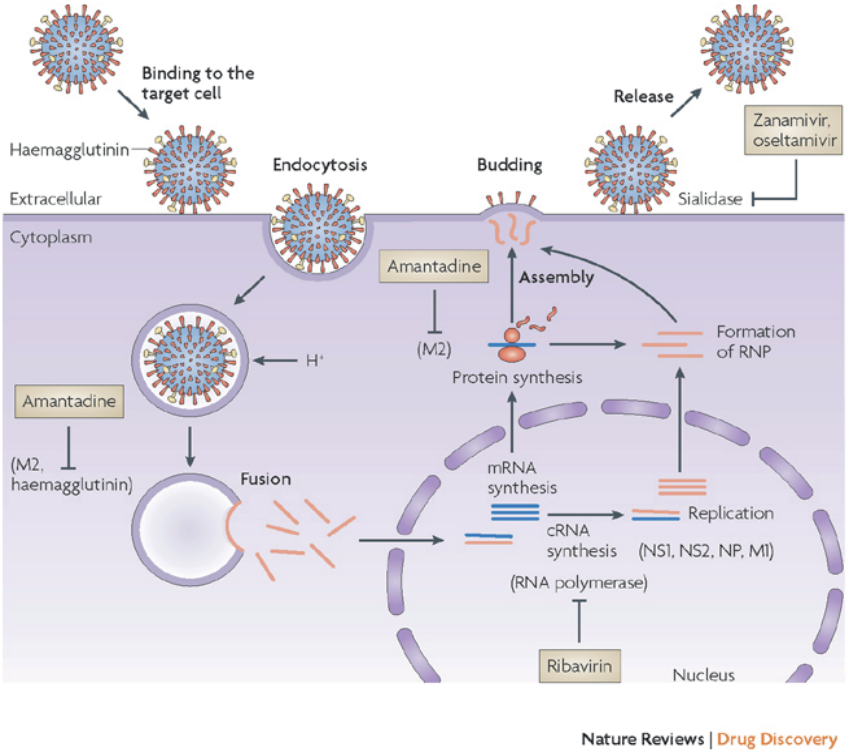

Figure 6.2: Life cycle of the influenza virus and targets for therapeutic interventions (from [34])

of the virus [155]. The main M2 ion channel inhibitors used were amantadine commercialized as Symmetrel® and Mantadix® and rimantadine commercialized as Flumadin®. Due to the large number of resistance to M2 inhibitors and the transmissibility of drug-resistant virus, neuraminidase inhibitors and especially oseltamivir were recommended for the prophylaxis and treatment of influenza in "at-risk" group [156].

Neuraminidases inhibitors, also called sialidases, impedes the release of virus and hence reduce its replicability [157]. Indeed, neuraminidases cleaves terminal sialic acid (N-acetylneuraminic acid) residues from cellular and viral glycoconjugates which promotes the release of progeny viruses and the spread of the virus from the host cell to uninfected surrounding cells. Inhibition of neuraminidase enzymatic action by antibody, mutation, or chemicals causes virus particles to aggregate at the cell surface and with each other [158]. Two neuraminidases are commercialized, namely oseltamivir, commer-

cialized as Tamiflu® and zanamivir, commercialized as Relenza®. A third compound is under development: peramivir which was experimentally used during the 2009 pandemic. Finally, laninamivir is in phase III clinical trials [159].

RNA polymerase inhibitors are still under development

***

Taken individually, each intervention has its limitation. Especially due to the proportion of transmission occurring prior to the onset of clinical symptoms as shown in Figure 6.3, the efficacy of measures aiming to reduce the contacts with patients is often limited [160]. In this context, understanding influenza infection timeline and its between subjects variations could be crucial to improve the strategies to mitigate the disease.

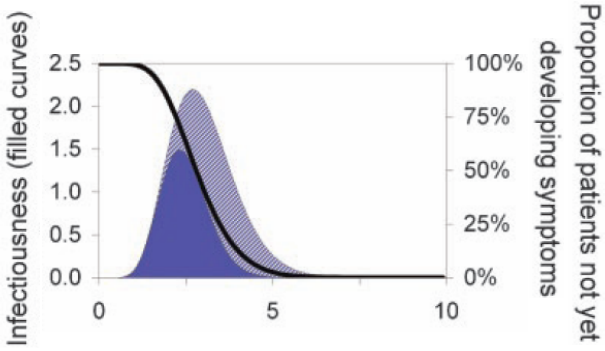

Figure 6.3: Key epidemiological determinants. These determinants describe the pattern of typical disease progression for an individual patient as a function of time since infection (measured in arbitrary units). Filled curves represent infectiousness through time (left axis). The black curve represents the probability of a person not having developed symptoms by a certain time (right axis). The basic reproduction number R0 is the area under the infectiousness curve (solid color plus cross-hatched section). The solid-colored area represents transmission arising prior to symptoms such that the proportion of presymptomatic transmission, is the proportion of the total area under the infectiousness curve that is solid-colored. (from [160])

Moreover, several studies showed that when different measures are combined their efficiency might be increased in favorable conditions and that the epidemic peak would be delayed and reduced [18–21, 25].

6.4 Modeling antivirals effects on viral kinetics and symptoms dynamics

6.4.1 Article *in progress*

Impact of different oseltamivir treatment regimens in the otherwise healthy or immunocompromised influenza infected subjects: insights from a modelling study

Laetitia Canini[1,2] and Fabrice Carrat[*,1,2,3].

Affiliations:

[1] UPMC – Paris 6, UMR-S 707, Paris, F-75012, France

[2] Inserm, UMR-S 707, Paris, F-75012, France

[3] Assistance Publique Hôpitaux de Paris, Hôpital Saint Antoine, Paris, F-75012, France

Address for correspondence:

F Carrat,

Epidémiologie, systèmes d'information, modélisation,

UMR-S 707,

Faculté de médecine Saint Antoine,

27, rue Chaligny,

75571 PARIS CEDEX 12,

phone: +33 1 44 73 84 51

fax: +33 1 44 73 84 53

e-mail: carrat@u707.jussieu.fr

Abstract

Several studies have proven oseltamivir to be efficient to reduce viral titre and symptoms intensity of influenza. However the usefulness of oseltamivir can be compromised by the emergence and the spread of drug-resistant viruses. The selective pressure exerted by oseltamivir and the effect of the regimen has received little attention.

In a previous work, we fitted a model of viral kinetics and symptom dynamic to human influenza infection data using a population approach. Using this model, we explored the virological and clinical efficacy of oseltamivir through simulated pharmacokinetics. We simulated populations of 1000 subjects using between-subject variability parameters to describe the observed heterogeneity and we modelled immunodeficiency as a lack of cytotoxic activity from the NK cells. We simulated random mutations conferring resistance to oseltamivir and emergence of resistant virus on treatment. We explored the effect of the dose, of the time of first intake, of intake frequency and of immunodeficiency on influenza infection, illness dynamics and resistant virus emergence. An early administration, i.e. administration prior to the average symptom onset time, provided a high efficacy, but led to resistant virus emergence if the oseltamivir carboxylate concentration was below the IC_{50} at the inoculation time. Immunodeficiency was associated with a substantially increased proportion of subjects shedding resistant virus and a clear dose effect was found on resistance emergence.

Our model provides a global picture of the effect of oseltamivir. It indicates that once subjects are infected, “the sooner the better” as it combines higher efficacy and lower risk of resistance emergence. In addition, it suggests that immunocompromised

subjects should be treated with high doses in order to reduce the risk of resistance emergence. Prophylaxis should be used with caution as it can lead to resistance emergence. This work provides new leads to understand neuraminidase effect at the population level.

Word count: 298 (max 300)

Introduction

In addition to influenza vaccination, neuraminidase inhibitors are currently the best recommended pharmaceutical intervention to reduce the burden of seasonal or pandemic influenza [1,2,3,4,5,6]. Neuraminidase inhibitors comprise two European marketed drugs: nebulised zanamivir (Relenza® ; Glaxo Wellcome) and oral oseltamivir (Tamiflu® ; Hoffmann-La Roche), which interfere by blocking the release of progeny influenza virus from infected host cells and hence, by reducing the spread of infection in the respiratory tract [7]. Oseltamivir has been stockpiled in many countries for pandemic preparedness and is the most frequently used neuraminidase inhibitor worldwide [8]. Treatment with oseltamivir accelerate time to alleviation of influenza-like illness and post-exposure prophylaxis with oseltamivir reduce secondary transmission of influenza [9]. However the effectiveness of oseltamivir strongly depends on the delay between infection (or onset of symptoms) and first antiviral intake. The effectiveness of oseltamivir can also be compromised by the emergence and further spread of drug-resistant viruses [10]. Most resistant isolates emerged during post-exposure prophylaxis [11] or under treatment in subject with intense or prolonged viral shedding, such as children [12] or immunocompromised persons [13,14,15].

The interactions between time of infection, first oseltamivir intake, dose regimens and host response to infection, with clinical and virological effectiveness and emerging resistance are complex. Moreover, influenza infection dynamics is highly variable between subjects [16] and the pharmacokinetics of oseltamivir leads to great concentration variations in time [17] that can lead to variable efficacy at the individual level. To the best of our knowledge, the between subject variability and the effect of

oseltamivir pharmacokinetics have never been studied in details. We therefore explored these interactions *in silico*, using a stochastic adaptation of both the pharmacokinetic (PK) model of oseltamivir [17] and the virus kinetics / symptoms dynamic (VKSD) model fitted to experimental human infection data [16]. We provided an integrative framework to assess antiviral treatment by simultaneously taking into account random mutations, oseltamivir efficacy and selective pressure.

Material and methods

Structural equations modelling

To describe the pharmacokinetic of oseltamivir, we used a model describing the pharmacokinetics of the prodrug, oselatmivir phosphate (OP) and its metabolite, oseltamivir carboxylate (OC) which is the active drug. We used a 7 compartments model with 2 compartments for OP disposition, 3 for OC disposition, a metabolism compartment describing the conversion of OP in OC, and a compartment for first-pass metabolism (Figure 1). The model used nine fixed parameters and five mixed parameters, which consist of a fixed and a random parameter [17] (cf. supplementary information).

The time-course of influenza infection and symptoms was described by a compartmental model including epithelial cells (infected or not), free virus, pro-inflammatory cytokines level, NK cells and systemic symptoms as shown in Figure 2 [16]. Influenza viral kinetics (VK) was expressed in $TCID_{50}$/mL of virus titres and the systemic symptoms as a score representing the intensity of fever or feverish feeling, headaches, muscular aches and fatigue. The systemic symptom score ranged from 0 to 12 when all symptoms were at their highest intensity. The infection and illness model used ten mixed parameters [16].

The effect of the OC was modelled as inhibiting virus release from productive infected cells as follows:

$$p' = p\left(1 - \frac{C}{IC_{50} + C}\right)$$

Where p' is the virus production rate under treatment, p is the virus production rate without treatment, C is the OC concentration and IC_{50} is the concentration of oseltamivir that provides 50% inhibition of the virus production. IC_{50} was set to 2µg/L for susceptible virus [18].

We modelled the emergence of resistant variant virus as a random event occurring in productive infected cells with a probability λ. We considered the kinetics of the resistant variant virus and of the wild type virus to be similar [19,20]. The IC_{50} of resistant virus was set to 800 µg/L as it was shown that resistant virus IC50 is 400 times higher than susceptible virus IC50 [21]. We assumed that the target cells could be infected only by one type of virus at a time, which is a common way to model resistant virus kinetics [25,26].

We set the resistant variant emergence rate to 2 10^{-7} resistance emergence/replication cycle based on previous observations showing that between 0.4 and 1% of treated patients would shed resistant virus when treated with 75 mg bid during 5 days as previously found [22,23]. We simulated that with 75 mg bid during 5 days in average 1% of the subjects treated after three days post inoculation would shed resistant virus over the limit of detection (LOD = 0.3 $\log_{10}(TCID_{50}/mL)$ [24]).

Response to infection in the immunocompromised was simply modelled by assuming that the NK cells had no cytotoxic effect on productive infected cells, all other parameters being unchanged.

We formulated the model [16] as a finite-cell-population stochastic model. The deterministic model, as well as the structure of the stochastic process, is presented in the Supplementary material.

Simulations

We simulated the PK and VKSD for two oseltamivir approved regimens in adults: 75 mg daily during 10 days (post-exposure prophylaxis regimen), 75 mg twice a day during 5 days (treatment regimen). For comparison purposes, we also explored 150 mg twice a day during 5 days (recommended regimen in severe pandemic influenza [27]) and 300mg twice a day during 5 days [6]. We chose six possible first intake times. We simulated a first intake 7 or 1 days before the inoculation time. To simulate post-exposure prophylaxis, the first intake was set 0.5 day after inoculation or 1 day before whether we considered that the subject was contaminated or not at the prophylaxis start. Finally, to simulate curative regimen, we set the first intake 2, 3 and 4 days after inoculation time which correspond to 0, 1 and 2 days after symptom onset [6]. The VKSD was simulated during 8 days for otherwise healthy and during 15 days for immunocompromised subjects, which corresponded to maximal durations of shedding when no treatment was taken.

Two populations of 1000 healthy and immunocompromised subjects were simulated.

Fixed parameters were considered equal to the mean population value. For mixed parameters, the individual parameters were drawn from a lognormal distribution $\ln N(\mu,\omega^2)$ where μ is the mean population value and ω^2 is the mean inter-individual variability [16,17].

We used a binomial leaping algorithm from the package GillespieSSA implemented in R [28] to simulate our system.

Endpoints

We primarily assessed the virological efficacy as the average decrease of the area under the curve (AUC) of viral titres (in natural scale) under treatment related to the AUC of viral titres without treatment. Clinical efficacy was measured as the average decrease of the AUC of systemic symptoms under treatment related to the AUC of systemic symptoms without treatment. The results are presented as the mean value and a 95% interval of simulation values (95% ISV) thereafter. The lower bound of the interval was the 25^{th} permille and the upper bound was the 975^{th} permille.

Emergence of resistant virus was evaluated as the proportion of subjects who could have been detected as shedding resistant virus during the infection period at any moment during the infection, i.e. when the quantity of resistant virus shedding exceeded the LOD. We used the normal approximation to compute the binomial prediction interval of this proportion.

Results

Baseline

Figure 3 shows the simulated average viral kinetics and symptoms dynamic in otherwise healthy subjects and the immunocompromised. The viral titre peak were 4.9 $\log_{10}(TCID_{50}/mL)$ (95% ISV 0 – 6.0 $\log_{10}(TCID_{50}/mL)$ in healthy subjects vs. 5.7 (95% ISV 0 – 6.6) in immunocompromised, and duration of viral shedding above the LOD was 6.5 days (95% ISV 2.1 – 7.7 days) in otherwise healthy subjects vs. 12.8 days (95% ISV 3.2 – 14.7 days) in immunocompromised). The incubation period was similar in both cases (1.9 days in average) but systemic symptoms score were much higher and lasted longer (6.3 days (95% ISV 1.1 – 13.6 days)) in immunocompromised subjects than in otherwise healthy subjects (respectively 3.9 points (95% ISV 0 - 12) and 2.4 days (95% ISV 0.2 -6.4 days)). The AUC of the viral

curve was 4.8 $log_{10}(TCID_{50}/mL)$ in otherwise healthy subjects vs. 5.3 $log_{10}(TCID_{50})$ in immunocompromised subjects. The AUC of the systemic symptoms curve was 5.2 points in otherwise healthy subjects vs. 37.4 points in immunocompromised subjects.

Pharmacokinetics

Our simulated PK model shows increases of OC concentrations with peaks occurring in average 4 hours after each intake. After last treatment intake a prolonged decrease (Figure 4) was observed. The height of the peak was proportionate to the dose regimen. OC concentrations above the IC50 for susceptible viruses were obtained in the first hour after first treatment intake.

Treatment effect

Figure 5 shows that in immunocompetent subjects, the virological and clinical efficacies were increased with higher doses. With a first intake 0.5 day after inoculation and with 75mg bid during 5 days, the virological efficacy was 91.2% (95%ISV: 0 – 100). When the dose was 150 mg bid during 5 days, the virological efficacy increased to 91.7% (95%ISV: 0 – 100) and with 300 mg during 5 days it increased to 99.9% (95%ISV: 0 – 100). Similarly the clinical efficacy increased from 94.8% (95%ISV: 26.6 – 100) to 96.4% (95%ISV: 51.5 – 100) and to 96.9 % (95%ISV: 58.2 – 100) when subjects received 75 mg, 150 mg and 300 mg bid during 5 days respectively.

The virological and clinical efficacies were significantly improved by a first intake around inoculation time: With 75mg bid during 5 days, the virological efficacy was 90.2% (95% ISV: 0 – 100) for a first intake occurring 1 day before infection, 91.2% (95% ISV: 0 – 100) during the incubation and fell to 37.0% (95% ISV: 0 – 99.9) three days after inoculation.

The frequency of oseltamir intake was associated with the virological and clinical efficacy when the first treatment intake occurred 7 days before inoculation. In this case the virological efficacy was 38.2% (95% ISV: 0 – 100) with 75 mg bid during 5 days and 46.0% (95% ISV: 0 – 100) with 75 mg ind during 10 days.

In immunocompromised subjects, we found a marked dose effect. The virological and clinical efficacies were increased with higher doses. With a first intake 0.5 day after inoculation and with 75mg bid during 5 days, the virological efficacy was 79.1% (95%ISV: 0 – 99.9). When the dose was 150 mg bid during 5 days, the virological efficacy increased to 83.8% (95%ISV: 0 – 100) and with 300 mg during 5 days it increased to 88.7% (95%ISV: 0 – 100). Similarly the clinical efficacy increased from 44.0% (95%ISV: 0 – 100) to 56.0% (95%ISV: 0 – 100) and to 68.5 % (95%ISV: 0 – 100) when subjects received 75 mg, 150 mg and 300 mg bid during 5 days respectively.

Virological and clinical efficacy were also improved by an early intake (Figure 5): With 75mg bid during 5 days, the virological efficacy was 71.7% (95% ISV: 0 – 100) for a first intake occurring 1 day before infection, 79.1% (95% ISV: 0 – 99.9) during the incubation (12 h after inoculation) and fell to 20.1% (95% ISV: 0 – 99.1) three days after inoculation. The frequency of oseltamir intake was associated with the virological and clinical efficacy. Specifically, for a first intake 1 day before the inoculation, the regimen 75mg ind during 10 days led to a virological efficacy 1.85 lower and a clinical efficacy 3.0 times lower than with 75mg bid during 5 days.

Resistance emergence

In immunocompetent subjects, the proportion of subjects shedding resistant virus remained below 1% with all possible regimens except in the case of a first intake 7 days before virus inoculation. With this regimen, the proportion of subjects shedding

resistant virus was 3.7% (95%ISV: 2.5 – 4.9) with 75 mg bid during 5 days, 5.7% (95%ISV: 4.3 – 7.1) with 150 mg bid during 5 days, 6.3% (95% ISV: 4.8 – 7.8) with 300mg bid during 5 days and 5.0% (95%ISV: 3.6 – 6.4) with 75mg ind during 10 days (Figure 5 – left lower panel).

Immunocompromised subjects had an increased risk of resistance emergence. The dose was associated with the proportion of subjects shedding resistant virus. For a first intake 0.5 day after inoculation, this proportion was 8.6% (95%ISV: 6.9 – 10.3) with the regimen 75 mg bid during 5 days, 6.3% (95%ISV: 4.8 – 7.8) with 150 mg bid during 5 days, and 6.0% (95%ISV: 4.5 – 7.5) with 300 mg bid during 5 days.

The proportion of subjects shedding resistant virus remained below 10% for first intakes between 1 day prior to inoculation and 3 days after inoculation and with intakes twice daily. It increased to 20.7% (95%ISV: 18.2 – 23.2) with 75 mg bid during 5 days, 19.4% (95%ISV: 16.9 – 21.9) with 150 mg bid during 5 days and 22.4% (95%ISV: 19.8 – 25.0) with 300 mg bid during 5 days when the first intake was 7 days before inoculation.

Spacing out the intakes to one intake per day led to modified efficacy and resistant emergence patterns. The proportion of subjects shedding resistant virus was overall higher than with the other regimens. More specifically, this proportion was 19.1% (95%ISV: 16.7 – 21.5) with 75 mg ind during 10 days for a first intake 1 day prior inoculation whereas it was 7.5% (95%ISV: 5.8 – 9.0) when oseltamivir is taken twice daily.

Discussion

Our simulations showed that the virological and clinical efficacies were consistent with previous results: early administration of oseltamivir increased virological and clinical efficacy [29]. We complete this picture with prophylaxis when the first intake occurs 7 days before infection which was associated with both a decreased efficacy and an increased risk of resistance emergence. We found a dose effect in the immunocompromised subjects but not the otherwise healthy subjects like in previous findings [30]. More specifically the mean virological efficacy was 37% when oseltamivir was taken within 3 days after inoculation which is consistent with what was found in an epidemiological study [30].

The resistance emergence we described herein is consistent with what was described in experimental studies [31] as well as in epidemiological studies [14,32]. The proportion of subjects shedding resistant virus under various oseltamivir regimens remains low in the otherwise healthy when the first intake was 1 day before inoculation or during the incubation period or as a treatment whereas it increases up to 6.3% when the first intake was 7 days before inoculation.

In a previous modeling study of oseltamivir effect on influenza infection, the treatment effect was considered constant over time and ineffective on resistant strains [33] We added interindividual variability for both the viral kinetics and pharmacokinetics which reflects the great heterogeneity observed in the population and we considered that the resistant strain might be susceptible to high OC concentrations [21].

In our model, we supposed that every subject was infected with susceptible virus and we did not consider the case of subjects infected with resistant virus or with a mixture of both.

We made several other assumptions. First, in previous studies, [22,23], drug susceptibility was measured only at one sample time. We thus believe that our hypothesis concerning the emergence of resistant virus should be considered as a mimimum risk.

Second, this study was limited to adult subjects as the parameters used were obtained from studies conducted in this population. However, even if the time course of influenza was found to be similar in adults and children [24], the pharmacokinetics might differ in children. Indeed, the recommended dose is 1.0 mg/kg and 2.0 mg/kg bid in neonates and children aged 1-5 years respectively, leading to lower concentration than in adults [34,35,36]. This could explain the increased risk of resistance emergence in children [36].

Finally, we used a simplistic mean for simulating subjects with deficient innate immune response. It was shown that a depletion in NK cells increases morbidity and mortality in case of influenza infection [37,38,39] and considering the prolonged shedding and the raise of the proportion of subjects shedding resistant virus, this model seems to provide reliable prediction of resistance emergence in this population [14].

This model needs to be confronted to real experimental data to be validated. It can also help to design new experiment.

This work provides a global and accurate picture of oseltamivir effects in terms of efficacy and resistance emergence. However, to study oseltamivir effect after 8 days of follow up, the model should be completed to take into account the adaptive immune response necessary to clear the virus [40].

Our model indicates that oseltamivir should be used with caution for prophylaxis as it increases the risk of resistance emergence if the OC concentration is below the IC_{50}

at the infection time. In addition, it suggests that immunocompromised subjects should be treated with high doses in order to reduce the risk of resistance emergence. Once subjects are infected, “the sooner the better” as it combines higher efficacy and lower risk of resistance emergence. Further works might focus on different antiviral treatments and other administration routes.

Aknowledgements

We would like to thanks Craig Rayner (Roche Pharmaceuticals, Clinical pharmacology, Melbourne, Australia), Patrick Smith (F.Hoffmann-La Roche Ltd., Clinical pharmacology, Nutley, NJ, USA), Stephen Toovey (F.Hoffmann-La Roche Ltd., Pharmaceuticals Division, Basel, Switzerland), Mohamed Kamal (F. Hoffmann-La Roche Inc, Modeling & Simulation, Nutley, NJ, USA) and Micaela Reddy (Modeling and simulation group, DMPK department, Roche Palo Alto) for their advices.

References

1. Burch J, Corbett M, Stock C, Nicholson K, Elliot AJ, et al. (2009) Prescription of anti-influenza drugs for healthy adults: a systematic review and meta-analysis. Lancet Infect Dis 9: 537-545.
2. Hayden FG, Osterhaus AD, Treanor JJ, Fleming DM, Aoki FY, et al. (1997) Efficacy and safety of the neuraminidase inhibitor zanamivir in the treatment of influenzavirus infections. GG167 Influenza Study Group. N Engl J Med 337: 874-880.
3. Hayden FG, Treanor JJ, Fritz RS, Lobo M, Betts RF, et al. (1999) Use of the oral neuraminidase inhibitor oseltamivir in experimental human influenza: randomized controlled trials for prevention and treatment. JAMA 282: 1240-1246.
4. Monto AS (2003) The role of antivirals in the control of influenza. Vaccine 21: 1796-1800.
5. NICE (2009) Amantadine, oseltamivir and zanamivir for the treatment, Review of NICE technology appraisal guidance 58. London: National Institute for Clinical Excellence.
6. World Health Organization (2004) WHO guidelines on the use of vaccines and antivirals during influenza pandemics. Geneva, Switzerland: [Online.] http://www.who.int/csr/resources/publications/influenza/11_29_01_A.pdf.
7. Gubareva LV, Kaiser L, Hayden FG (2000) Influenza virus neuraminidase inhibitors. Lancet 355: 827-835.
8. Patel A, Gorman SE (2009) Stockpiling antiviral drugs for the next influenza pandemic. Clin Pharmacol Ther 86: 241-243.
9. Jefferson T, Jones M, Doshi P, Del Mar C (2009) Neuraminidase inhibitors for preventing and treating influenza in healthy adults: systematic review and meta-analysis. BMJ 339: b5106.
10. Sheu TG, Deyde VM, Okomo-Adhiambo M, Garten RJ, Xu X, et al. (2008) Surveillance for neuraminidase inhibitor resistance among human influenza A and B viruses circulating worldwide from 2004 to 2008. Antimicrob Agents Chemother 52: 3284-3292.
11. World Health Organization (2009) Pandemic (H1N1) 2009 - update 67. [Online.] http://www.who.int/csr/don/2009_09_25/en/index.html.
12. Kiso M, Mitamura K, Sakai-Tagawa Y, Shiraishi K, Kawakami C, et al. (2004) Resistant influenza A viruses in children treated with oseltamivir: descriptive study. Lancet 364: 759-765.
13. Chen LF, Dailey NJ, Rao AK, Fleischauer AT, Greenwald I, et al. (2010) Cluster of oseltamivir-resistant 2009 pandemic influenza A (H1N1) virus infections on a hospital ward among immunocompromised patients--North Carolina, 2009. J Infect Dis 203: 838-846.
14. Renaud C, Boudreault AA, Kuypers J, Lofy KH, Corey L, et al. (2011) H275Y Mutant Pandemic (H1N1) 2009 Virus in Immunocompromised Patients. Emerg Infect Dis 17: 653-660.
15. World Health Organization (2010) Update on oseltamivir resistant pandemic A (H1N1) 2009 influenza virus: January 2010. Weekly Epidemiological Record 85: 37-40.
16. Canini L, Carrat F (2011) Population Modeling of Influenza A/H1N1 Virus Kinetics and Symptom Dynamics. J Virol 85: 2764-2770.
17. Rayner CR, Chanu P, Gieschke R, Boak LM, Jonsson EN (2008) Population pharmacokinetics of oseltamivir when coadministered with probenecid. J Clin Pharmacol 48: 935-947.

18. Jullien V, Hubert D, Launay O, Babany G, Lortholary O, et al. (2011) Pharmacokinetics and diffusion into sputum of oseltamivir and oseltamivir carboxylate in cystic fibrosis adults. Antimicrob Agents Chemother.
19. Bloom JD, Gong LI, Baltimore D (2010) Permissive secondary mutations enable the evolution of influenza oseltamivir resistance. Science 328: 1272-1275.
20. Hamelin ME, Baz M, Abed Y, Couture C, Joubert P, et al. (2010) Oseltamivir-resistant pandemic A/H1N1 virus is as virulent as its wild-type counterpart in mice and ferrets. PLoS Pathog 6: e1001015.
21. Gubareva LV, Webster RG, Hayden FG (2001) Comparison of the activities of zanamivir, oseltamivir, and RWJ-270201 against clinical isolates of influenza virus and neuraminidase inhibitor-resistant variants. Antimicrob Agents Chemother 45: 3403-3408.
22. Hayden FG (2001) Perspectives on antiviral use during pandemic influenza. Philos Trans R Soc Lond B Biol Sci 356: 1877-1884.
23. Treanor JJ, Hayden FG, Vrooman PS, Barbarash R, Bettis R, et al. (2000) Efficacy and safety of the oral neuraminidase inhibitor oseltamivir in treating acute influenza: a randomized controlled trial. US Oral Neuraminidase Study Group. JAMA 283: 1016-1024.
24. Cowling BJ, Chan KH, Fang VJ, Lau LL, So HC, et al. (2010) Comparative epidemiology of pandemic and seasonal influenza A in households. N Engl J Med 362: 2175-2184.
25. Rong L, Z. F, Perelson AS (2007) Emergence of HIV-1 drug resistance during antiretroviral treatment. Bulletin of Mathematical Biology 69: 2027-2060.
26. Vaidya NK, Rong L, Marconi VC, Kuritzkes DR, Deeks SG, et al. (2010) Treatment-mediated alterations in HIV fitness preserve CD4+ T cell counts but have minimal effects on viral load. PLoS Comput Biol 6: e1001012.
27. World Health Organization (2010) WHO Guidelines for Pharmacological Management of Pandemic Influenza A(H1N1) 2009 and other Influenza Viruses - Part I Recommendations. [online] http://www.who.int/csr/resources/publications/swineflu/h1n1_guidelines_pharmaceutical_mngt.pdf.
28. Pineda-Krch M (2008) GillespieSSA: Implementing the stochastic simulation algorithm in R. J Stat Softw 25: 1-18.
29. Aoki FY, Macleod MD, Paggiaro P, Carewicz O, El Sawy A, et al. (2003) Early administration of oral oseltamivir increases the benefits of influenza treatment. J Antimicrob Chemother 51: 123-129.
30. Nicholson KG, Aoki FY, Osterhaus AD, Trottier S, Carewicz O, et al. (2000) Efficacy and safety of oseltamivir in treatment of acute influenza: a randomised controlled trial. Neuraminidase Inhibitor Flu Treatment Investigator Group. Lancet 355: 1845-1850.
31. Gubareva LV, Kaiser L, Matrosovich MN, Soo-Hoo Y, Hayden FG (2001) Selection of influenza virus mutants in experimentally infected volunteers treated with oseltamivir. J Infect Dis 183: 523-531.
32. Monto AS, McKimm-Breschkin JL, Macken C, Hampson AW, Hay A, et al. (2006) Detection of influenza viruses resistant to neuraminidase inhibitors in global surveillance during the first 3 years of their use. Antimicrob Agents Chemother 50: 2395-2402.
33. Handel A, Longini IM, Jr., Antia R (2007) Neuraminidase inhibitor resistance in influenza: assessing the danger of its generation and spread. PLoS Comput Biol 3: e240.

34. Maltezou HC, Drakoulis N, Siahanidou T, Karalis V, Zervaki E, et al. (2011) Safety and Pharmacokinetics of Oseltamivir for Prophylaxis of Neonates Exposed to Influenza H1N1. The Pediatric Infectious Disease Journal.
35. Oo C, Hill G, Dorr A, Liu B, Boellner S, et al. (2003) Pharmacokinetics of anti-influenza prodrug oseltamivir in children aged 1-5 years. Eur J Clin Pharmacol 59: 411-415.
36. Whitley RJ, Hayden FG, Reisinger KS, Young N, Dutkowski R, et al. (2001) Oral oseltamivir treatment of influenza in children. Pediatr Infect Dis J 20: 127-133.
37. Monteiro JM, Harvey C, Trinchieri G (1998) Role of interleukin-12 in primary influenza virus infection. J Virol 72: 4825-4831.
38. Santoli D, Trinchieri G, Koprowski H (1978) Cell-mediated cytotoxicity against virus-infected target cells in humans. II. Interferon induction and activation of natural killer cells. J Immunol 121: 532-538.
39. Stein-Streilein J, Guffee J (1986) In vivo treatment of mice and hamsters with antibodies to asialo GM1 increases morbidity and mortality to pulmonary influenza infection. J Immunol 136: 1435-1441.
40. Miao H, Hollenbaugh JA, Zand MS, Holden-Wiltse J, Mosmann TR, et al. (2010) Quantifying the early immune response and adaptive immune response kinetics in mice infected with influenza A virus. J Virol 84: 6687-6698.
41. White MR, Doss M, Boland P, Tecle T, Hartshorn KL (2008) Innate immunity to influenza virus: implications for future therapy. Expert Rev Clin Immunol 4: 497-514.
42. Baccam P, Beauchemin C, Macken CA, Hayden FG, Perelson AS (2006) Kinetics of influenza A virus infection in humans. J Virol 80: 7590-7599.
43. Wattanagoon Y, Stepniewska K, Lindegardh N, Pukrittayakamee S, Silachamroon U, et al. (2009) Pharmacokinetics of high-dose oseltamivir in healthy volunteers. Antimicrob Agents Chemother 53: 945-952.

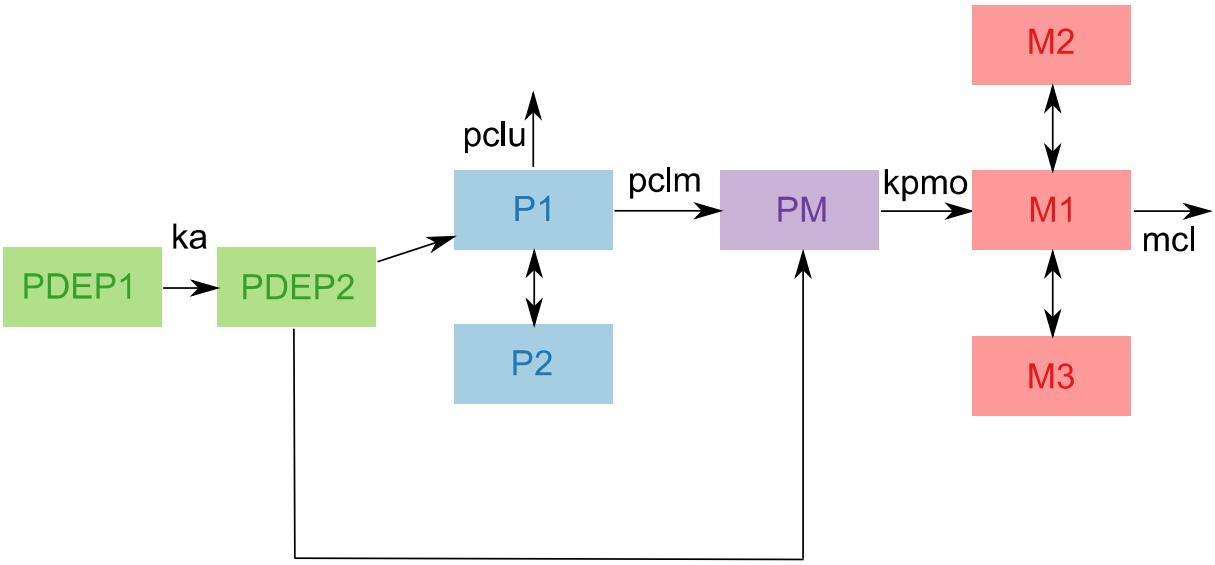

Figure 1: Graphical presentation of the PK model of oseltamivir. *$PDEP_1$,* oseltamivir phosphate before absorption; *$PDEP_2$,* oseltamivir phosphate before first-pass effect;*P*, oseltamivir phosphate; *PM*, conversion compartment*; M*, oseltamivir carboxylate. The five mixed parameters are: *ka*, absorption rate constant; *pclu*, urinary clearance of *P* from compartment 1; *pclm*, metabolic clearance of *P* from compartment 1; *kpmo*, *P −M* conversion rate; *mcl*, total elimination clearance of *M* from compartment 1.

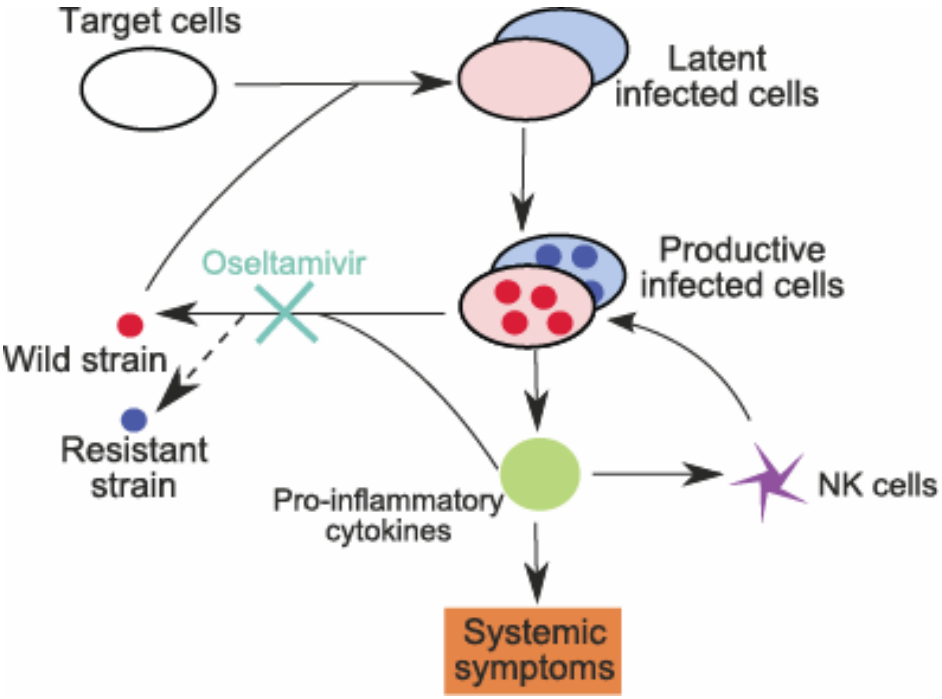

Figure 2: Graphical presentation of the VKSD model with resistance emergence and treatment effect. The free virus infects target epithelial cells, which become latent infected cells i.e. not yet producing virus, before becoming productive infected cells. These latter cells produce free virus and lead to the production of pro-inflammatory cytokines, either directly or via activation of macrophages or dendritic cells. Cytokines reduce the virus production rate, activate natural killer (NK) cells and induce systemic symptoms. NK cells kill infected cells. Resistant virus can emerge during replication

and will itself infects target cell and induce the whole VKSD cycle. Moreover, oseltamivir treatment acts by blocking the release of free viruses.

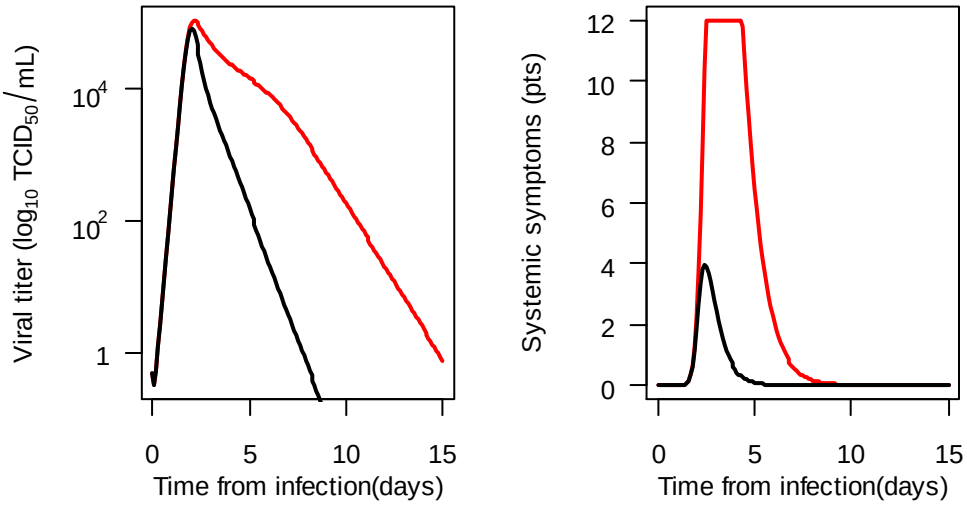

Figures 3: Population viral kinetics (left panel) and symptoms dynamic (right panel) for healthy (black) and immunocompromised (red) subjects

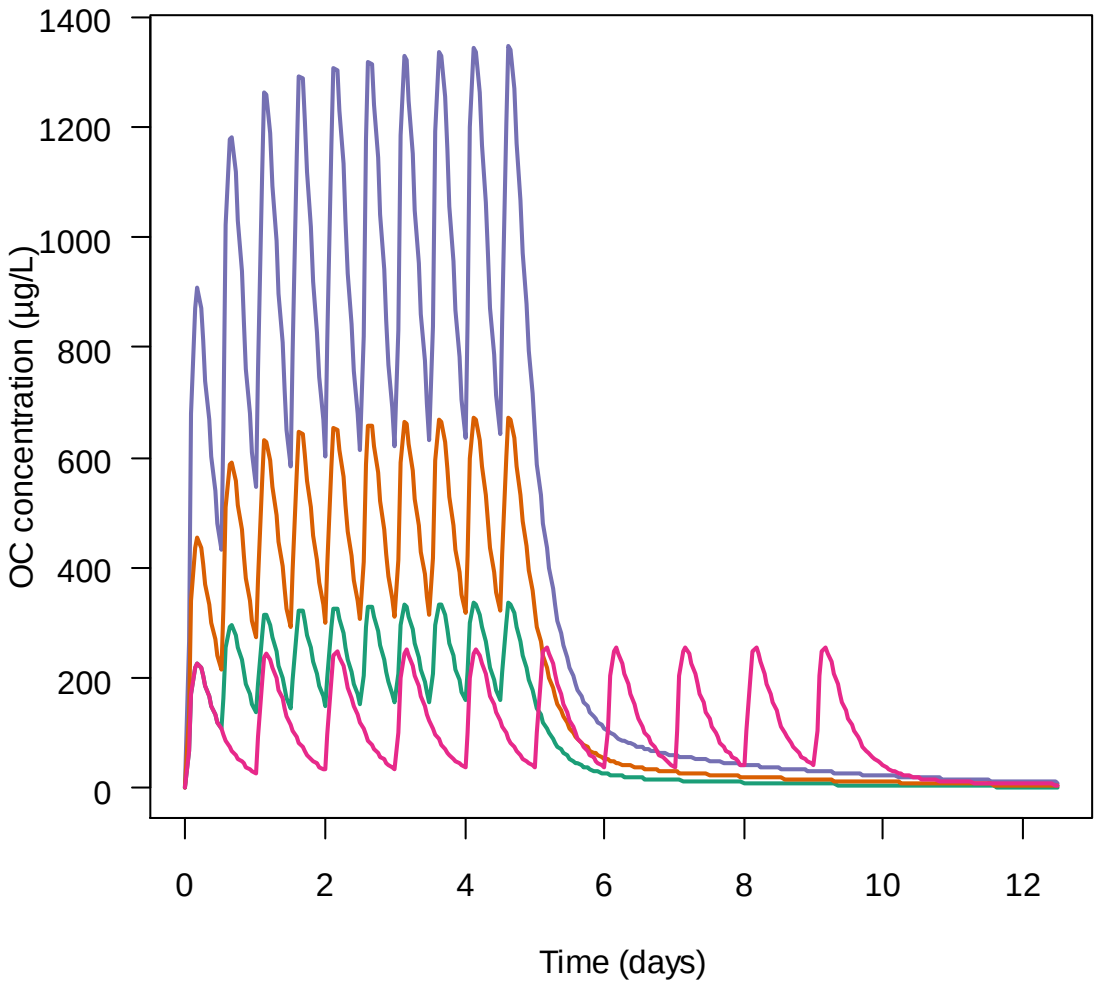

Figure 4: Oseltamivir carboxylate kinetics (purple line: 300 mg bid during 5 days, orange line: 150 mg bid suring 5 days, green line: 75 mg bid during 5 days, pink line: 75mg in.d. 10 days)

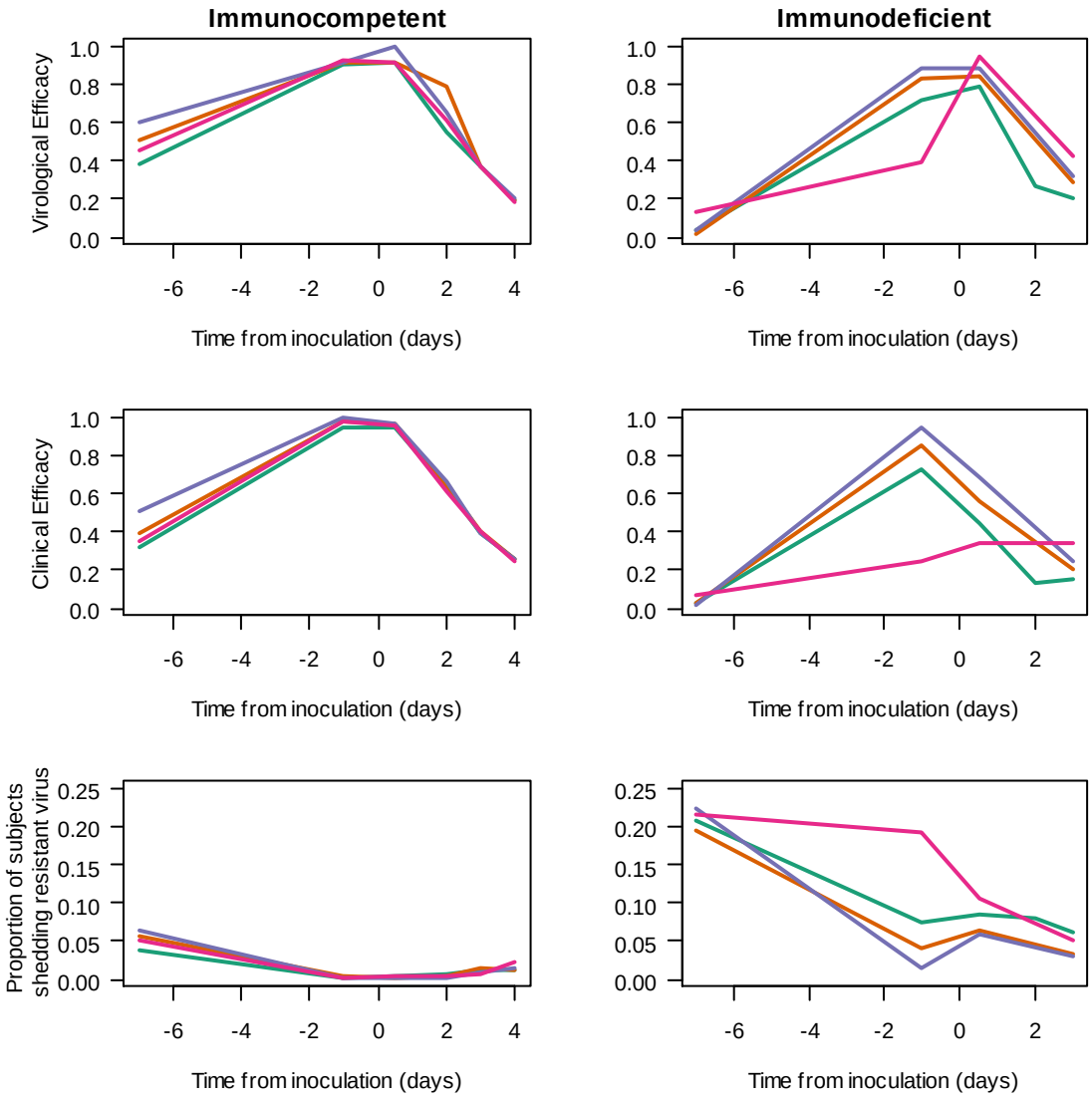

Figure 5: Oseltamivir efficacy: (R1: 75mg in d. 10 days, R2: 75 mg bid 5 days, R3: 150mg bid 5 days, R4: 300mg bid, 5 days). 0 stands for the inoculation time; negative times represent prophylaxis intakes and positive times treatment intakes.

The upper panel represents the virological efficacy, i.e. the decrease of virus shedding over time depending on the time of first oseltamivir intake. The middle panel represents the clinical efficacy, i.e. the decrease of systemic symptoms intensity over time depending on the time of first oseltamivir intake. The lower panel represents the emergence of resistant virus, i.e. the proportion of patients shedding resistant virus above the LOD.

Supplementary material

The PK model for oseltamivir used a set of ordinary differential equations.

$$\frac{d\,PDEP_1}{dt} = -ka\ PDEP_1$$

$$\frac{d\,PDEP_2}{dt} = ka\ (PDEP_1 - PDEP_2)$$

$$\frac{d\,P_1}{dt} = -(k_{10P} + kpmi)\,P_1 - k_{12P}\,P_1 + k_{21P}\,P_2 + fx\ ka\ PDEP_2$$

$$\frac{d\,P_2}{dt} = k_{12p}\,P_1 - k_{21P}\,P_2$$

$$\frac{d\,PM}{dt} = kpmi\ P_1 - kpmo\ PM + (1 - fx)\,ka\ PDEP_2$$

$$\frac{d\,M_1}{dt} = kpmo\ mwf\ \ PM - k_{10M}\,M_1 - k_{12M}\,M_1 + k_{21M}\,M_2 - k_{13M}\,M_1 + k_{31M}\,M_3$$

$$\frac{d\,M_2}{dt} = k_{12M}\,M_1 - k_{21M}\,M_2$$

$$\frac{d\,M_3}{dt} = k_{13M}\,M_1 - k_{31M}\,M_3$$

Where $PDEP_i$, stands for oseltamivir phosphate before absorption; *P*, oseltamivir phosphate; *M*, oseltamivir carboxylate; *PM*, conversion compartment. The index is related to the compartment in which the compound is at time t. 1 is used for the central compartement whereas 2 and 3 are peripherical compartements in which the molecule is distributed.

The model was parameterized with *pclm*, metabolic clearance of *P* from compartment 1; *pclu*, urinary clearance of *P* from compartment 1; pv_1, volume of distribution of *P* in compartment 1; *ka*, absorption rate constant; *fx*, bioavailability; pq_2, distribution clearance of *P* from compartment 1 to 2; pv_2, volume of distribution of *P* in compartment 2; *kpmo*, *P* −*M* conversion rate; mwf, molecular weight correction;*mcl*, total elimination clearance of *M* from compartment 1; mv_1, volume of distribution of *M* in compartment 1; mq_2, distribution clearance of *M* from compartment 1 to 2; mv_2,

volume of distribution of *M* in compartment 2; mq_3, distribution clearance of *M* from compartment 1 to 3; mv_3, volume of distribution of *M* in compartment 3.

The VKSD model used a set of ordinary differential equations. The compartments were uninfected target cells (T), unproductive infected cells (I1), productive infected cells (I2), infectious viral titers expressed in TCID50/mL (V), natural killer cells (Nk) and cytokines (F) (Figure 1-b). Note that here the cytokines compartment is taken “as a whole" and not restricted to the IFN only as in the Baccam model. It involves a large number of cytokines as immunomodulators [41].

$$\frac{dT}{dt} = -\beta TV$$

$$\frac{d\,I_1}{dt} = \beta TV - k\,I_1$$

$$\frac{d\,I_2}{dt} = k\,I_1 - \delta\,I_2 - \tau\,I_2 N_k$$

$$\frac{dF}{dt} = I - \alpha F$$

$$\frac{d\,N_k}{dt} = F - \xi\,N_k$$

$$\frac{dV}{dt} = \frac{p}{1+\psi F}\,I_2 - cV$$

Compartmental models were parameterized in terms of the infection rate (β), cytokines clearance (α), the transition rate from unproductive to productive infected cells (k), the mortality rate of infected cells (δ), the rate of virus production by infected productive cells (p), the effect of cytokines on p (ψ), the effect of NK cells on infected cells (τ), the NK cells clearance (ξ) and the virus clearance (c). T0, the initial number of target cells in the upper respiratory tract, was set to $4x10^8$ cells [42]. We set the

cytokines and NK cells production rates to 1, as this changes only the units in which the early immune response is measured and does not lead to a loss of generality.

Individual parameters were simulated as $\theta_i = \theta_{pop} e^{\eta_{\theta i}}$, where θ_i is the individual parameter for the subject i, θ_{pop} and $\eta_{\theta i}$ are the population parameter and the random effect. θ_{pop} and ω_θ were drawn from lognormal distributions $lnN(\mu_\theta, \sigma^2_\theta)$ and $lnN(\mu_\omega, \sigma^2_\omega)$ respectively, where μ_x and σ^2_x were the mean and variance estimated in previous works [16,17,43]. $\eta_{\theta i}$ was drawn from a Gaussian distribution $N(0, \omega^2_\theta)$, where ω_θ represents the inter-individual variability of the parameter $\tilde{\theta}$

Supplementary Table 1: Structure of the stochastic process: *$PDEP_1$,* oseltamivir phosphate before absorption; *$PDEP_2$,* oseltamivir phosphate before first-pass effect;*P*, oseltamivir phosphate; *M*, oseltamivir carboxylate; *PM*, conversion compartment; *pclm*, metabolic clearance of *P* from compartment 1; *pclu*, urinary clearance of *P* from compartment 1; *pv_1*, volume of distribution of *P* in compartment 1; *ka*, absorption rate constant; *fx*, bioavailability; *pq_2*, distribution clearance of *P* from compartment 1 to 2; *pv_2*, volume of distribution of *P* in compartment 2; *kpmo*, *P −M* conversion rate; mwf, molecular weight correction;*mcl*, total elimination clearance of *M* from compartment 1; *mv_1*, volume of distribution of *M* in compartment 1; *mq_2*, distribution clearance of *M* from compartment 1 to 2; *mv_2*, volume of distribution of *M* in compartment 2; *mq_3*, distribution clearance of *M* from compartment 1 to 3; *mv_3*, volume of distribution of *M* in compartment 3.

	Event	**Population at t**	→	**Population at t+Δt**	**Probability**
Pharmacokinetics	Absorption of OP	$PDEP_1$ $PDEP_2$	→	$PDEP_1$-1 $PDEP_2$+1	$kaPDEP_1\ \Delta t$
	Diffusion of OP to compartment 1	$PDEP_2$ P_1	→	$PDEP_2$-1	$fx\ ka\ PDEP_2\ \Delta t$
	Urinary clearance of OP	P_1	→	P_1+1	$pclu/pv_1\ P_1\ \Delta t$
	Metabolic clearance of OP	P_1 PM	→	P_1-1 PM+1	$pclm/pv_1\ P_1\ \Delta t$
	Distribution of OP from compartment 1 to 2	P_1 P_2	→	P_1-1 P_2+1	$pq_2/pv_1\ P_1\ \Delta t$
	Distribution of OP from compartment 2 to 1	P_1 P_2	→	P_1+1 P_2-1	$pq_2/pv_2\ P_2\ \Delta t$
	Conversion of OP into OC	PM M_1	→	PM-1 M_1+1	$kpmo\ mwf\ PM\ \Delta t$
	By-pass of the first-pass effect	$PDEP_2$ PM	→	$PDEP_2$-1 PM+1	$(1\text{-}fx)ka\ PDEP_2\ \Delta t$
	Clearance of OC	M_1	→	M_1-1	$mcl/mv_1\ M_1\ \Delta t$
	Distribution of OC from compartment 1 to 2	M_1 M_2	→	M_1-1 M_2+1	$mq_2/mv_1\ M_1\ \Delta t$
	Distribution of OC from compartment 2 to 1	M_1 M_2	→	M_1+1 M_2-1	$mq_2/mv_2\ M_2\ \Delta t$
	Distribution of OC from compartment	M_1 M_3	→	M_1-1 M_3+1	$mq_3/mv_1\ M_1\ \Delta t$

	1 to 3				
	Distribution of OC from compartment 3 to 1	M_1 M_3	→	M_1+1 M_3-1	$mq_3/mv_3\ M_3\ \Delta t$
Viral kinetics	Production of latent cells infected by susceptible virus	T I_1	→	T-1 I_1+1	$\beta TV\ \Delta t$
	Production of cells producing susceptible virus	I_1 I_2	→	I_1-1 I_2+1	$kI_1\ \Delta t$
	Production of pro-inflammatory cytokines	F	→	F+1	$(I2+J2)\ \Delta t$
	Production of susceptible virus	V	→	V+1	$(1-M_1/(IC_{50}+M_1))pI_2/(1+\psi F)\ \Delta t$
	Clearance of susceptible virus	V	→	V-1	$cV\ \Delta t$
	Clearance of pro-inflammatory cytokines	F	→	F-1	$\alpha F\ \Delta t$
	Death of infected cells producing susceptible virus	I_2 D	→	I_2-1 D+1	$(k/(k-1)I_2+\tau I_2 NK)\ \Delta t$
	Production of NK cells	NK	→	NK+1	$F\ \Delta t$
	Death of NK cells	NK	→	NK-1	$\xi NK\ \Delta t$
	Production of latent cells infected by resistant virus	T J_1	→	T-1 J_1+1	$\beta TR\ \Delta t$
	Production of cells producing resistant virus	J_1 J_2	→	J_1-1 J_2+1	$kJ_1\ \Delta t$
	Production of resistant virus	R	→	R+1	$(1-M_1/(IC'_{50}+M_1))p(\lambda I_2+J_2)/(1+\psi F)\ \Delta t$
	Death of infected cells producing	J_2 D	→	J_2-1 D+1	$(k/(k-1)J_2+\tau J_2 NK)\ \Delta t$

	resistant virus				
	Clearance of resistant virus	R	→	R-1	cR Δt
Symptoms dynamics	Production of systemic symptoms	S	→	S+1	γF Δt
	Alleviation of systemic symptoms	S	→	S-1	hS Δt

6.4.2 Comments

We simulated the effect of oseltamivir treatment on viral kinetics and systemic symptoms dynamics as well as on resistant virus emergence. We explored for the first time the effect of time of first intake, of regimen and of immune status. We used parameter estimates from two studies [120, 161] and we derived the resistant variant emergence based upon observations of the proportion of treated patients shedding resistant virus [162, 163]. We found that the clinical and virological efficacy as well as the resistant variant emergence depended on the time of first intake, on the immune status and we found a stronger dose effect in immunocompromised than in otherwise healthy subjects. We also found that when the first intake was set 7 days prior inoculation time, it led to high proportion of subjects shedding resistant virus in both immunocompromised and otherwise healthy subjects, respectively between 19.4 and 22.4% and between 3.7 and 6.3% depending on the dose. This situation can occur in the case of a seasonal or post-exposure prophylaxis. We can also doubt of the subjects' compliance in the real world in the absence of symptoms or in the absence of cases in their circle. This could lead to an even more increased proportion of subjects shedding resistant virus.

Eventhough this model needs to be confronted to real experimental data to be validated, simulation is useful to consider hypotheses that cannot be investigated during a trial, such as testing regimens likely to generate resistant virus or experimental inoculation of influenza virus in immunocompromised subjects.

7 Conclusion & perspectives

Influenza epidemiology has been intensively studied. Several models were developed to describe the disease transmission in the population and the effect of mitigating measures [18–21, 25]. These models use natural history parameters which are directly connected to influenza dynamics.

Thus understanding influenza infection dynamics within host and its variability between subjects is crucial. Key parameters of influenza transmission models such as infectiousness and generation time depend directly on viral shedding as shown in part 2.2.2.
In this thesis, we used an integrative approach to describe the complex phenomenon which is influenza infection. It combines biological knowledge about influenza infection and immune response, mathematical modeling and epidemiology.

We develop the first model of kinetics of influenza infection taking into consideration the subject's symptoms such as fever as presented in part 4.5. We used for this work a population approach which allows one to use the information from a set of patients to infer the distribution of parameters that characterize the infection and patient symptoms in the population as well as in each individual.
The models presented in this thesis were developed for specific populations experimentally inoculated for simplicity purpose.
This model also proposed an innate immune response model to describe the time course of NK cell activity and even though the results concerning the pro-inflammatory cy-

tokines and NK cells were speculative, they were in accordance with what was previously oberved [45, 117]. By definition, a model is a simplified representation of reality and is thus imperfect. The approximations have little impact on the viral kinetics or symptoms dynamics conclusions, as they are descriptive. However, the findings about innate immune response should be carefully considered as they were based on speculation. This shows the importance of adapting the study design.

We derived natural history parameters from the viral kinetics and symptoms dynamics, based upon the hypothesis that infectiousness is proportional to the viral titer. Some ongoing studies are using viral titers as a primary source for transmission model parameter estimation.

Another novelty of this work was the use an appropriate statistical method to describe the different levels of variability. Influenza infection and illness variability is responsible for several issues in epidmiological studies. For instance, influenza-like illness clinical case definition is temperature over 37.8°C with cough or sore throat. We found a high rate of asymptomatic infection explaining that it is difficult to clearly identify the chain transmission.

Viral kinetics was only recently studied. Indeed, the data are scarce and difficult to collect, especially in the case of naturally acquired infections. On the other hand, experimental inoculation of influenza virus can be seen as unethical. This is why, planning rationalized study design is crucial. We need data that are enough informative to fit the model and easy to collect for practical reasons. We then proposed a design that meets this requirement in part 5. This design needs 50% less samples and allows precise estimates of the model parameters. We suggest to add sample times for pro-inflammatory cytokines and/or NK cells to bring information about the innate immune response and to refine the model previously developed.

A better understanding of influenza infection dynamics could also enhance the strategies to mitigate influenza. Several measures might be ineffective due to a bad synchronisation of their application with the disease dynamics. For instance patient isolation occurs often after the infectious period which making it ineffective. During the 2009 pandemic, according to World Health Organization, the virus was identified in May. However, vaccination campaign in France started in October, five months after the first cases. In case of a new pandemic, several weeks will be necessary to develop an adapted vaccine. Contrary to vaccine the mechanism of action of antivirals is independent of the viral strain and could hence be used in the early stage of a pandemic when vaccine could not be developed in time [164, 165]. The use of antivirals is thus essential in the initial response to pandemic influenza. An other matter is resistance emergence. There is indeed a high level of resistance of circulating influenza strains to anti-influenza drugs, such as oseltamivir. We need to rich a balance between efficacy and resistance emergence to preserve the usefulness of such drugs. We hence used the model from part 3 and modified it to take into account oseltamivir pharmacokinetics and resistant strains emergence. Our result suggest that prophylaxis should be avoided as it may dramatically increase the risk of resistance emergence.

Many perspectives can be considered. First, fitting the model to data enriched with pro-inflammatory and/or NK cells dynamics data is necessary to validate our results.
Second, repiratory symptoms could be modeled to complete the picture of influenza dynamics. Respiratory symptoms are associated with the spread of the virus in the environment and most probably modify the infectiousness in time.
Third, some avenues of research should be investigated to explain the great variability observed in influenza dynamics. For instance, transcriptional dynamics role on influenza infection and illness variability could be studied as it was shown to be associated with influenza illness severity and could explain a great part of influenza infection variability.

Also, the influence of the viral strains of influenza dynamics should be studied. The role of pre-existing adaptive immune on susceptibility to influenza could also be explored. As the protection towards influenza varies with the antibody titers, studying antibodies kinetics could bring new elements for influenza epidemiology. Little is known about adaptive immune response dynamics in humans and immune response dynamics after vaccine was never studied to our knowledge.

These improvements are aimed to describe influenza infection and illness dynamics to provide an image as close as possible to naturally acquired infection. Undersanding the disease dynamics without interventions is a first step to figure out the effect of measures such as antiviral use. This work point out the importance of learning as much as we can about dealing with influenza infection and mitigating its impact.

Bibliography

[1] Smith W, Andrewes C, BLaidlwa P. A virus isolated from influenza patients. The Lancet. 1933;2:66–68.

[2] Alexander D, Brown I, et al. Recent zoonoses caused by influenza A viruses. Revue scientifique et technique (International Office of Epizootics). 2000;19(1):197.

[3] Guang-jian Z, Zong-shuai L, Yan-li Z, Shi-jin J, Zhi-jing X. Genetic characterization of a novel influenza A virus H5N2 isolated from a dog in China. Veterinary Microbiology. 2011;.

[4] Francis T. A new type of virus from epidemic influenza. Science. 1940;92(2392):405.

[5] Cox N, Subbarao K. Global epidemiology of influenza: past and present. Annual review of medicine. 2000;51(1):407–421.

[6] Neumann G, Noda T, Kawaoka Y. Emergence and pandemic potential of swine-origin H1N1 influenza virus. Nature. 2009;459(7249):931–939.

[7] Taubenberger JK, Morens DM. The pathology of influenza virus infections. Annual review of pathology. 2008;3:499.

[8] Webster RG, Bean WJ, Gorman OT, Chambers TM, Kawaoka Y. Evolution and ecology of influenza A viruses. Microbiological reviews. 1992;56(1):152–179.

[9] Viboud C, Alonso WJ, Simonsen L. Influenza in tropical regions. PLoS medicine. 2006;3(4):e89.

[10] Carrat F, Flahault A. Influenza vaccine: the challenge of antigenic drift. Vaccine. 2007;25(39-40):6852–6862.

[11] Dushoff J, Plotkin JB, Viboud C, Earn DJD, Simonsen L. Mortality due to influenza in the United States—an annualized regression approach using multiple-cause mortality data. American Journal of Epidemiology. 2006;163(2):181.

[12] Langmuir AD, Worthen TD, Solomon J, Ray CG, Petersen E. The Thucydides syndrome. New England Journal of Medicine. 1985;313(16):1027–1030.

[13] Potter CW. Chronicle of influenza pandemics. In: Nicholson KG, Webster RF, Hay AJ, editors. Textbook of Influenza. Oxford: Blackwell Science Ltd.; 1998. p. 3–18.

[14] Taubenberger JK, Reid AH, Krafft AE, Bijwaard KE, Fanning TG. Initial genetic characterization of the 1918 "Spanish" influenza virus. Science. 1997;275(5307):1793.

[15] Shope RE. Swine influenza: III Filtration experiments and etiology. The Journal of experimental medicine. 1931;54(3):373–385.

[16] Chang W. National influenza experience in Hong Kong, 1968. Bulletin of the World Health Organization. 1969;41(3-4-5):349.

[17] Chowell G, Bertozzi SM, Colchero MA, Lopez-Gatell H, Alpuche-Aranda C, Hernandez M, et al. Severe respiratory disease concurrent with the circulation of H1N1 influenza. New England Journal of Medicine. 2009;361(7):674–679.

[18] Ferguson N, Cummings D, Cauchemez S, Fraser C, Riley S, Meeyai A, et al. Strategies for containing an emerging influenza pandemic in Southeast Asia. Nature. 2005;437(7056):209.

[19] Ferguson NM, Cummings DAT, Fraser C, Cajka JC, Cooley PC, Burke DS. Strategies for mitigating an influenza pandemic. Nature. 2006;442(7101):448–452.

[20] Longini IM, Nizam A, Xu S, Ungchusak K, Hanshaoworakul W, Cummings DAT, et al. Containing pandemic influenza at the source. Science. 2005;309(5737):1083.

[21] Carrat F, Luong J, Lao H, Sallé AV, Lajaunie C, Wackernagel H. A'small-world-like'model for comparing interventions aimed at preventing and controlling influenza pandemics. BMC medicine. 2006;4(1):26.

[22] Cauchemez S, Carrat F, Viboud C, Valleron A, Boelle P. A Bayesian MCMC approach to study transmission of influenza: application to household longitudinal data. Statistics in medicine. 2004;23(22):3469–3487.

[23] Cauchemez S, Donnelly CA, Reed C, Ghani AC, Fraser C, Kent CK, et al. Household transmission of 2009 pandemic influenza A (H1N1) virus in the United States. New England Journal of Medicine. 2009;361(27):2619–2627.

[24] Elveback LR, Fox JP, Ackerman E, Langworthy A, Boyd M, Gatewood L. An influenza simulation model for immunization studies. American Journal of Epidemiology. 1976;103(2):152.

[25] Germann TC, Kadau K, Longini Jr IM, Macken CA. Mitigation strategies for pandemic influenza in the United States. PNAS. 2006;103(15):5935–5940.

[26] Chao DL, Halloran ME, Obenchain VJ, Longini IM. FluTE, a publicly available stochastic influenza epidemic simulation model. PLoS computational biology. 2010;6(1):e1000656.

[27] Mills CE, Robins JM, Lipsitch M. Transmissibility of 1918 pandemic influenza. Nature. 2004;432(7019):904–906.

[28] Baccam P, Beauchemin C, Macken CA, Hayden FG, Perelson AS. Kinetics of influenza A virus infection in humans. Journal of virology. 2006;80(15):7590.

[29] Handel A, Longini Jr IM, Antia R. Towards a quantitative understanding of the within-host dynamics of influenza A infections. Journal of The Royal Society Interface. 2010;7(42):35–47.

[30] Handel A, Longini IM, Antia R. Neuraminidase inhibitor resistance in influenza: assessing the danger of its generation and spread. PLoS Computational Biology. 2007;3(12):e240.

[31] Miao H, Hollenbaugh JA, Zand MS, Holden-Wiltse J, Mosmann TR, Perelson AS, et al. Quantifying the early immune response and adaptive immune response kinetics in mice infected with influenza A virus. Journal of virology. 2010;84(13):6687–6698.

[32] Saenz RA, Quinlivan M, Elton D, MacRae S, Blunden AS, Mumford JA, et al. Dynamics of influenza virus infection and pathology. Journal of virology. 2010;84(8):3974.

[33] Whittaker GR. Intracellular trafficking of influenza virus: clinical implications for molecular medicine. Expert Reviews in Molecular Medicine. 2001;3(05):1–13.

[34] De Clercq E, Neyts J. Avian influenza A (H5N1) infection: targets and strategies for chemotherapeutic intervention. Trends in pharmacological sciences. 2007;28(6):280–285.

[35] Carrat F, Vergu E, Ferguson NM, Lemaitre M, Cauchemez S, Leach S, et al. Time lines of infection and disease in human influenza: a review of volunteer challenge studies. American journal of epidemiology. 2008;167(7):775.

[36] Cowling BJ, Chan KH, Fang VJ, Lau LLH, So HC, Fung ROP, et al. Comparative epidemiology of pandemic and seasonal influenza A in households. New England Journal of Medicine. 2010;362(23):2175–2184.

[37] Couch RB, Kasel JA. Immunity to influenza in man. Annual Reviews in Microbiology. 1983;37(1):529–549.

[38] French AR, Yokoyama WM. Natural killer cells and viral infections. Current opinion in immunology. 2003;15(1):45–51.

[39] Huang Y, Zaas AK, Rao A, Dobigeon N, Woolf PJ, Veldman T, et al. Temporal dynamics of host molecular responses differentiate symptomatic and asymptomatic influenza a infection. PLoS Genet. 2011;7(8):e1002234.

[40] Doherty PC, Topham DJ, Tripp RA, Cardin RD, Brooks JW, Stevenson PG. Effector CD4+ and CD8+ T-cell mechanisms in the control of respiratory virus infections. Immunological reviews. 1997;159(1):105–117.

[41] Doherty PC, Allan W, Eichelberger M, Carding SR. Roles of alphabeta and gammadelta T Cell Subsets in Viral Immunity. Annual review of immunology. 1992;10(1):123–151.

[42] Bridges CB, Thompson WW, Meltzer MI, Reeve GR, Talamonti WJ, Cox NJ, et al. Effectiveness and cost-benefit of influenza vaccination of healthy working adults. JAMA: The Journal of the American Medical Association. 2000;284(13):1655.

[43] Canini L, Andréoletti L, Ferrari P, D'Angelo R, Blanchon T, Lemaitre M, et al. Surgical mask to prevent influenza transmission in households: a cluster randomized trial. PLoS One. 2010;5(11):e13998.

[44] Cowling BJ, Chan KH, Fang VJ, Cheng CKY, Fung ROP, Wai W, et al. Facemasks and hand hygiene to prevent influenza transmission in households. Annals of Internal Medicine. 2009;151(7):437–446.

[45] Hayden FG, Fritz R, Lobo MC, Alvord W, Strober W, Straus SE. Local and systemic cytokine responses during experimental human influenza A virus infection. Relation to symptom formation and host defense. Journal of Clinical Investigation. 1998;101(3):643.

[46] Hayden FG, Gwaltney JMJ. Viral infections. In: Philadelphia WSC, editor. Textbook of Respiratory Medicine. J.F. Murray and JA. Nadel; 1994. p. 977–1035.

[47] Hayden FG, Palese PA. Influenza virus. In: Richmond DD, Whitley RJ, Hayden FG, editors. Clinical virology. Churchill Livingstone, Inc., New York; 1997. p. 911–942.

[48] Fabian P, McDevitt JJ, DeHaan WH, Fung ROP, Cowling BJ, Chan KH, et al. Influenza virus in human exhaled breath: an observational study. PLoS One. 2008;3(7):e2691.

[49] Blachere FM, Lindsley WG, Pearce TA, Anderson SE, Fisher M, Khakoo R, et al. Measurement of airborne influenza virus in a hospital emergency department. Clinical Infectious Diseases. 2009;48(4):438.

[50] Riley RL. Airborne infection. The American journal of medicine. 1974;57(3):466–475.

[51] Alford RH, Kasel JA, Gerone PJ, Knight V. Human influenza resulting from aerosol inhalation. Experimental Biology and Medicine. 1966;122(3):800.

[52] Brankston G, Gitterman L, Hirji Z, Lemieux C, Gardam M. Transmission of influenza A in human beings. The Lancet infectious diseases. 2007;7(4):257–265.

[53] Bridges CB, Kuehnert MJ, Hall CB. Transmission of influenza: implications for control in health care settings. Clinical Infectious Diseases. 2003;37(8):1094–1101.

[54] Tellier R. Review of aerosol transmission of influenza A virus. Emerging Infectious Diseases. 2006;12(11):1657–62.

[55] Grassly NC, Fraser C. Mathematical models of infectious disease transmission. Nature Reviews Microbiology. 2008;6(6):477–487.

[56] Lowen AC, Mubareka S, Tumpey TM, García-Sastre A, Palese P. The guinea pig as a transmission model for human influenza viruses. Proceedings of the National Academy of Sciences. 2006;103(26):9988.

[57] Herlocher ML, Elias S, Truscon R, Harrison S, Mindell D, Simon C, et al. Ferrets as a transmission model for influenza: sequence changes in HA1 of type A (H3N2) virus. Journal of Infectious Diseases. 2001;184(5):542.

[58] Anderson RM, May RM. Directly transmitted infections diseases: control by vaccination. Science. 1982;215(4536):1053.

[59] Svensson Å. A note on generation times in epidemic models. Mathematical biosciences. 2007;208(1):300–311.

[60] Casanova JL, Abel L. The human model: a genetic dissection of immunity to infection in natural conditions. Nature Reviews Immunology. 2004;4(1):55–66.

[61] Schaffer F, Soergel M, Straube D. Survival of airborne influenza virus: effects of propagating host, relative humidity, and composition of spray fluids. Archives of virology. 1976;51(4):263–273.

[62] Eccles R. An explanation for the seasonality of acute upper respiratory tract viral infections. Acta oto-laryngologica. 2002;122(2):183–191.

[63] Cannell J, Vieth R, Umhau J, Holick M, Grant W, Madronich S, et al. Epidemic influenza and vitamin D. Epidemiology and Infection. 2006;134(06):1129–1140.

[64] Wang TT, Nestel FP, Bourdeau V, Nagai Y, Wang Q, Liao J, et al. Cutting edge: 1, 25-dihydroxyvitamin D3 is a direct inducer of antimicrobial peptide gene expression. The Journal of Immunology. 2004;173(5):2909.

[65] Liu PT, Stenger S, Li H, Wenzel L, Tan BH, Krutzik SR, et al. Toll-like receptor triggering of a vitamin D-mediated human antimicrobial response. Science. 2006;311(5768):1770.

[66] Young Jr GA, Underdahl NR, Carpenter LE. Vitamin D Intake and Susceptibility of Mice to Experimental Swine Influenza Virus Infection. Experimental Biology and Medicine. 1949;72(3):695.

[67] Cannell JJ, Zasloff M, Garland CF, Scragg R, Giovannucci E, et al. On the epidemiology of influenza. Virol J. 2008;5(1):29.

[68] Hope-Simpson RE. The role of season in the epidemiology of influenza. The Journal of hygiene. 1981;86(1):35.

[69] Shaman J, Jeon CY, Giovannucci E, Lipsitch M. Shortcomings of vitamin D-based model simulations of seasonal influenza. PloS one. 2011;6(6):e20743.

[70] Webster RG, Laver WG, Air GM, Schild GC. Molecular mechanisms of variation in influenza viruses. Nature. 1982;296(5853):115–121.

[71] Domingo E, Holland JJ. RNA virus mutations and fitness for survival. Annual Reviews in Microbiology. 1997;51(1):151–178.

[72] Drake JW, Charlesworth B, Charlesworth D, Crow JF. Rates of spontaneous mutation. Genetics. 1998;148(4):1667.

[73] Nachman MW, Crowell SL. Estimate of the mutation rate per nucleotide in humans. Genetics. 2000;156(1):297.

[74] Lauring AS, Andino R. Quasispecies theory and the behavior of RNA viruses. PLoS pathogens. 2010;6(7):e1001005.

[75] Russell RJ, Haire LF, Stevens DJ, Collins PJ, Lin YP, Blackburn GM, et al. The structure of H5N1 avian influenza neuraminidase suggests new opportunities for drug design. Nature. 2006;443(7107):45–49.

[76] Collins PJ, Haire LF, Lin YP, Liu J, Russell RJ, Walker PA, et al. Crystal structures of oseltamivir-resistant influenza virus neuraminidase mutants. Nature. 2008;453(7199):1258–1261.

[77] Ives JA, Carr JA, Mendel DB, Tai CY, Lambkin R, Kelly L, et al. The H274Y mutation in the influenza A/H1N1 neuraminidase active site following oseltamivir phosphate treatment leave virus severely compromised both in vitro and in vivo. Antiviral Research. 2002 August;55(2):307–317.

[78] Duan S, Boltz DA, Seiler P, Li J, Bragstad K, Nielsen LP, et al. Oseltamivir–Resistant Pandemic H1N1/2009 Influenza Virus Possesses Lower Transmissibility and Fitness in Ferrets. PLoS pathogens. 2010;6(7):e1001022.

[79] Bloom JD, Gong LI, Baltimore D. Permissive secondary mutations enable the evolution of influenza oseltamivir resistance. Science. 2010;328(5983):1272.

[80] Bloom JD, Nayak JS, Baltimore D. A Computational-Experimental Approach Identifies Mutations That Enhance Surface Expression of an Oseltamivir-Resistant Influenza Neuraminidase. PloS one. 2011;6(7):e22201.

[81] Alberts R, Srivastava B, Wu H, Viegas N, Geffers R, Klawonn F, et al. Gene expression changes in the host response between resistant and susceptible inbred mouse strains after influenza A infection. Microbes and infection. 2010;12(4):309–318.

[82] Trammell RA, Liberati TA, Toth LA. Host genetic background and the innate inflammatory response of lung to influenza virus. Microbes and Infection. 2011;.

[83] Horby P, Sudoyo H, Viprakasit V, Fox A, Thai P, Yu H, et al. What is the evidence of a role for host genetics in susceptibility to influenza A/H 5 N 1? Epidemiology and infection. 2010;138(11):1550–1558.

[84] Albright FS, Orlando P, Pavia AT, Jackson GG, Albright LAC. Evidence for a heritable predisposition to death due to influenza. Journal of Infectious Diseases. 2008;197(1):18.

[85] Gottfredsson M, Halldórsson BV, Jónsson S, Kristjánsson M, Kristjánsson K, Kristinsson KG, et al. Lessons from the past: Familial aggregation analysis of fatal pandemic influenza (Spanish flu) in Iceland in 1918. Proceedings of the National Academy of Sciences. 2008;105(4):1303.

[86] Loosli CG, Hamre D, Gerber P. Antigenic variants of influenza A virus (PR8 strain). V. Virulence, antigenic potency, and cross-protection tests in mice of the original and second series. Journal of Experimental Medicine. 1958;107:857–868.

[87] Rambaut A, Pybus OG, Nelson MI, Viboud C, Taubenberger JK, Holmes EC. The genomic and epidemiological dynamics of human influenza A virus. Nature. 2008;453(7195):615–619.

[88] Ginaldi L, Loreto MF, Corsi MP, Modesti M, De Martinis M. Immunosenescence and infectious diseases. Microbes and Infection. 2001;3:851–857.

[89] Viboud C, Boëlle PY, Cauchemez S, Lavenu A, Valleron AJ, Flahault A, et al. Risk factors of influenza transmission in households. British Journal of General Practice. 2004;54(506):684–689.

[90] Ho DD, Neumann AU, Perelson AS, Chen W, Leonard JM, Markowitz M, et al. Rapid turnover of plasma virions and CD4 lymphocytes in HIV-1 infection. Nature. 1995;373(6510):123–126.

[91] Perelson AS, Neumann AU, Markowitz M, Leonard JM, Ho DD. HIV-1 dynamics in vivo: virion clearance rate, infected cell life-span, and viral generation time. Science. 1996;271(5255):1582.

[92] Nowak MA, Bonhoeffer S, Hill AM, Boehme R, Thomas HC, McDade H. Viral dynamics in hepatitis B virus infection. Proceedings of the National Academy of Sciences. 1996;93(9):4398.

[93] Neumann AU, Lam NP, Dahari H, Gretch DR, Wiley TE, Layden TJ, et al. Hepatitis C viral dynamics in vivo and the antiviral efficacy of interferon-α therapy. Science. 1998;282(5386):103.

[94] Bonhoeffer S. Models of viral kinetics and drug resistance in HIV-1 infection. AIDS Patient Care and STDs. 1998;12(10):769–774.

[95] Bonhoeffer S, May RM, Shaw GM, Nowak MA. Virus dynamics and drug therapy. Proceedings of the National Academy of Sciences. 1997;94(13):6971.

[96] Bonhoeffer S, May RM, Shaw GM, Nowak MA. Virus dynamics and drug therapy. Proceedings of the National Academy of Sciences. 1997;94(13):6971.

[97] Hancioglu B, Swigon D, Clermont G. A dynamical model of human immune response to influenza A virus infection. Journal of theoretical biology. 2007;246(1):70–86.

[98] Lee HY, Topham DJ, Park SY, Hollenbaugh J, Treanor J, Mosmann TR, et al. Simulation and prediction of the adaptive immune response to influenza A virus infection. Journal of virology. 2009;83(14):7151–7165.

[99] Smith AM, Perelson AS. Influenza A virus infection kinetics: quantitative data and models. Wiley Interdisciplinary Reviews: Systems Biology and Medicine. 2010;.

[100] Belz GT, Wodarz D, Diaz G, Nowak MA, Doherty PC. Compromised influenza virus-specific CD8+-T-cell memory in CD4+-T-cell-deficient mice. Journal of virology. 2002;76(23):12388.

[101] Tridane A, Kuang Y. Modeling the interaction of cytotoxic T lymphocytes and influenza virus infected epithelial cells. Math Biosci Eng. 2010;7:171–185.

[102] Saccomani MP, Audoly S, Bellu G, D'Angiņ L. Examples of testing global identifiability of biological and biomedical models with the DAISY software. Computers in biology and medicine. 2010;40(4):402–407.

[103] Smith AM, Adler FR, Perelson AS. An accurate two-phase approximate solution to an acute viral infection model. Journal of mathematical biology. 2010;60(5):711–726.

[104] Carson ER, Cobelli C. Modelling methodology for physiology and medicine. Academic Pr; 2001.

[105] Sheiner LB, Steimer JL. Pharmacokinetic/pharmacodynamic modeling in drug development. Annu Rev Pharmacol Toxicol. 2000;40:67–95.

[106] Karlsson MO, Sheiner LB. The importance of modeling interoccasion variability in population pharmacokinetic analyses. J Pharmacokinet Biopharm. 1993 Dec;21(6):735–750.

[107] Pinheiro JC. Topics in mixed effects models. UNIVERSITY OF WISCONSIN; 1994.

[108] Sheiner LB, Beal SL. Evaluation of methods for estimating population pharmacokinetic parameters II. Biexponential model and experimental pharmacokinetic data. Journal of Pharmacokinetics and Pharmacodynamics. 1981;9(5):635–651.

[109] Beal S, Sheiner L, et al. Estimating population kinetics. Critical reviews in biomedical engineering. 1982;8(3):195.

[110] Lindstrom MJ, Bates D. Nonlinear Mixed Effects Models. Biometrics. 1990;46:673–687.

[111] Wolfinger R. Laplace's approximation for nonlinear mixed models. Biometrika. 1993;80(4):791–795.

[112] Chan PLS, Jacqmin P, Lavielle M, McFadyen L, Weatherley B. The use of the SAEM algorithm in MONOLIX software for estimation of population pharmacokinetic-pharmacodynamic-viral dynamics parameters of maraviroc in asymptomatic HIV subjects. Journal of pharmacokinetics and pharmacodynamics. 2011;38(1):41–61.

[113] Spiegelhalter D, Thomas A, Best N, Gilks W. BUGS: Bayesian inference using Gibbs sampling, Version 0.50. MRC Biostatistics Unit, Cambridge. 1995;.

[114] Dempster AP, Laird NM, Rubin DB. Maximum likelihood from incomplete data via the EM algorithm. Journal of the Royal Statistical Society Series B (Methodological). 1977;p. 1–38.

[115] Delyon B, Lavielle M, Moulines E. Convergence of a stochastic approximation version of the EM algorithm. Annals of Statistics. 1999;p. 94–128.

[116] Kuhn E, Lavielle M. Maximum likelihood estimation in nonlinear mixed effects models. Computational statistics & data analysis. 2005;49(4):1020–1038.

[117] Zhang Y, Wallace DL, De Lara CM, Ghattas H, Asquith B, Worth A, et al. In vivo kinetics of human natural killer cells: the effects of ageing and acute and chronic viral infection. Immunology. 2007;121(2):258–265.

[118] Eccles R. Understanding the symptoms of the common cold and influenza. The Lancet Infectious Diseases. 2005;5(11):718–725.

[119] Mathews JD, McCaw CT, McVernon J, McBryde ES, McCaw JM. A biological model for influenza transmission: pandemic planning implications of asymptomatic infection and immunity. PLoS One. 2007;2(11):e1220.

[120] Canini L, Carrat F. Population modeling of influenza A/H1N1 virus kinetics and symptom dynamics. J Virol. 2011 Mar;85(6):2764–2770.

[121] Boëlle PY, Ansart S, Cori A, Valleron AJ. Transmission parameters of the A/H1N1 (2009) influenza virus pandemic: a review. Influenza and Other Respiratory Viruses. 2011;.

[122] Bazzoli C. Evaluation et optimisation de protocoles dans les modčles non linéaires ŕ effets mixtes - Application ŕ la modélisation de la pharmacologie des antiretroviraux. Université Paris 7 - Denis Diderot Ecole doctorale de santé publique: Epidémiologie et sciences de l'information biomedicale; 2009.

[123] Al-Banna MK, Kelman AW, Whiting B. Experimental design and efficient parameter estimation in population pharmacokinetics. Journal of Pharmacokinetics and Pharmacodynamics. 1990;18(4):347–360.

[124] Jonsson EN, Wade JR, Karlsson MO. Comparison of some practical sampling strategies for population pharmacokinetic studies. Journal of Pharmacokinetics and Pharmacodynamics. 1996;24(2):245–263.

[125] Bouillon-Pichault M, Jullien V, Bazzoli C, Pons G, Tod M. Pharmacokinetic design optimization in children and estimation of maturation parameters: example of cytochrome P450 3A4. Journal of pharmacokinetics and pharmacodynamics. 2011;p. 1–16.

[126] Overholser BR, Brophy DF, Sowinski KM. Development of an efficient sampling strategy to predict enoxaparin pharmacokinetics in stage 5 chronic kidney disease. Therapeutic drug monitoring. 2006;28(6):807.

[127] Tod M, Jullien V, Pons G. Facilitation of drug evaluation in children by population methods and modelling. Clinical pharmacokinetics. 2008;47(4):231–243.

[128] Atkinson AC, Donev AN. Optimum experimental design. Press C, editor. Oxford Statistical Science Series; 1992.

[129] Walter E, Pronzato L. Identification of parametric models from experimental data. Communications and Control Engineering Series. Springer, editor. Springer, London; 1997.

[130] Mentre F, Mallet A, Baccar D. Optimal design in random-effects regression models. Biometrika. 1997;84(2):429–442.

[131] Retout S, Mentré F, Bruno R. Fisher information matrix for non-linear mixed-effects models: evaluation and application for optimal design of enoxaparin population pharmacokinetics. Statistics in medicine. 2002;21(18):2623–2639.

[132] Retout S, Mentre F. Optimization of individual and population designs using Splus. Journal of pharmacokinetics and pharmacodynamics. 2003;30(6):417–443.

[133] Fedorov VV. Theory of optimal experiments. Academic press; 1972.

[134] Guedj J, Bazzoli C, Neumann AU, Mentré F. Design evaluation and optimization for models of hepatitis C viral dynamics. Statistics in Medicine. 2011;.

[135] Bates DM, Watts DG. Relative curvature measures of nonlinearity. Journal of the Royal Statistical Society Series B (Methodological). 1980;p. 1–25.

[136] Jones B, Wang J. Constructing optimal designs for fitting pharmacokinetic models. Statistics and Computing. 1999;9(3):209–218.

[137] Cook RD, Goldberg ML. Curvatures for parameter subsets in nonlinear regression. The Annals of Statistics. 1986;p. 1399–1418.

[138] Mentré F, Dubruc C, Thénot JP. Population pharmacokinetic analysis and optimization of the experimental design for mizolastine solution in children. Journal of pharmacokinetics and pharmacodynamics. 2001;28(3):299–319.

[139] Retout S, Comets E, Samson A, Mentré F. Design in nonlinear mixed effects models: Optimization using the Fedorov–Wynn algorithm and power of the Wald test for binary covariates. Statistics in medicine. 2007;26(28):5162–5179.

[140] Reed MD. Optimal sampling theory: An overview of its application to pharmacokinetic studies in infants and children. Pediatrics. 1999;104(Supplement):627.

[141] Hennig S, Waterhouse TH, Bell SC, France M, Wainwright CE, Miller H, et al. A d-optimal designed population pharmacokinetic study of oral itraconazole in adult cystic fibrosis patients. British journal of clinical pharmacology. 2007;63(4):438–450.

[142] WHO. Regulatory Preparedness for Human Pandemic Influenza Vaccines. Expert committee on Biological Standardization (ECBS); 2007.

[143] Ambrose CS, Wu X, Knuf M, Wutzler P. The efficacy of intranasal live attenuated influenza vaccine in children 2 through 17 years of age: A meta-analysis of 8 randomized controlled studies. Vaccine. 2011;.

[144] Akira S. Innate immunity and adjuvants. Philosophical Transactions of the Royal Society B: Biological Sciences. 2011;366(1579):2748–2755.

[145] Aiello AE, Murray GF, Perez V, Coulborn RM, Davis BM, Uddin M, et al. Mask use, hand hygiene, and seasonal influenza-like illness among young adults: a randomized intervention trial. Journal of Infectious Diseases. 2010;201(4):491.

[146] Cowling BJ, Fung ROP, Cheng CKY, Fang VJ, Chan KH, Seto WH, et al. Preliminary findings of a randomized trial of non-pharmaceutical interventions to prevent influenza transmission in households. PLoS One. 2008;3(5):e2101.

[147] Loeb M, Dafoe N, Mahony J, John M, Sarabia A, Glavin V, et al. Surgical mask vs N95 respirator for preventing influenza among health care workers. JAMA: the journal of the American Medical Association. 2009;302(17):1865.

[148] MacIntyre CR. Hand hygiene and face mask use within 36 hours of index patient symptom onset reduces flu transmission to household contacts. Evidence Based Medicine. 2010;15(2):48–49.

[149] Grayson ML, Melvani S, Druce J, Barr IG, Ballard SA, Johnson PDR, et al. Efficacy of soap and water and alcohol-based hand-rub preparations against live H1N1 influenza virus on the hands of human volunteers. Clinical infectious diseases. 2009;48(3):285.

[150] Bell D, et al. Non-pharmaceutical interventions for pandemic influenza, national and community measures. Emerging infectious diseases. 2006;12(1):88.

[151] Burch J, Corbett M, Stock C, Nicholson K, Elliot AJ, Duffy S, et al. Prescription of anti-influenza drugs for healthy adults: a systematic review and meta-analysis. The Lancet infectious diseases. 2009;9(9):537–545.

[152] Hayden FG, Osterhaus ADME, Treanor JJ, Fleming DM, Aoki FY, Nicholson KG, et al. Efficacy and safety of the neuraminidase inhibitor zanamivir in the treatment of influenzavirus infections. New England Journal of Medicine. 1997;337(13):874–880.

[153] Hayden FG, Treanor JJ, Fritz RS, Lobo M, Betts RF, Miller M, et al. Use of the oral neuraminidase inhibitor oseltamivir in experimental human influenza. JAMA: the journal of the American Medical Association. 1999;282(13):1240.

[154] Kiso M, Mitamura K, Sakai-Tagawa Y, Shiraishi K, Kawakami C, Kimura K, et al. Resistant influenza A viruses in children treated with oseltamivir: descriptive study. The Lancet. 2004;364(9436):759–765.

[155] Shimbo K, Brassard DL, Lamb RA, Pinto LH. Ion selectivity and activation of the M2 ion channel of influenza virus. Biophysical journal. 1996;70(3):1335–1346.

[156] NICE. Amantadine, oseltamivir and zanamivir for the treatment, Review of NICE technology appraisal guidance 58. National Institute for Clinical Excellence; 2011.

[157] Gubareva LV, Kaiser L, Hayden FG. Influenza virus neuraminidase inhibitors. The Lancet. 2000;355(9206):827–835.

[158] Liu C, Eichelberger MC, Compans RW, Air GM. Influenza type A virus neuraminidase does not play a role in viral entry, replication, assembly, or budding. Journal of virology. 1995;69(2):1099.

[159] Watanabe A, Chang SC, Kim MJ, Chu DW, Ohashi Y, et al. Long-acting neuraminidase inhibitor laninamivir octanoate versus oseltamivir for treatment of influenza: a double-blind, randomized, noninferiority clinical trial. Clinical Infectious Diseases. 2010;51(10):1167.

[160] Fraser C, Riley S, Anderson RM, Ferguson NM. Factors that make an infectious disease outbreak controllable. Proceedings of the National Academy of Sciences of the United States of America. 2004;101(16):6146.

[161] Rayner CR, Chanu P, Gieschke R, Boak LM, Jonsson EN. Population pharmacokinetics of oseltamivir when coadministered with probenecid. The Journal of Clinical Pharmacology. 2008;48(8):935.

[162] Hayden FG. Perspectives on antiviral use during pandemic influenza. Philos Trans R Soc Lond B Biol Sci. 2001;356(1416):1877–1884.

[163] Treanor JJ, Hayden FG, Vrooman PS, Barbarash R, Bettis R, Riff D, et al. Efficacy and safety of the oral neuraminidase inhibitor oseltamivir in treating acute influenza. JAMA: the journal of the American Medical Association. 2000;283(8):1016.

[164] Monto AS. The role of antivirals in the control of influenza. Vaccine. 2003;21(16):1796–1800.

[165] WHO. WHO guidelines on the use of vaccines and antivirals during influenza pandemics. World Health Organization; 2004.